

B D Simons<sup>1</sup> and Alexander Altland<sup>2</sup>

<sup>1</sup>*Cavendish Laboratory, Madingley Road, Cambridge CB3 0HE, UK*

<sup>2</sup>*Institut für theoretische Physik, Zùlpicher Str. 77, 50937 Kùln, Germany*

(May 16, 2001)

A course of lectures on mesoscopic quantum interference phenomena: we begin with a qualitative survey of the manifestations of quantum phase coherence and interaction in mesoscopic structures. This will be followed by a more methodologically oriented part which aims to introduce the construction of effective field theories of mesoscopic systems. The remaining sections of the course will be devoted to the discussion of various applications, with an emphasis on recent developments. Specifically, we will discuss electron-electron interaction phenomena, review the status of the ballistic  $\sigma$ -model and its application to problems of ‘quantum chaos’, and introduce basic elements of mesoscopic superconductivity. Some emphasis will be given to the discussion of the concept of seven ‘new’ symmetry classes. We discuss why the three-fold symmetry classification of Wigner and Dyson is not exhaustive and where ‘non-standard’ symmetries are realized. This will be followed by the discussion of a number of applications, notably disordered hybrid superconducting-normal structures, dirty  $d$ -wave superconductivity, and chiral fermion systems.

## Contents

<b>I</b>	<b>Introduction to Mesoscopic Physics</b>	<b>1</b>
A	Manifestations of Phase Coherence in Mesoscopic Structures . . . . .	3
1	Magneto-fingerprints . . . . .	4
2	Aharonov-Bohm Effects . . . . .	5
B	Qualitative Considerations: Feynman Paths . . . . .	5
1	Weak Localization . . . . .	9
2	Fluctuations . . . . .	10
3	Aharonov-Bohm Oscillations . . . . .	10
4	Energy Level Repulsion and Universality . . . . .	11
5	Universal Conductance Fluctuations . . . . .	11
6	Breakdown of Perturbation Theory: RMT . . . . .	12
7	Scaling Theory of Localization . . . . .	13
8	Summary . . . . .	14
C	Interaction Phenomena . . . . .	15
1	Coulomb Blockade . . . . .	15
2	Zero-Bias Anomaly . . . . .	16
3	Inelastic Scattering Rate and Dephazing . . . . .	17
D	Impurity Diagram Technique . . . . .	18
<b>II</b>	<b>Field Theory of Disordered Conductors</b>	<b>20</b>
A	Derivation of the $\sigma$ -Model Action . . . . .	20
1	Field Integral . . . . .	21
2	Impurity Averaging . . . . .	22
3	Hubbard-Stratonovich Decoupling . . . . .	22
4	Saddle-Point Equation . . . . .	23
5	Gradient Expansion . . . . .	24
6	Magnetic Field . . . . .	24
B	Applications of the $\sigma$ -Model . . . . .	25
1	Perturbation Theory . . . . .	25
2	Weak Localization, Scaling and the RG . . . . .	25

---

\*a five lecture course to be published in the proceedings of the CRM Summer school entitled “Theoretical Physics at the End of the XXth Century”, Banff (Springer-Verlag) 2001.

3	Level Statistics . . . . .	26
4	Zero-Mode . . . . .	26
C	Zero-Mode Integration . . . . .	27
D	Random Matrix Theory . . . . .	27
E	Theories of Mesoscopic Systems . . . . .	28
<b>III</b>	<b>Quantum Chaos . . . . .</b>	<b>28</b>
A	Spectral Statistics: A Brief History . . . . .	31
1	Wigner Surmise . . . . .	31
2	Gor'kov-Eliashberg Theory . . . . .	31
3	Supersymmetry: Efetov's Non-linear $\sigma$ -Model . . . . .	32
4	Bohigas-Giannoni-Schmidt Conjecture . . . . .	32
B	Semi-classics and the Trace formula . . . . .	33
C	Ballistic $\sigma$ -Model . . . . .	34
D	Perturbation Theory . . . . .	34
E	Quantum Hall Effect . . . . .	36
<b>IV</b>	<b>Coulomb Interaction Phenomena . . . . .</b>	<b>38</b>
A	Matsubara Field Integral . . . . .	39
B	Plasma Theory of the Free Electron Gas . . . . .	40
C	Plasma Theory of the Disordered Electron Gas . . . . .	42
D	Gauge Fixing: Low-Energy Saddle-Point . . . . .	43
E	Zero-Bias Anomaly . . . . .	44
<b>V</b>	<b>Novel Symmetry Classes . . . . .</b>	<b>45</b>
A	Realizations of Novel Symmetries . . . . .	46
B	Dirty Superconductivity . . . . .	47
1	Field Theory of the Dirty Superconductor . . . . .	48
2	Mean-Field Theory . . . . .	49
3	Fluctuations . . . . .	49
C	Hybrid Superconductor-Normal Systems . . . . .	50
1	SN Phenomenology . . . . .	50
2	Field Theory of SN-Structures . . . . .	52
D	Dirty d-Wave Superconductivity . . . . .	54
1	Field Theory of a Single Dirac Node . . . . .	55
2	Gradient Expansion . . . . .	55
3	Mode Locking . . . . .	56
E	Systems with Chiral Symmetries . . . . .	58
F	Bond-Disordered Fermion Systems . . . . .	58
1	Field Theory of the RF-Model . . . . .	59
2	Color-Flavor Transformation . . . . .	60
3	Properties of the Field Theory . . . . .	62

## I. INTRODUCTION TO MESOSCOPIC PHYSICS

As students we are usually introduced to the phenomena of solid state physics within the framework of the “nearly-free electron” theory of metals in which electrons are thought to interact only weakly with a *regular* (i.e. ordered) crystalline lattice potential [1]. The interaction between electrons is limited to the quantum mechanical exclusion principle. Yet, in the majority of metals, the Coulomb interaction between electrons is by no means small — the energy associated with Coulomb interaction is typically comparable to the kinetic energy. However, the validity of the non-interacting theory is, in many cases, assured by the *Fermi liquid theory*.

The fundamental principle underlying Fermi liquid

theory is one of “adiabatic continuity” [2]: In the absence of an electronic phase transition (such as “Wigner crystallization” of the electrons, or a “Mott-Hubbard transition” to a magnetic insulating state), a non-interacting ground state evolves smoothly or adiabatically into the interacting ground state as the strength of interaction is increased. An elementary excitation of the non-interacting system represents an “approximate excitation” of the interacting system (i.e. the “lifetime” of an elementary excitation is long).

However, the integrity of a fully ordered lattice potential is more questionable. Electrons in metals and semiconductors typically experience an irregular lattice potential arising from defects or lattice imperfections, grain boundaries, vacancies, and doped impurities. At length

scales in excess of the (temperature dependent) phase coherence length  $L_\varphi$  (i.e. the scale over which the electron dynamics is phase coherent), the transport properties in such a disordered environment can be simply understood within the framework of quasi-classical techniques such as the Kinetic or Boltzmann theory [3]. However, at length scales smaller than  $L_\varphi$ , the quantum phase coherence of the electron degrees of freedom dramatically influence the nature of the dynamics. Here at the “mesoscopic” scale, new physical principles emerge.

- ▷ **What is mesoscopic physics?** As a subject, Mesoscopic physics involves the domain of length scales in between the microscopic and macroscopic where the influence of quantum phase coherence effects find manifestations in observed physical properties. Yet, as we will see in these lectures, the subject of mesoscopic physics is not confined to the study of electrons in disordered conductors.
- ▷ **Where can one find mesoscopic structures?** The development of modern fabrication techniques combined with the routine availability of millikelvin temperatures in the laboratory have exposed a novel class of materials macroscopic in their constitution, yet smaller than the typical scales over which phase coherence is established. The market forces that drive the semiconductor industry have driven this “nanostructure” technology to a level of unprecedented sophistication. These days, artificial semiconductor devices can be manufactured with a resolution of 100 nm or less (see below). Even “nanotubes” of carbon have been successfully incorporated into small conducting bridges.
- ▷ **Why study mesoscopic physics?** Leaving aside the obvious benefits brought about by the continual miniaturization of quantum devices, such structures present a unique opportunity to study new and fundamental physical phenomena. Where phase coherence is established, the manifestations of quantum mechanics on the observed physical properties is often substantial. Therefore, the fabrication of mesoscopic structures such as low-dimensional, nanostructure or “quantum dot” devices provides a laboratory in which one can explore the fundamental properties of many-particle systems from the influence of disorder to strong electron interaction phenomena.

**Aim of these lectures:** Mesoscopic physics is an old subject which, since the late '70's has engaged a vast number of researchers. To embark on a comprehensive review of the entire field would be foolhardy. An attempt to achieve such a goal in just a few lectures would be futile. Instead, the aim of these lectures will be to introduce some of the guiding principles, to highlight some of the more recent developments and generalizations, and, perhaps most importantly, expose many unresolved questions in the field. In doing so, we will exploit

novel methods of quantum statistical field theory which will establish useful and, sometimes, surprising connections to other branches of physics from atomic physics to QCD. Finally, a disclaimer: in preparing this course, it is inevitable that the subjective choice of material reflects to a large extent our own polarized interests and for which we should apologize.

The outline of the course is as follows: in the remainder of this chapter we will introduce the central ideas and concepts that shape the subject of mesoscopic physics. In doing so, we aim to review the main questions presented by experiment as well as providing interpretations in terms of simple quasi-classical phenomenology. These qualitative ideas are put on a firm footing in chapter II where a statistical field theory of weakly disordered metallic conductors is developed within the framework of a supersymmetric non-linear  $\sigma$ -model. In applying the field theory, particular emphasis is placed on establishing connections which tie together the phenomenology of “weak localization” and “universality” (the random matrix theory).

To broaden the class of applications of the statistical approach, chapter III is concerned with the generalization of the quantum field theory to the properties of non-stochastic chaotic quantum structures — “quantum chaos”. Here we will stress the importance of the intuition afforded by the characteristic mesoscopic phenomena observed in weakly disordered metallic systems, and point out some of the outstanding problems in the field.

Chapters I, II and III focus largely on the properties of *non-interacting* quantum structures. Yet, the influence of Coulomb interaction, particularly in the environment of disorder, is strong. In chapter IV we will establish a generalization of the statistical field theory of disordered conductors to encompass the important effects of Coulomb interaction. Applications of this theory will be limited as much by the current state of the technology, as by the constraints placed on the scope of these lectures.

Phase coherence effects in weakly disordered structures can be usually classified into three universality classes which reflect the fundamental symmetries of the bare Hamiltonian. Yet, such a classification is not exhaustive: recent attempts to extend theories of disordered systems to encompass superconducting structures and sublattice models have identified novel universality classes which exhibit qualitatively new phenomena. Surprisingly, it is mostly through the study of such systems that unusual connections to other branches of physics have been identified. In chapter V we introduce and explore the unusual spectral and localization properties associated with these novel symmetry classes pointing out their close connection to the study of lattice QCD, and the dynamical properties of random *classical* operators.

The program is broad: it is therefore not the intention of these lectures to provide a complete or comprehensive

review of the field. Rather, we hope to convey the central concepts of this diverse subject, as well as developing some of the general technology which has proved to be so successful in the exploration of this field. Finally, we have attempted to keep the prerequisites for this course to a minimum: we will, however, assume a familiarity with the fundamental principles of elementary solid state physics, and an exposure to some basic concepts in advanced statistical mechanics and quantum field theory.

### A. Manifestations of Phase Coherence in Mesoscopic Structures

To begin our investigation of mesoscopic physics we start with a survey of several of the classic experiments which explore mechanisms of quantum phase coherence (for a review see, e.g., Ref. [4]). In doing so, where possible, we will separate those experiments which find their origin in Coulomb interaction effects from those which can be understood within the framework of a purely non-interacting theory.

The majority of the experiments which we discuss below are performed on low-dimensional semi-conducting GaAs or Si heterostructures. Without going into extensive detail, we remark that the latter involve “sandwich” structures where abrupt changes of doping concentration of donor and acceptor impurities trap electrons in a narrow regions known as “inversion layers”. The inversion layer potential can be used to confine electrons (or holes) to two-dimensional regions, one-dimensional channels (wires), and zero-dimensional wells (known as “quantum dots”) — for a review see, e.g., Refs. [5,7,6]. Here, by confinement, we mean that the Fermi energy lies in an interval of energy well below the energy required to excite the lowest “transverse” mode. (For a review of device technology see, e.g., Ref. [8,36].)

For simplicity, we will not dwell on specific fabrication techniques. Nor will we assess the integrity of device characteristics. However, to orient our discussion, we note the typical range of relevant physical parameters below:

Parameter	GaAs	Si	Units
Density $n$	4.0	4.0	$10^{11} \text{ cm}^{-2}$
Mobility $\mu$	$10^5$	$10^4$	$\text{cm}^2/\text{Vs}$
Scattering Time $\tau$	3.8	1.1	$10^{-12}\text{s}$
Fermi Wavevector $\lambda_F$	1.6	1.6	$10^6 \text{ cm}^{-1}$
Fermi Velocity $v_F$	2.76	0.97	$10^7 \text{ cm/s}$
Elastic m.f.p. $\ell$	1.05	0.107	$10^{-4} \text{ cm}$

Before we turn to the experiments, as preparation for our discussion, let us first recall some elementary concepts in the theory of electron transport. Firstly, in a degenerate electron gas, the conductivity  $\sigma$  and the diffusion constant  $D$  are fundamentally connected by the Einstein relation [1]

$$\sigma = e^2 \nu D \quad (1)$$

where  $\nu$  denotes the density of states at the Fermi level. The diffusion constant can, in turn, be obtained from the time-integrated velocity-velocity correlation function

$$D = \frac{1}{d} \int_0^\infty dt \langle \mathbf{v}(t) \cdot \mathbf{v}(0) \rangle$$

where the average is taken over all initial velocities  $\mathbf{v}(0)$ .

Now, within the framework of classical transport or kinetic theory, the velocity of an electron is randomized on a time scale set by the mean free scattering time between collisions,  $\tau$ . In this approximation, the diffusion constant is specified by  $D = v_F^2 \tau / d$ , where  $v_F = p_F / m$  denotes the Fermi velocity and  $d$  the dimensionality. The latter, in turn, leads to the classical Drude formula for the conductivity,

$$\sigma = \frac{ne^2\tau}{m}$$

where  $n \sim \nu E_F$  represents the electron density, and  $E_F$  denotes the Fermi energy.

Finally, from the conductivity, we can define the conductance  $G = \sigma L^{2-d}$  which, making use of the Einstein relation (1) can be expressed as

$$G = \frac{e^2}{\hbar} \nu L^d \frac{\hbar D}{L^2} = \frac{e^2}{\hbar} g, \quad g \equiv \frac{E_c}{\Delta} \quad (2)$$

where  $\Delta = 1/\nu L^d$  denotes the average energy level spacing, and  $E_c = \hbar D / L^2$  represents the typical inverse diffusion time for an electron to cross a sample of dimension  $L^d$ . This result shows that the conductance of a metallic sample can be expressed as the product of the quantum unit of conductance  $e^2/\hbar = (4.1k\Omega)^{-1}$ , and a *dimensionless conductance*  $g$  equal to the number of levels inside an interval  $E_c$ . In a good metallic sample, the dimensionless conductance is large,  $g \gg 1$ . Note, however, that the control parameter  $g$  must not be categorically identified with the conductance observed in experiment. E.g. in systems with pronounced quantum localization effects, to be discussed below, the microscopic *conductivity* and the *conductance* are not related by the simple scaling relation (2). In such cases, the parameter  $g$  becomes a purely formal, and largely meaningless quantity.

#### 1. Magneto-fingerprints

With this background, we turn our attention to experiment: fig. 1 shows a series of magneto-conductance measurements [10] (i.e. the dependence of  $g$  as a function of magnetic field) performed on a SiGaAs wire after repeated heating and cooling.

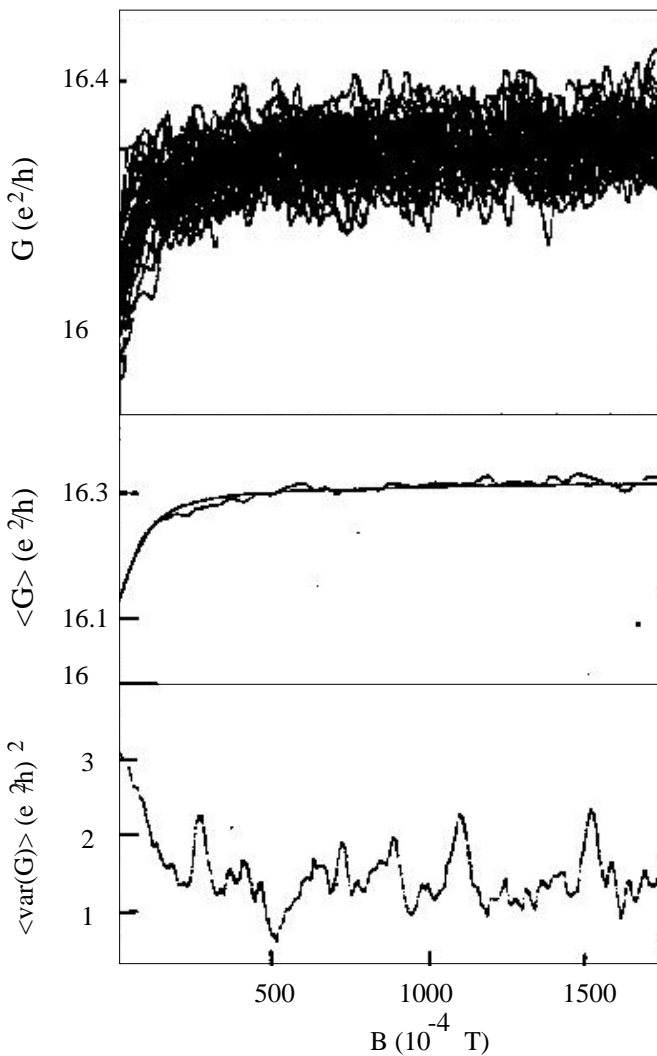


FIG. 1. Magneto-conductance measurements of a SiGaAs wire taken from Ref. [10]. (a) Conductance as a function of magnetic field for samples which differ by thermal cycling. (b) The conductance averaged over different realizations. (c) The variation of the variance of the conductance fluctuations measured as a function of magnetic field. (Courtesy of Ref. [10].)

Although each individual trace appears to fluctuate randomly around some uniform value, the measurements are completely reproducible. (I.e. when held at a constant low temperature, the fluctuations of the conductance do not change with time.) However, by thermal cycling, the accompanying rearrangement of the impurities completely changes the pattern of magneto-conductance fluctuations. These results, which are typical of those observed in phase coherent devices, suggest that sample-sample fluctuations provide a characteristic signature (a “magneto-fingerprint”) of an individual system [11,12].

Yet characteristic fluctuations of this kind are not limited to wires. Figs. 2 and 3 show the variation of two-terminal magneto-conductance measurements together with an applied gate voltage potential performed on a

mesoscopic GaAs quantum dot. Again, the qualitative behavior is similar: the system shows a reproducible magneto-fingerprint with the same characteristic scale of fluctuations,  $e^2/h$ .

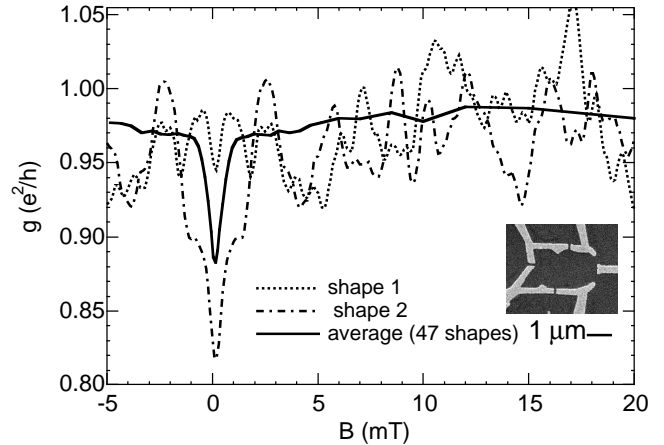


FIG. 2. Magneto-conductance measurements of a GaAs quantum dot taken from Ref. [13]. The device, shown inset, has a transport mean free path and phase coherence length greatly in excess of the dimensions of the device (ca.  $1\mu\text{m}$ ). The “shape” of the quantum dot can be changed by tuning a gate or “plunger”. Separate traces are shown for two particular shapes together with the average over an ensemble of different realizations. Note the universal scale of the fluctuations, and the conductance minimum at zero field. (Courtesy of Ref. [13].)

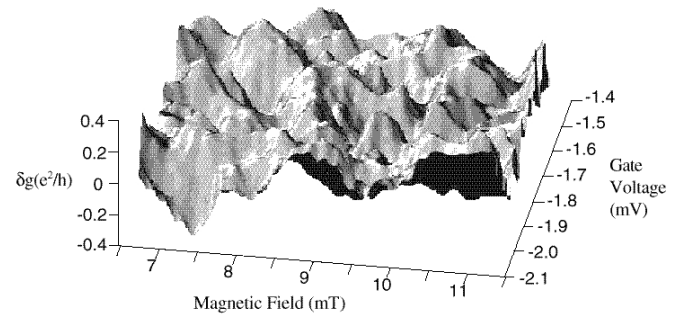


FIG. 3. Conductance measurements as a function of magnetic field and external gate voltage for a quantum dot qualitatively similar to that shown in Fig. 2. (Courtesy of Ref. [13].)

Taken together, these measurements pose the following questions:

- ▷ Firstly, why is the magnitude of the conductance fluctuations *universal*? That is, for any size or geometry of the sample, the conductance is found to fluctuate on a scale comparable to  $e^2/h$ . More precisely, defining  $\langle \dots \rangle$  as the ensemble average over realizations of the impurity potential (gen-

erated in the present case by thermal cycling),  $\langle(\delta G)^2\rangle \simeq (e^2/h)^2$ , where  $\delta G \equiv G - \langle G \rangle$  — i.e. the characteristic scale of fluctuations is independent of the system size.

▷ Secondly, why are these fluctuations so large? Naively, in a metallic  $d$ -dimensional sample, it is reasonable to suppose that each block of dimension  $\ell_c^d$ , where  $\ell_c$  represents a macroscopic length scale (e.g. mean distance between impurities), contributes independently to the total conductance. With this assumption, one can expect the magnitude of conductance fluctuations to vanish in the thermodynamic limit as the power law  $\langle(\delta G)^2\rangle/\langle G \rangle^2 \sim (\ell_c/L)^d$ . In this sense, the conductance is expected to be *self-averaging*. However, taking  $\langle G \rangle = \sigma L^{2-d}$  (i.e. Ohm's law), the experimental measurements above are compatible with fluctuations of magnitude  $\langle(\delta G)^2\rangle/\langle G \rangle^2 \sim L^{4-2d}$  which, at least in dimensions  $d < 4$ , are substantially larger! Evidently, there exist substantial *non-local* correlations which, in turn, lead to the absence of *self-averaging*.

▷ Finally, why is the strength of both the ensemble averaged conductance, as well as its fluctuation, magnetic field dependent? More precisely, the measurements above show two clear effects: firstly, the conductivity increases with the application of a weak magnetic field (i.e. a field small enough that the influence of orbital effects can be ruled out). Secondly, on the same field scale, the magnitude of the fluctuations is substantially diminished.

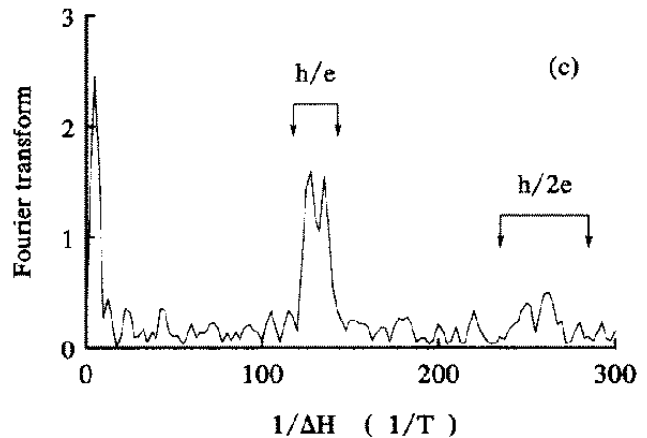
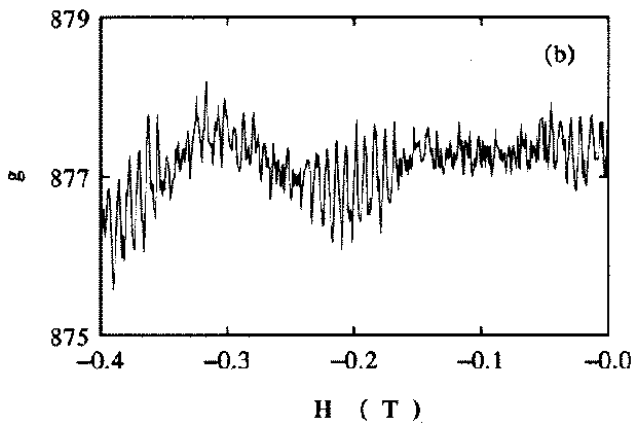


FIG. 4. Magneto-conductance measurements of a single Au loop together with the corresponding power spectrum showing periodic oscillations at  $h/e$  and  $h/2e$  taken from Ref. [14].

## 2. Aharonov-Bohm Effects

A second classic experiment involves the Aharonov-Bohm effect. Fig. 4 shows the magneto-resistance measurements of a single gold metallic ring. As with the quantum wire, the results show a characteristic pattern of magneto-fingerprint fluctuations. However, these fluctuations are modulated by periodic oscillations. These oscillations are manifest most clearly in the power spectrum which indicate Fourier components at a frequencies of  $1/\Delta H$  corresponding to values of  $h/e$  and  $h/2e$ . Furthermore, separate measurements of a statistical ensemble of mesoscopic rings shows the  $h/e$  oscillations to vanish on averaging, while the  $h/2e$  oscillations remain. To our list above, we can, therefore, add the questions:

- ▷ In the Aharonov-Bohm geometry, what is the physical origin of the  $h/e$  and  $h/2e$  oscillations?
- ▷ And how can we understand the action of ensemble averaging on these two types of oscillations?

## B. Qualitative Considerations: Feynman Paths

To find qualitative answers to the questions raised above, it is useful to consider a simplified model of electron dynamics in the background of a random scattering potential. In doing so, we should first recognize the crucial distinction between the two types of scattering an electron can undergo. *Elastic scattering* (e.g. by lattice defects or impurities) imparts on the electron a well-defined phase shift. By contrast, *inelastic scattering*, which involves the exchange of energy with other degrees of freedom (e.g. phonons, other electrons, and spins), introduces uncertainty in the phase. It is this uncertainty which is responsible for the destruction of quantum interference. In the following, we will assume that the time

scale over which phase coherence is maintained, the inelastic scattering time  $\tau_\varphi$ , is greatly in excess of the time scale on which an electron is scattered across the Fermi surface, the elastic scattering time  $\tau$ .

At its simplest level, the dynamics of an electron in a phase coherent environment can be described by a non-interacting or single-particle Hamiltonian

$$\hat{H} = \frac{\hat{\mathbf{p}}^2}{2m} + V(\mathbf{r}), \quad (3)$$

where  $\hat{\mathbf{p}} = -i\hbar\partial$  denotes the momentum operator, and  $V(\mathbf{r})$  represents a random impurity potential. Now, even for this simplified model, a given realization of the random impurity potential is associated with a complex spectrum. Yet, if the potential fluctuations are weak as compared with the typical energy scale of the particle, the influence of quantum interference on the particle dynamics can be determined both qualitatively and, as we shall see later, quantitatively.

To stay within the domain in which a quasi-classical analysis is valid, we will focus on the hierarchy of length scales shown in Fig. 5.

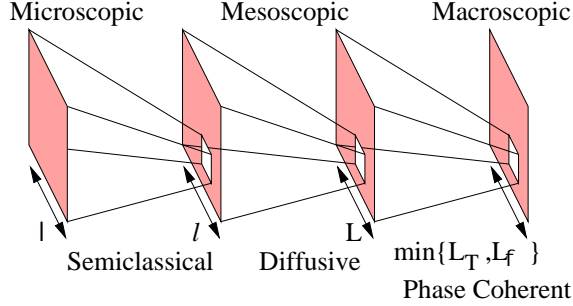


FIG. 5. Hierarchy of length scales which electron dynamics is phase coherent and diffusive.

Specifically, we will focus on the *semi-classical* regime in which the mean free path of the particle  $\ell$  is greatly in excess of the corresponding wavelength of the particle  $\lambda_F$  (or, equivalently  $E_F\tau \gg \hbar$ ). Moreover, to stay within the regime in which the particle dynamics is diffusive, we will require the system size  $L$  to be greatly in excess of  $\ell$ . Finally, we will take the system size to be much smaller than the typical length scale  $L_\varphi$  over which the particle dynamics is phase coherent.

With this definition, the quantum transfer *probability amplitude* for a particle to propagate from a point  $\mathbf{r}_I$  to a point  $\mathbf{r}_F$  in a time  $t$  is specified by the quantum mechanical Feynman propagator

$$G(\mathbf{r}_F, \mathbf{r}_I; t) = \int_{\mathbf{r}(0)=\mathbf{r}_I}^{\mathbf{r}(t)=\mathbf{r}_F} D\mathbf{r}(t) e^{\frac{i}{\hbar} \int_0^t dt \left( \frac{m\dot{\mathbf{r}}^2}{2} - V(\mathbf{r}(t)) \right)}. \quad (4)$$

Now, for an arbitrary configuration of the impurity potential, an exact evaluation of the path integral is, of course, infeasible. However, we can gain a qualitative

understanding of the problem by visualizing the path integral as an infinite sum of separate paths  $i$  each with its own amplitude  $A_i$  and phase  $\varphi_i$ ,

$$G(\mathbf{r}_F, \mathbf{r}_I; t) = \sum_i A_i e^{i\varphi_i}.$$

i.e. the superposition of randomly scattered waves.

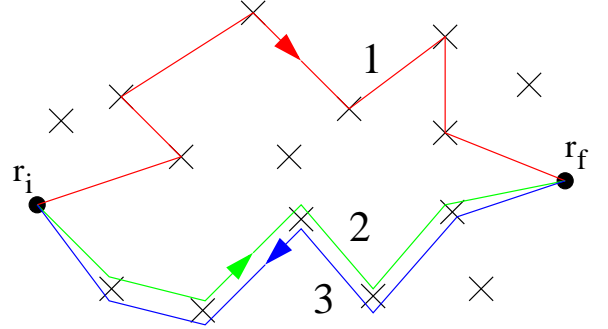


FIG. 6. Typical Feynman paths connecting lattice sites  $\mathbf{r}_I$  and  $\mathbf{r}_F$ . When summed over all configurations of the random impurity potential, the contribution of paths such as 1 and 2 add incoherently to the average probability amplitude or Green function. However, the diagonal contribution from paths 2 and 3 (which follow the same path) contribute coherently to the average probability density.

Typically, different paths have lengths that differ substantially implying a statistical independence of the phases  $\varphi_i$  (i.e. for two paths  $i$  and  $j$ ,  $|\varphi_i - \varphi_j| \gg 2\pi$ ). Therefore, applied to the propagator, an ensemble average over different realizations of the random impurity potential leads to a random phase cancellation which is manifest as an exponential decay of the average on the time scale of the mean free scattering time  $\tau$ . Equivalently, the ensemble average of the propagator decays on a length scale comparable to the mean free path  $\ell$ .

By contrast, the corresponding transfer *probability density* of a particle from a position  $\mathbf{r}_I$  to  $\mathbf{r}_F$

$$\begin{aligned} P(\mathbf{r}_F, \mathbf{r}_I; t) &\equiv |G(\mathbf{r}_F, \mathbf{r}_I; t)|^2 \\ &= \sum_i A_i^2 + 2 \sum_{i \neq j} A_i A_j \cos(\varphi_i - \varphi_j), \end{aligned}$$

involves long-ranged correlations. More precisely, when subjected to an ensemble average, while the *interference* contribution averages to zero, a long-ranged *diagonal* contribution survives:

$$\langle P(\mathbf{r}_F, \mathbf{r}_I; t) \rangle = \sum_i \langle A_i^2 \rangle.$$

Here the random phase accumulated by a particle propagating from a point  $\mathbf{r}_I$  to  $\mathbf{r}_F$  is cancelled by the phase acquired on the return providing the two paths coincide on the scale of Fermi wavelength,  $\lambda_F$  of the particle (see Fig. 6, paths 2 and 3).

How can the qualitative Feynman path picture be promoted to a quantitative theory? In a sense, much of the rest of the course will deal with just this question. However, for the moment let us restrict ourselves to some preliminary considerations of the two theoretical approaches most directly related to the path picture: semi-classics and diagrammatic perturbation theory.

The exact path integral representation (4) of the Green function is, in general, not amenable to rigorous analytical manipulations. However, in the vast majority of problems of mesoscopic physics, semi-classical stationary phase approximations schemes can be applied to reduce the complexity of the problem. Let us recall that Feynman path integrals can be evaluated by stationary phase methods whenever the action  $S = \int (m\dot{r}^2/2 - V)$  is greatly in excess of  $\hbar$ . An action of  $\mathcal{O}(\hbar)$  is accumulated whenever a quantum particle has propagated over a distance of  $\mathcal{O}(\lambda_F)$ , the Fermi wave length. As pointed out above,  $\lambda_F$  is substantially smaller than any other relevant length scale, i.e. we are working under conditions where the path integral can be evaluated by stationary phase schemes.

This observation forms the basis to the so-called **semi-classical approach** to mesoscopic systems, i.e. an approach that attempts to make the summation over classical stationary phase paths quantitative. The application of such methods to *effectively clean* mesoscopic structures has been a great success story. (In the context of mesoscopic physics, a ‘clean’ system is one where the disorder concentration is so low that on the length/time scales of interest the electron dynamics is effectively ballistic. Examples include high mobility two-dimensional electron gases. More will be said about such systems in section III below.) They are, however, far less suited to the analysis of disordered structures wherefore the orthodox semi-classical approach will not play the main role in this course. Closely related, but now tailor made to problems with disorder, are methods of **diagrammatic perturbation theory**.

The starting point of the diagrammatic approach is a formal series expansion of the single particle Green function,

$$\hat{G} \equiv (\hat{G}_0^{-1} - \hat{V})^{-1} = \hat{G}_0 + \hat{G}_0 \hat{V} \hat{G}_0 + \hat{G}_0 \hat{V} \hat{G}_0 \hat{V} \hat{G}_0 + \dots, \quad (5)$$

where  $\hat{G}_0 = (\epsilon - \hat{H}_0)^{-1}$  denotes the free Green function, controlled by the kinetic part of the Hamilton operator,  $\hat{H}_0$ , and  $\hat{V}$  is some kind of disorder potential. As usual with diagrammatic approaches, individual terms contributing to the series are represented graphically like in Fig. 7.

FIG. 7. Graphical series representation of the single particle Green function.

Here the thin and thick lines stand for the free and full Green function, respectively, and the crosses symbolize scattering off the potential. At this stage, the series expansion of Fig. 7 merely represents a formal expression for the scattering paths depicted schematically in Fig. 6. However, the real advantage of the formal diagrammatic expansion is that it can be made quantitative. For that one first needs to specify a probability measure defining the characteristics of the scattering potential  $V$ . E.g., a popular choice is to assume that  $V$  is short range Gaussian correlated,

$$\langle V(\mathbf{r}) \rangle = 0, \quad \langle V(\mathbf{r}) V(\mathbf{r}') \rangle = \frac{\hbar}{2\pi\nu\tau} \delta^d(\mathbf{r} - \mathbf{r}'), \quad (6)$$

where the average should be understood as over many realizations of the scattering potential.

Of course, in order for the whole approach to make sense the outcome of the diagrammatic analysis (i.e. predictions for the long range behaviour of observables of interest) must be insensitive to the particular modeling of the potential distribution. In the vast majority of applications this condition is met. Yet there are a few prominent exceptions, e.g. the  $d$ -wave superconductor (to be discussed below) whose low energy spectral properties sensitively depend on the microscopic features of the scattering potential.

In practical terms, Eq. (6) states that, on average, scattering events are pairwise correlated. One can interpret this rule by saying that the scattering phase shift accumulated by the Green function in any scattering event must be compensated for by a second scattering process with equal but opposite phase shift. A set of diagrams conforming with this rule is shown in Fig. 8 where the dashed lines indicate the pairwise, or Gaussian, correlation of the scattering process.

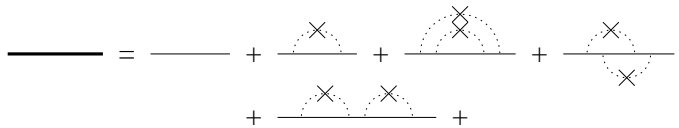


FIG. 8. Set of diagrams contributing to the averaged single particle Green function.

The pair correlation rule entails enormous simplifications and enables one to compute objects like averaged Green functions in quantitative detail. (Referring to the literature [15] for detailed expositions of the technicalities we have included a brief review of diagrammatic methods in section I D.) E.g., application of the diagram technique to the average of a single Green function obtains

$$\langle G(\mathbf{r}_F, \mathbf{r}_I; t) \rangle = G_0(\mathbf{r}_F - \mathbf{r}_I; t) e^{-t/2\tau},$$

i.e. an object that decays rapidly on the scale of  $l = v_F \tau$ . This result conforms with our previous qualitative considerations on the short-ranged behaviour of the averaged



Green function. However, the diagrammatic formalism can equally well be applied to averages of products of Green functions, as they appear in the analysis of transport *probabilities*. One then encounters (see section ID for details) diagrams of the topology shown in Fig. 9 (a). This diagram formally describes correlated pair propagation, as depicted qualitatively in Fig. 6, bottom. Again the scattering events occur pairwise, where now the scattering phase picked up by one Green function gets compensated by a matching term in the other Green function.

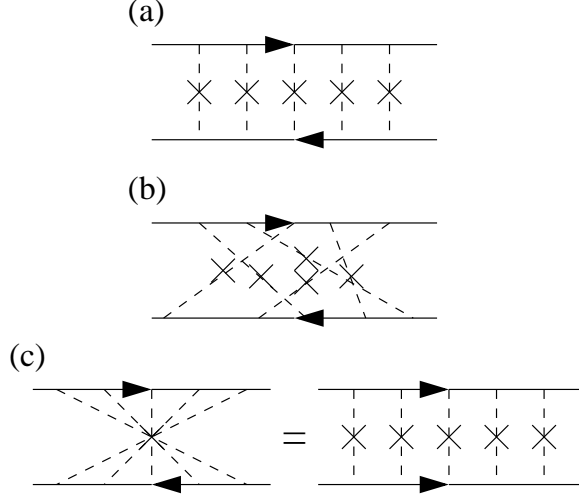


FIG. 9. Diagrammatic representation of the two particle Green function: (a) Diffuson, (b) a short-ranged non-singular contribution, and (c) Cooperon. Note that the maximally crossed Cooperon diagram can be re-expressed as a ladder series by time-reversing the advanced Green function.

Quantitative evaluation of the pair propagation process shown in Fig. 9 (a) leads to the result

$$\begin{aligned} \langle P(\mathbf{r}_F, \mathbf{r}_I; t) \rangle &= \langle |G(\mathbf{r}_F, \mathbf{r}_I; t)|^2 \rangle \equiv \Pi_D(\mathbf{r}_F - \mathbf{r}_I, t) = \\ &= \frac{1}{(2\pi Dt)^{d/2}} \exp \left[ -\frac{(\mathbf{r}_F - \mathbf{r}_I)^2}{2Dt} \right], \end{aligned} \quad (7)$$

where  $D = v^2\tau/d$  denotes the bare classical diffusion constant. This equation predicts diffusive long time relaxation, as one would expect on the basis of the close analogy between the diagram of Fig. 9 (a) and the pair-correlated scattering paths shown in Fig. 6, bottom. Within the context of diagrammatic perturbation theory, a process like Fig. 9 (a) is known as a **soft mode**. The origin of the phrase can be understood by representing the diagram in frequency/momentum space. Fourier transformation of Eq. (7) obtains the result  $\Pi_D(\mathbf{q}, \Omega) = (-i\Omega + \hbar Dq^2)^{-1}$ , where  $\mathbf{q}$  and  $\Omega$  are conjugate to  $\mathbf{r}_I - \mathbf{r}_F$  and  $t$ , respectively. Notice that  $\Pi_D$  diverges in the limit of small  $\mathbf{q}$  (large length scales) and  $\Omega$  (large time scales) which is symptomatic for an effective theory with low, or soft excitations. In the mesoscopic literature, the mode  $\Pi_D$  is known as the **Diffuson**.

Notice, however, that so far the analysis accounted only for a very restrictive set of diagrams contributing to the series expansion of the pair Green function: not only did the scattering events occur in a pairwise correlated manner, they were also ordered in a highly regular, ‘ladder’ type sequence. (c.f. the ‘irregular’ contribution shown in Fig. 9 (b) that also contributes to the two particle Green function.) Why is the ladder contribution more relevant than generic processes? The point is that we are interested in computing contributions to the pair Green function with low phase mismatch. To fulfill this condition the two Green functions constituting the pair propagator must run ‘in parallel’, so that the two dynamical quantum phases picked up during the propagation through the medium largely cancel out. Re-interpreting a diagram like Fig. 9 (b) in terms of real space scattering paths, it is clear that the phase cancellation condition is not fulfilled. For a more rigorous formulation, see section ID.

However, is the diagram shown in Fig. 9 (a) the only one with small phase mismatch? Indeed, there is one more process of relevance, viz. Fig. 9 (c). From the topology of this diagram, it should be clear that it describes propagation of two Green functions through the same scattering path, albeit in reversed direction. That such processes might play a role in phase coherent transport can be seen in Fig. 10. The origin of the relevancy of this contribution is that, in the absence of time reversal symmetry breaking perturbations, the quantum phase picked up during propagation through any one path equals the phase of propagation in reversed direction. This symmetry gives rise to a second soft mode, the so-called **Cooperon**,  $\Pi_C(\mathbf{q}, \Omega) = (-i\Omega + \hbar Dq^2)^{-1}$ . (Technically, this results obtains from summation over all diagrams of the type Fig. 9 (b) [c.f. section ID]). Contrary to the Diffuson, which basically represents the quantum descriptor of classical diffusive motion, the Cooperon does not have a classical counterpart; its existence essentially hinges on the fact that the fundamental object of quantum dynamics is amplitudes, not densities. The name ‘Cooperon’ derives from the strong analogy to Cooper pair propagation in the theory of superconductivity, a point we will discuss in more detail below.

Quantitative evaluation of the contribution of time reversed path propagation to the return probability  $\langle P(\mathbf{r}_F = \mathbf{r}_I, \mathbf{r}_I; t) \rangle$  gives

$$\langle P(\mathbf{r}_F = \mathbf{r}_I, \mathbf{r}_I; t) \rangle = 2 \times \sum_i \langle A_i^2 \rangle,$$

i.e. the coherent superposition of a path  $i$  with its time-reversed counterpart  $j \equiv \bar{i}$  leads to doubling of the classical result.

What happens to the Diffuson and Cooperon modes in cases where time reversal invariance is broken, e.g. through the application of a magnetic field. Under such conditions the parity between Diffuson and Cooperon gets lost: while the former remains invariant, the latter

assumes the form (for the calculation see, e.g., [15])

$$\Pi_C(\mathbf{q}, \Omega) = \frac{1}{L^d} \frac{1}{2\pi\nu\tau^2} \frac{1}{D(\mathbf{q} - e\mathbf{A}/\hbar c)^2 - i\Omega},$$

where  $\mathbf{A}$  is the vector potential representing the time reversal breaking perturbation. Notice that the Cooperon denominator no longer diverges in the limit  $(\mathbf{q}, \Omega) \rightarrow (0, 0)$ , i.e. the Cooperon is no longer a soft mode.

The structure of this result can be made plausible as follows: (for weak enough fields) classical diffusion of a particle is not affected which is why the Diffuson remains invariant. However, the Cooperon gets modified, the reason being that the quantum phases for propagation through a path in reversed order are no longer identical. The analytical structure of the perturbed Cooperon pole is largely dictated by gauge invariance; as with conventional quantum-mechanics a “covariant” combination like  $(\mathbf{q} - e\mathbf{A}/\hbar c)^2$  describes the minimal gauge invariant coupling of a vector potential.

Together, the Diffusion and Cooperon modes represents the fundamental “building blocks” out of which quantum coherence phenomena can be described. As a first example, we will identify the main quantum interference corrections to the classical conductivity.

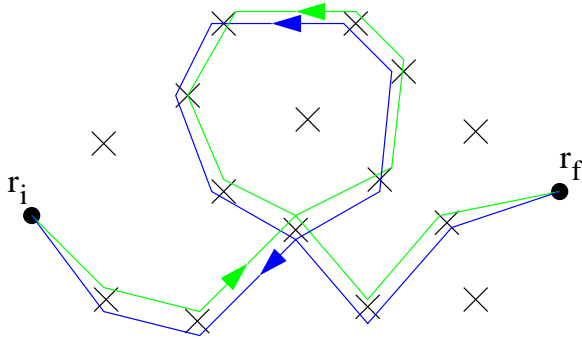


FIG. 10. Quantum phase coherent paths contributing to the transfer probability. Note that the constructive interference of a path with its time-reversed counterpart leads to an enhancement of the return probability which renormalizes down the diffusion constant.

### 1. Weak Localization

Applied to the transfer probability density, the phase coherent superposition of time-reversed paths (the Cooperon mode) provides the leading quantum correction to classical conductivity (see Fig. 10). The enhanced return probability has a tendency to “delay”, or “weakly localize” the particle, and has important implications for localization and transport properties. An estimate of the quantum correction to the diffusion constant can be obtained by evaluating the reduction in transfer probability along a diffusing path due to redundant excursions (see Fig. 11). Requiring that a returning path stays within

a wavelength of the outgoing path, an estimate for the relative change in the diffusion constant can be obtained by accounting for the return probability  $1/(Dt)^{d/2}$  at any point along the trajectory [16]

$$\begin{aligned} \frac{\delta D}{D} &= \frac{\delta P}{P} \simeq -v_F \lambda_F^{d-1} \int_{\tau}^{t_D} \frac{dt}{(Dt)^{d/2}} \\ &= -\frac{1}{\hbar\nu_d D} \frac{2}{2-d} (L^{2-d} - \ell^{2-d}). \end{aligned} \quad (8)$$

Here  $t_D = L^2/D$  denotes the typical diffusion time across a sample of size  $L^d$ , and  $\nu_d$  is the  $d$ -dimensional density of states (DoS).

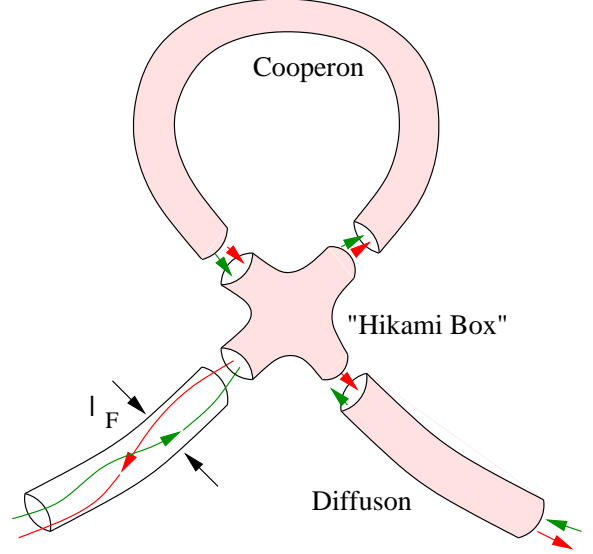


FIG. 11. The weak localization correction shown in Fig. 10 can be separated into a three stage process: two Diffuson ladders connected to a Cooperon ladder by a junction region known as an “Hikami box”. Here, the “tubular” representation of the soft modes emphasizes that the maximum real space resolution of the quantum propagation, as described by the two-particle Green function modes, is given by  $\lambda_F$ . Weak localization arises when the two Green functions constituting a diffuson mode split up to form a Cooperon mode (see Fig. 10.) Note that the magnitude of the correction is constrained by the condition to return to the same point in real space all with a resolution of the Fermi wavelength.

Applying the Einstein relation for the conductivity,  $\sigma = e^2\nu_d D$ , this estimate of the weak localization correction (8) is in accord with the diagrammatic calculation showing that, in two dimensions [17],

$$\delta\sigma = -\frac{e^2}{\pi^2\hbar} \ln\left(\frac{L}{\ell}\right). \quad (9)$$

This result resolves one of the puzzles presented by experiment: when subjected to a weak magnetic field, a given path no longer interferes constructively with its time-reversed counterpart. As a result, to leading order, the

conductivity is predicted to increase in agreement with the observed negative magneto-resistance measurements.

The long-ranged Diffuson and Cooperon modes provide the key elements from which a consistent diagrammatic theory of quantum coherence phenomena in disordered conductors can be assembled. Later, in section II, their existence will be used to motivate the existence of a low-energy quantum field theory of disordered conductors.

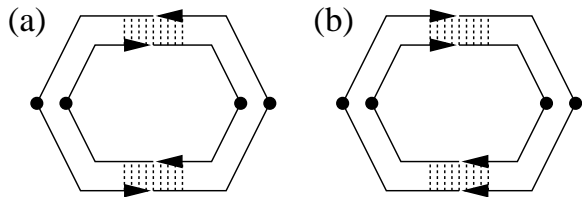


FIG. 12. Diagrammatic representation of the main phase coherent contributions to the fluctuations of the transfer probability density from (a) the diffuson channel, and (b) the Cooperon channel.

## 2. Fluctuations

While the random phase cancellation of different Feynman paths restricts the long-range contributions to the transfer probability density to classical diagonal contributions, their influence on *fluctuations* is substantial. In particular, phase coherent contributions to the quadratic fluctuations can arise from paths that are non-diagonal (see Fig. 12). More precisely, since  $\langle \cos^2(\varphi_i - \varphi_j) \rangle = 1/2$ , fluctuations of the probability density differ from the classical transfer probability by an amount

$$\langle (P(\mathbf{r}_F, \mathbf{r}_I; t) - \langle P(\mathbf{r}_F, \mathbf{r}_I; t) \rangle)^2 \rangle = 2 \sum_{i \neq j} \langle A_i^2 A_j^2 \rangle$$

Mechanisms of quantum interference between different Feynman trajectories induce fluctuations in the probability density which depend *non-locally* on the particular realization of the impurity potential. These fluctuations resolve a second puzzle concerning the existence of the characteristic magneto-fingerprint pattern observed in the conductance measurements: The phase accumulated by a closed Feynman path depends sensitively on the external magnetic field according to the relation

$$\varphi = \frac{e}{\hbar c} \oint \mathbf{A} \cdot d\mathbf{l} \equiv \frac{e}{\hbar c} \int \mathbf{H} \cdot d\mathbf{a}. \quad (10)$$

Thus, a change of magnetic field by an amount  $\phi_0/L^2$ , where  $\phi_0 = hc/e$  denotes the *magnetic flux quantum*, effectively changes the configuration space of the system which in turn induce reproducible, characteristic fluctuations of the conductance. Equivalently, defining the magnetic length  $L_H = \sqrt{\phi_0/H}$  as the typical length scale

over which phase coherence of Cooperon modes is maintained, we can estimate

$$\langle \delta G(0) \delta G(H) \rangle \sim \left( \frac{L_H}{L} \right)^d \left( \frac{e^2}{h} \right)^2.$$

Later we will find an explanation for the universality of the magnitude of the conductance fluctuations. However, before doing so, let us see how these ideas can be used to explain the nature of the Aharonov-Bohm oscillations.

FIG. 13. Schematic diagram showing the interference correction to a two-terminal conductance measurement of a device with the geometry of a ring. The second diagram shows a Cooperon correction from trajectories which circulate around the ring. The latter is responsible for the  $h/2e$  oscillations.

## 3. Aharonov-Bohm Oscillations

Both mechanisms of quantum interference shown in Figs. 11 and 12 are manifest in the transport properties of a metallic ring threaded by a magnetic flux,  $\phi$ . In the Aharonov-Bohm geometry (see Fig. 13) Feynman trajectories which pass anti-clockwise around the ring experience an additional phase shift relative to those that move clockwise. A contribution to the transfer probability or conductance which involves a pair of Feynman paths which traverse the ring in opposite directions will therefore experience an Aharonov-Bohm oscillation of period  $hc/e$ . Yet, such contributions add incoherently and do not appear in the ensemble average conductance. However, following on from our discussion above, phase coherent contributions to the fluctuations do survive. Altogether these results suggest a periodic modulation of the magneto-conductance fluctuations with a period set by the flux quantum  $\langle \delta G(0) \delta G(\varphi) \rangle \sim \cos(2\pi\phi/\phi_0)$ . These

fluctuations account for the  $\hbar c/e$  oscillations observed in the experiment.

The  $\hbar c/2e$  oscillations of the average conductance itself finds its origin in the mechanism of weak localization. In the Aharonov-Bohm geometry the application of a magnetic flux imparts a relative phase into the time-reversed paths encircling the ring (see Fig. 13). Here, each particle has to completely circumnavigate the ring once. As a result the average conductance itself is expected to exhibit oscillations periodic in  $\hbar c/2e$ . This effect, predicted by Altshuler and Aronov [18], was first observed by Sharvin and Sharvin [19].

#### 4. Energy Level Repulsion and Universality

Our considerations above were primarily concerned with understanding the influence of quantum phase coherence on the transport properties of mesoscopic systems. However, the same phase coherence phenomena are responsible for characteristic fluctuations in spectral properties. Although clearly there are no low-energy scale correlations between the energy levels belonging to completely different impurity configurations, within any given realization the eigenvalues are strongly correlated. An estimate of the degree of correlation can be established from the two-point correlator of DoS fluctuations,

$$R_2(\Omega) \equiv \Delta^2 \langle \nu(E + \Omega/2) \nu(E - \Omega/2) \rangle - 1, \quad (11)$$

where  $\nu(E) = \text{tr } \delta(E - \hat{H})$  denotes the DoS operator, and  $\Delta \equiv 1/L^d \nu$  denotes the average level spacing. (For convenience, here and throughout, the smooth average DoS is expressed as the shorthand,  $\nu \equiv \langle \nu(E) \rangle$ .)

To interpret the origin of the statistical correlations within the framework of interfering trajectories, we can exploit the identity connecting the Feynman propagator with the DoS. Defining the advanced Green function  $\hat{G}^- = [E - \hat{H} - i0]^{-1} \equiv (\hat{G}^+)^{\dagger}$ , the DoS is defined by

$$\nu(E) = \frac{1}{\pi} \text{tr } \text{Im } \hat{G}^-(E). \quad (12)$$

In this representation, the DoS is seen to be associated with the return probability of Feynman trajectories. As before, when subjected to an ensemble average, the long-time contributions to the DoS vanish due to the random phase cancellation of Feynman paths. Only the very short-time  $t \ll \tau$  trajectories, which give rise to a smooth part of the DoS survive.

However, as with the transfer probability, phase coherent long-time contributions to the fluctuations can be identified (see Fig. 14). The complete phase cancellation of Feynman trajectories is achieved by matching paths with two diffusion modes (c.f. the diagrammatic representation of the fluctuation correction.) Formally, the existence of long-range correlations arises from the exchange of two diffusion ladders between two closed loops, and gives the result [20]

$$R_2(\Omega) = \frac{1}{2\pi^2} \text{Re} \sum_{\mathbf{q}} \frac{\Delta^2}{(-i\Omega + \hbar D \mathbf{q}^2)^2}. \quad (13)$$

In systems invariant under time-reversal, a second mechanism arising from the exchange of Cooperon ladders is accounted by a further factor of two (see Fig. 14b).

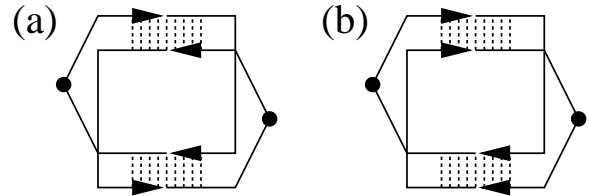


FIG. 14. Diagrams showing the leading contribution to the two-point auto-correlator of DoS fluctuations. The first diagram (a) represents the exchange of two diffusion ladders between two closed loops while the second denotes the exchange of two Cooperon ladders.

While this result shows that on energy scales  $\Omega$  in excess of the “Thouless energy” (i.e. the inverse transport time),

$$E_c \equiv \frac{\hbar}{t_D} = \frac{\hbar D}{L^2}, \quad (14)$$

level statistics depend explicitly on material properties such as geometry and morphology, on scales  $\Omega \ll E_c$ , the zero spatial diffusion mode  $\mathbf{q} = 0$  dominates, and

$$R_2(\Omega) \simeq -\frac{1}{2\pi^2} \left( \frac{\Delta}{\Omega} \right)^2. \quad (15)$$

In this limit fluctuations of the DoS are *universal*, independent of detailed properties of the system. In fact Eq. (15) is a manifestation of “rigidity” in the spectrum: taking  $N(\Omega)$  to be the number of levels inside a band of width  $\Omega$ , Eq. (15) shows fluctuations in  $N$  to increase only logarithmically with  $\Omega$ ,

$$\langle N^2(\Omega) \rangle_c \simeq \frac{1}{\pi^2} \ln \langle N \rangle. \quad (16)$$

This compares with a hypothetical random or Poisson distribution of energy levels in which fluctuations of  $N$  grow as  $\sqrt{\langle N \rangle}$ .

#### 5. Universal Conductance Fluctuations

Spectral rigidity (16) provides a simple physical interpretation of the characteristic scale of conductance fluctuations [21]: as we have seen, the bare conductance of a metallic sample of dimension  $L$  can be expressed through the Einstein relation (1) as a ratio of characteristic energy

scales,  $G = ge^2/\hbar$ , where  $g = E_c/\Delta$ ; i.e. the dimensionless conductance  $g$  is equivalent to the number of levels inside a window of energy  $E_c$ . Thus, while the average conductance  $\langle G \rangle = ge^2/\hbar$ , is large in a good metal ( $g \gg 1$ ), Eq. (16) implies that the characteristic scale of fluctuations,

$$\sqrt{\langle (\delta G)^2 \rangle_c} \sim O(e^2/\hbar),$$

is universal [11,12], independent of the average conductance, system size, etc. Spectral rigidity of the spectrum of the disordered quantum Hamiltonian therefore provides a natural way to understand the characteristic universal conductance fluctuations observed in experiment.

## 6. Breakdown of Perturbation Theory: RMT

The estimate for the spectral correlation function (15) also signals a warning concerning the domain of validity of the diagrammatic perturbation theory which will be of relevance in future. At energy scales  $\Omega \ll \Delta$ , or equivalently at time scales in excess of the inverse level spacing (known as the “Heisenberg time”),  $t \gg t_H = \hbar/\Delta$ , response functions obtained with diagrammatic perturbation theory show unphysical IR divergences. Taking into account contributions higher order in perturbation theory doesn’t help. Indeed, the strength of the divergence just becomes enhanced.

In fact, the validity of diagrammatic perturbation theory relies on two independent parameters: firstly, the disorder potential should be sufficiently weak that a quasi-classical approximation is valid (i.e.  $\lambda_F/\ell \ll 1$ ). Furthermore, the influence of quantum interference corrections should be small. More precisely, the validity of Eq. (13) relies on the further condition,

$$\left(\frac{\Delta}{E_c}\right)^{d/2} \left(\frac{\Delta}{\Omega}\right)^{(2-d)/2} \ll 1.$$

To understand the structure of this criterion, consider the first order quantum interference correction to the classical diffusion constant, (8). For any given value of the frequency  $\Omega$ , the self returning Cooperon mode can propagate for a time  $\sim \Omega^{-1}$  before phase coherence is lost. This means that for  $\Omega > t_D^{-1}$ , the upper limit in (8) must be replaced by  $\Omega^{-1}$ . Doing the integral and expressing all parameters in terms of  $\Delta$  and  $E_c$  we arrive at the criterion above.

In the *quantum regime* (i.e. where  $\Omega \lesssim \Delta$ ), this condition is not met. Here the intuition afforded by the diagrammatic picture breaks down.

In fact, the universality of the low-energy sector of the correlation function gives a clue to the true behavior in the quantum regime. On time scales in excess of  $t_D = L^2/D$ , the entire phase space of the system has been explored. In this “ergodic regime” spectral and transport properties of a quantum particle ought to become fully

universal, dependent only on (a) the fundamental symmetries of the system and (b) the total number,  $N$ , of energetically accessible states. Under these conditions (and with the benefit of a good deal of hindsight) one would expect the dynamics of the particle in a disordered environment to be indistinguishable from that of a “random matrix” Hamiltonian, i.e. an  $N$ -dimensional matrix  $H$  drawn from some distribution  $P(H)dH$  that is compatible with the symmetries of the system but otherwise maximally entropic.

In fact, Random Matrix Theory (RMT), as it has come to be known, provides a convenient way of modelling low energy regimes of disordered electronic systems. Temporarily restricting the discussion to ordinary normal metals (thereby excluding superconductors, relativistic Fermion systems and other less conventional species), three principal universality classes

$$P(H)dH \propto \exp \left[ -\frac{N\beta}{\lambda^2} \text{tr} H^2 \right] dH,$$

can be identified [22] according to whether the matrix  $H$  is constrained to be real symmetric ( $\beta = 1$ , *Orthogonal*), complex Hermitian ( $\beta = 2$ , *Unitary*), or real quaternion ( $\beta = 4$ , *Symplectic*). Hamiltonians invariant under time-reversal belong to the orthogonal ensemble, while those which are not belong to the unitary ensemble. Time-reversal invariant systems with half-integer spin and broken rotational symmetry belong to the third symplectic ensemble. (Later on we will see that an exhaustive description of the ergodic low energy phases of all stochastic quantum systems requires the introduction of seven more ensembles.)

Now, expressed in the basis of eigenstates  $H = U^\dagger \Lambda U$ , where  $\Lambda$  denotes the matrix of eigenvalues, the probability distribution can be recast in the form

$$P(H)dH = J(\{E_i\}) \exp \left[ -\frac{\beta N}{\lambda^2} \sum_i E_i^2 \right] \prod_l dE_l dU$$

where the invariant measure  $J(\{E_i\}) = \prod_{i < j} |E_i - E_j|^\beta$  reveals the characteristic repulsion of the energy levels. As with the disordered Hamiltonian, the rigidity of the complex eigenvalue spectrum is revealed in the two-point correlator of DoS fluctuations. In particular, applied to the unitary class of complex Hermitian matrices, to leading order in  $N$  random matrix analysis [23,24] reveals a universal (i.e. independent of the distribution) correlation function

$$R_2(\Omega) = 1 - \frac{\sin^2(\pi\Omega/\Delta)}{(\pi\Omega/\Delta)^2}. \quad (17)$$

This result, non-perturbative in  $\Delta/\Omega$ , interpolates smoothly onto the result of Eq. (13) if we set  $\sin^2(\pi\Omega/\Delta) \rightarrow 1/2$ .

In fact, the connection between RMT and the long-time or low-energy properties of disordered conductors is even more robust extending to statistical properties of the wavefunctions themselves.

To close this section on coherence effects in non-interacting disordered systems, let us return to the phenomena of weak localization. Previously, we saw that the constructive interference of time-reversed paths gave rise to a quantum correction to the conductivity which was interpreted as the renormalization of the classical diffusion constant to a lower value. This invites the question, how does the accumulation of quantum interference corrections finally affect the transport in a disordered environment.

This question finds its origin in the pioneering work by Anderson in a seminal paper entitled “The absence of diffusion in certain random lattices” [25]. Based on the consideration of a simple random “tight-binding” Hamiltonian, Anderson proposed that, above a certain critical strength of the disorder potential, there is a qualitative change in the nature of the electronic wavefunction in which its envelope becomes exponentially localized.

Here a distinction should be drawn between qualitatively different mechanisms of localization. Evidently, the lowest energy states in a disordered system will be dictated by “optimal fluctuations” of the random impurity potential. These “tail states” can be interpreted as “bound states” localized in regions where the potential is unusually low and uniform [26,27]. Instead, here we are interested in the localization properties of states with energies greatly in excess of the typical magnitude of the impurity potential, i.e.  $E_F\tau \gg 1$ . Here, the mechanism of localization can derive only from the accumulation of subtle interference corrections.

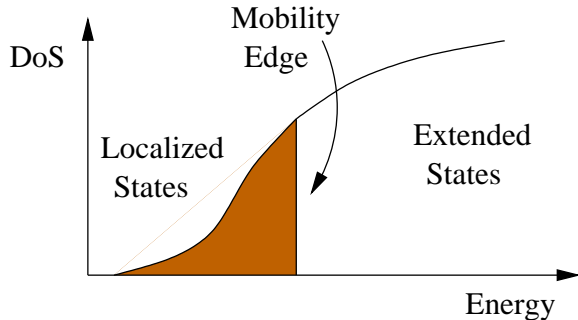


FIG. 15. Schematic diagram showing the typical variation of the DoS with energy. A mobility edge separates regions of extended and localized states.

According to its energy  $E$ , Anderson proposed that a given state is either extended or localized depending on the degree of disorder. Following an argument due to Mott, it is also plausible that extended and localized states at the same energy do not coexist — in such circumstances, the admixture of the former due to arbitrarily small perturbations would lead to the delocalization of the latter. Moreover, it is natural that states at the band edge are more susceptible to the formation of bound or

localized states. These considerations suggest a profile for the DoS in which the low-lying localized states are separated from higher-energy extended states by a **Mobility edge**. The transition signalled by the Mobility edge is known as the **Anderson transition**.

Since the pioneering work of Anderson, almost two decades past before a consistent theory of localization emerged. Its basis was a simple yet powerful scaling hypothesis which followed naturally from arguments of Thouless [28,29]. Building on this work, Abrahams, Anderson, Licciardello, and Ramakrishnan [30] proposed a *one-parameter scaling theory of localization* according to which the conductance of a system of size  $bL$ , where  $b$  is some dimensionless scaling parameter, is a function of  $g(L)$  only:

$$g(bL) = f_b(g(L)).$$

The important point is that  $f_b$  does not explicitly depend on the system size  $L$ . Independently of Thouless’s argument, this restriction can be made plausible by dimensional analysis: since  $g$  is dimensionless, the only way for the parameter  $L$  to appear in  $f$  is through a dimensionless ratio  $L/a$ . Here,  $a$  is some compensating scale of dimensionality ‘length’. This, however, would imply explicit dependence of the conductance on a microscopic reference scale which conflicts with the presumption of universal scaling behaviour. Differentiation of the scaling form with respect to  $b$  then obtains the Gell-Mann Low equation

$$\frac{d \ln g}{d \ln L} = \beta(g).$$

The scaling function  $\beta(g) \equiv f(g)/g$  is universal, independent of the microscopic properties of the sample, such as the bare microscopic conductance and  $\ell/\lambda_F$ . Reassuringly, this scaling picture fits neatly into the perturbative scheme of weak localization. In fact the weak localization correction (8) represents just the first term in a perturbative series which accumulate into a renormalization or scaling of the diffusion constant  $D$ .

The one-parameter scaling theory has profound consequences for the localization properties of disordered conductors. For an ohmic conductor, the scaling function takes a constant value  $\beta = d - 2$ , while deep in the insulating regime, where states are exponentially localized,  $\beta(g) \sim \ln g$  (i.e.  $g \sim e^{-L/\xi}$ ). A smooth interpolation between these limits (see Fig. 16) suggests that below two-dimensions all states are localized, while above there is a critical conductance,  $g_*$ , above which states are extended. The unstable fixed point is associated with the Anderson localization transition.

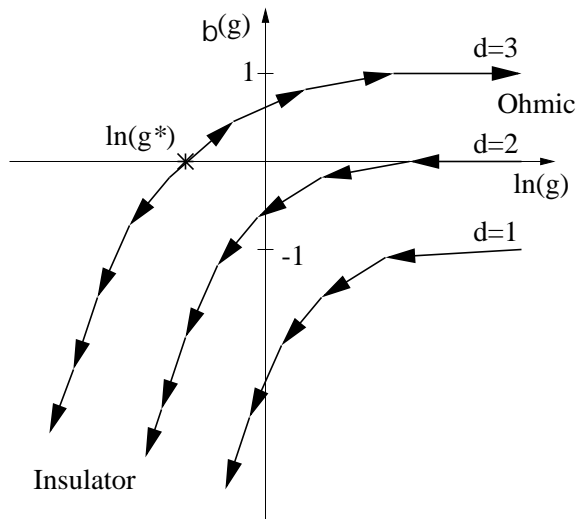


FIG. 16. Scaling function of the dimensionless conductance,  $\beta(g)$ , in dimensions  $d = 1, 2$  and  $3$ . At large values of the conductance, the scaling function approaches the asymptotic  $\beta(g) \rightarrow d-2$  corresponding to Ohmic behavior. For very small values of conductance, the scaling function approaches  $\beta(g) \rightarrow \ln(g)$  characteristic of insulating behavior. According to the weak localization expansion, a localization transition is predicted in dimensions *greater* than two.

The situation in two-dimensions is more delicate. Localization properties depend sensitively on the asymptotic approach of the  $\beta$  function to the metallic limit. However, taking the first quantum correction from Eq. (9), one obtains  $\beta(g) = -1/\pi^2 g$  which is consistent with localization of all states in two-dimensions. While the one-parameter scaling theory of localization has yet to find a truly rigorous mathematical proof, it nevertheless represents an important milestone in phenomenology. At the same time, trust in the phenomenology places important constraints on the theories of disordered materials.

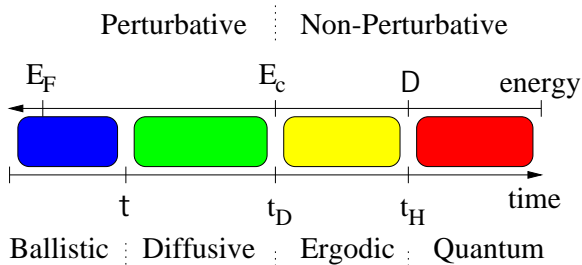


FIG. 17. Schematic diagram showing the relevant time and energy scales in disordered transport. Also shown is the regime over which properties can be treated within a perturbative framework.

This concludes our preliminary survey of the quantum interference phenomena which characterize mesoscopic structures. To summarize our findings, let us consider the influence of quantum interference processes on the dynamics of a spreading wavepacket in a background of weakly scattering random impurities. (Here we imagine a wavepacket whose spectral resolution is confined to a narrow interval (i.e.  $\Delta \ll E_{\text{width}} \ll \hbar/\tau$ ) around the Fermi level.) The fate of the wave package sensitively depends on whether the size of the host system is larger or smaller than the localization length. We begin by considering the latter case: absence of pronounced Anderson localization effects. The different regimes encountered by the diffusing particle are summarized in Fig. 17.

- ▷ **Ballistic Regime:** here, on time scales  $t < \tau$  a wavepacket spreads ballistically at the Fermi velocity. Within this regime, particle dynamics is largely insensitive to the impurity background.
- ▷ **Diffusive Regime:** one time scales  $\tau < t < t_D \equiv L^2/D$ , the quantum interference due to scattering off the background impurity potential leads to diffusive dynamics of the wavepacket. Within the Diffusive regime, quantum weak localization corrections renormalize the diffusion constant below the bare value. In dimensions  $d \leq 2$ , these quantum corrections accumulate, and ultimately lead to the complete localization of the wavepacket.
- ▷ **Ergodic Regime:** if the particle does not localize, or if the localization length is greatly in excess of the system size  $\xi \gg L$ , on time scales  $t > t_D \equiv L^2/D$  the wavepacket extends over the whole system. In this sense, the particle dynamics is said to be “ergodic”. Here the dynamics becomes universal, independent of the geometrical and material properties of the system. Spectral properties of the system become indistinguishable from those of random matrix ensembles.
- ▷ **Quantum Regime:** finally, on time scales  $t > t_H \equiv \hbar/\Delta$ , the particle enters a regime in which its properties are dictated by the universal properties associated with the resolution of individual levels. In particular, the rigidity of the spectrum cooperates to produce a “dynamical echo” of the wavepacket [31] (c.f. the dynamics of a wavepacket confined to an harmonic oscillator potential).

For a large system with  $L \gg \xi$ , the initial stages of the propagation process, ballistic and diffusive motion, are identical to those sketched above. However, the diffusive spreading of the particle is now limited by the localization length and not by the system size. On large time scales  $t > \xi^2/D$  the particle enters the analog of the

‘ergodic regime’, i.e. it has uniformly explored its accessible phase space. On still larger scales  $t > \Delta_\xi$ , where  $\Delta_\xi$  is the characteristic level spacing of a system of volume  $\xi^d$ , it enters the ‘quantum regime’. Many of the non-perturbative phenomena observed in the quantum regime of finite size systems carry over to the localized case. However, since neither  $\xi$  nor  $\Delta_\xi$  are sharply defined scales, the notorious level-spacing oscillatory behaviour displayed by finite size systems is not observed (see, e.g., Ref. [32] for a discussion of this point).

### C. Interaction Phenomena

Although, as we have seen, many of the characteristic mesoscopic phenomena can be satisfactorily understood within the framework of a non-interacting theory, the effects of Coulomb interaction give rise to a number of important manifestations in experiment, including charging effects, dephasing and various realizations of the Kondo effect. Indeed the slow dynamics of electrons in a disordered environment can lead to an enhancement of interaction effects. In this section, we will discuss several of the classic experiments in which interaction effects are important.

#### 1. Coulomb Blockade

Perhaps the most direct and simplest manifestation of Coulomb interaction in charge transport arises in measurements of the resonant conductance through almost closed quantum structures. Previously, we saw that in open dots, two-terminal conductance measurements showed characteristic mesoscopic fluctuations — magneto-fingerprints (see, e.g. Fig. 1). Suppose that a changing gate potential narrows the constriction to the dot so that the number of transverse quantum channels is diminished down to one open channel. When the constriction is narrowed even further, an incoming electron experiences a tunnel barrier. In this regime, one would expect charge transport to be limited to resonant transmission through the discrete energy levels of the device when the chemical potential of the leads matches the dot.

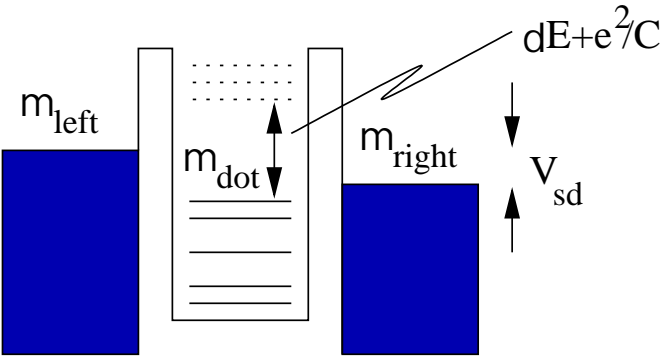


FIG. 18. Schematic diagram showing the condition for charge transfer through a quantum dot. The continuum of states in the reservoirs are filled up to the chemical potential  $\mu_{\text{left}}$  and  $\mu_{\text{right}}$  which are related by the external Source-Drain voltage  $V_{\text{sd}}$ . Discrete states of the zero-dimensional quantum dot are filled up to a chemical potential  $\mu_{\text{dot}}$ . Charge transfer is possible when the chemical potential  $\mu_{\text{dot}}$  lies between  $\mu_{\text{right}}$  and  $\mu_{\text{left}}$ .

Experimentally, resonant conductance peaks are observed as a function of the chemical potential (i.e. external gate voltage), but the separation of the peak spacing is typically controlled not by the single electron-energy level spacing of the dot  $\Delta$ , but rather by a more substantial charging energy incurred when an electron is transferred onto the dot. In the simplest approximation, the Coulomb interaction of the electrons on the device can be taken into account phenomenologically by including in the Hamiltonian a ‘‘classical’’ charging energy  $E_c(n) = n^2 e^2 / 2C$ , where  $C$  denotes the capacitance. According to this ‘‘orthodox model’’, charge transfer is forbidden unless the excess charging energy vanishes,

$$(E_c(n+1) - (n+1)eV_g) - (E_c(n) - eV_g n) = 0,$$

where  $V_g$  is a gate potential controlling the chemical potential of the dot. This condition under which charge transfer is allowed is met when  $V_g = (n + 1/2)e^2/C$ . Away from this value charge transfer is strongly suppressed — the ‘‘Coulomb blockade’’ [33,34]. (For a review see, e.g., Refs. [35–38].)

Despite its simplicity, the orthodox model of the Coulomb blockade gives a good qualitative explanation of experiment. Fig. 19 shows the resonant conductance measurements of a ballistic GaAs quantum dot. These results show resonant conductance peaks separated by a uniform energy scale reflecting the charging energy  $e^2/2C$  of device. Fluctuations in the height of the peaks can be ascribed to mesoscopic fluctuations of the wavefunction amplitude at the contacts [39] (although their correlation from one peak to another is harder to explain).

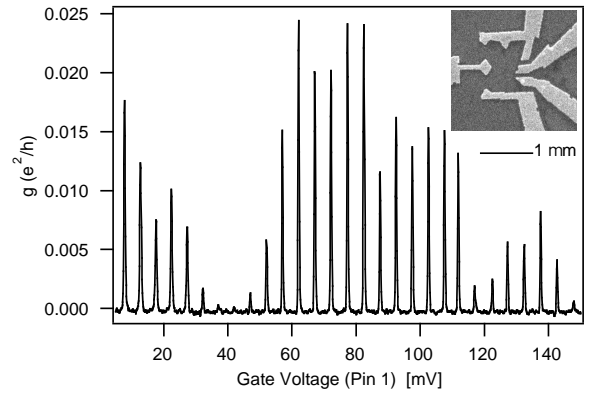


FIG. 19. Resonant tunneling conductance of a ballistic quantum dot (with the geometry as shown inset) courtesy of Ref. [13].



Coulomb blockade oscillations are usually periodic in the charging energy. However, in a dot containing a very small number of electrons, both the electron-electron interaction and the effects of confinement become sufficiently strong that the spacings between the Coulomb blockade peaks becomes irregular. In such cases, the quantum dot behaves as an artificial atom showing “magic numbers” at which angular momentum states form a closed shell and electronic configurations are highly stable. Fig. 20 shows a grey-scale plot of the conductance as a function of gate and source-drain voltage of a device known as a vertical quantum dot [40]. At zero source-drain bias, the Coulomb blockade oscillations reveal stable configurations in which the total number of electrons on the dot are  $N = 2, 6$  and  $12$  (c.f. the “noble gas” configurations). At non-zero bias, features appear corresponding to the many-body electronic excitations in the dot.

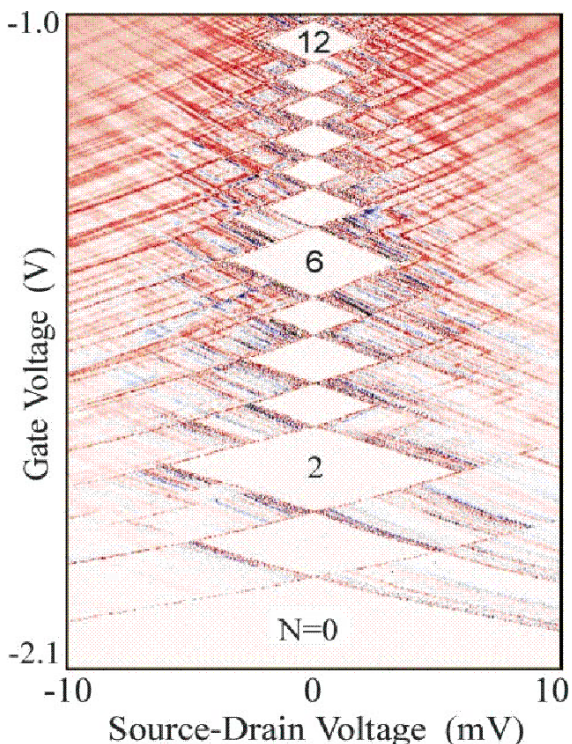


FIG. 20. Measurements of the conductance of a vertical quantum dot as a function of gate and source-drain voltage courtesy of Ref. [40].

Despite the apparent success of the orthodox theory, the agreement between theory and experiment reported in the early literature has, in recent years, been called into question. Correlation between the parametric dependences of the resonant peaks both as a function of changing gate voltage and magnetic field point at the existence of interaction effects which lie outside the orthodox scheme [41,42]. The continuing attempts to reconcile these effects with many-body theories of electron

interactions is the subject of on-going research.

## 2. Zero-Bias Anomaly

Surprisingly, an effect analogous to the Coulomb blockade described above occurs in the tunneling of a particle onto an *open* system (i.e. where the net charging energy vanishes). The transfer of an electron onto a metal involves two steps: traversing the barrier, followed by spreading within the metal. Typically the traversal time is much shorter than the relaxation time in the electron liquid. Accordingly, it is legitimate to separate tunneling into a single-electron, and a many-electron process. At small bias voltages, the first contribution, which is described by the transmission coefficient of the barrier, can typically be taken as constant. The second process by which the electron is accommodated on the device, involves the collective motion of a large number of electrons. At low bias voltages, the second collective effect may dominate the tunneling rate.

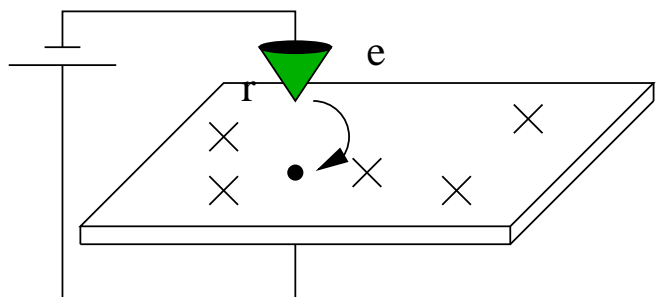


FIG. 21. Schematic diagram showing the geometry for the measurement of the tunneling conductance of a disordered metallic conductor.

The effect of charge relaxation on the tunneling rate has a simple qualitative interpretation. Following the discussion of Ref. [43], let us consider a situation when at small bias voltages, one electron is transferred across a tunnel barrier into a disordered conductor. Since the traversal time is typically much shorter than the relaxation time in the metal, while the electron traverses the barrier, other electrons practically do not move. Thus instantly, a large electrostatic potential is established, both due to the tunneling electron itself, and due to the screening hole left behind. The jump in electrostatic energy by an amount much bigger than the bias  $eV$  means that immediately after the one electron transfer, the system is found to be in a classically forbidden state under the Coulomb barrier. In order to accomplish tunneling, the charge yet has to spread over a large area, so that the potential of the charge fluctuation is reduced below  $eV$ . If the conductivity is finite, the spreading over large distances takes a long time, and thus the cooperative under-barrier action is much bigger than  $\hbar$ .

Taking the effective Coulomb interaction to be short-

anged, a crude estimate of the excess charging energy suggests  $E_{\text{Coulomb}}(t) \sim \lambda \int d\mathbf{r} \rho(\mathbf{r}, t)^2$  where  $\lambda$  denotes the interaction constant. If the charge relaxation is diffusive, the charge is distributed approximately uniformly over a radius  $r(t) \sim (Dt)^{1/2}$  (i.e.  $\rho(\mathbf{r}, t) = 1/r(t)^d$ ). With this assumption, we obtain the following estimate for the excess action,

$$S_{\text{int}} \sim \int_{\tau}^{1/eV} dt E_{\text{Coulomb}} \sim \lambda \int_{\tau}^{1/eV} \frac{v_F dt}{k_F^{d-1}} \frac{1}{(Dt)^{d/2}}. \quad (18)$$

Applied to the tunneling conductance,  $\delta G(V)/G \sim \delta \nu(V)/\nu \sim \exp[-S_{\text{int}}/\hbar]$  implying, for example, a logarithmic suppression of the tunneling DoS in two-dimensions, and a square root singularity in three [44].

Transport properties such as the conductivity and magneto-resistance are also affected by interaction. For example, if  $k_B T > E_c$ , the interaction correction to the conductivity is given by

$$\delta \sigma(T) \sim \begin{cases} \sqrt{T} & d = 3 \\ \ln T & d = 2, \end{cases}$$

and competes directly with the localization corrections.

### 3. Inelastic Scattering Rate and Dephazing

A second important manifestation of Coulomb interaction is through the phenomena of inelastic energy relaxation and dephazing. As a warmup to our discussion of electronic interactions in dirty media, let us recapitulate the concept of the quasi-particle lifetime in the theory of the Fermi liquid.

Consider an electron with some energy  $\epsilon > 0$  at zero temperature. (In this section, all energies are measured from the Fermi energy.) Energy relaxation occurs through interaction with a partner electron of energy

$\epsilon' < 0$  (see Fig. 22). For large initial energies, processes of this type will lead to a rapid creation of a cascade of particle-hole excitations and, thereby, to a swift decay of the single particle spectral weight into a many body continuum. However, at small energies, energy/momentum conservation, and the conditions imposed by the Pauli exclusion principle impose tight phase space restrictions on the scattering process; for asymptotically small excitation energies, the quasi-particle becomes stable.

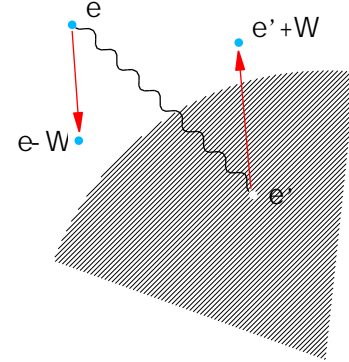


FIG. 22. Schematic illustration of the scattering process underlying the inelastic relaxation rate. An electron with energy  $\epsilon > 0$  transfers energy  $\Omega$  to an electron with energy  $\epsilon' < 0$ . The phase space accessible to the scattering process is limited by the condition of energy and momentum conservation, and by the Pauli exclusion principle.

To get a quantitative estimate for the quasi-particle life time, one can compute the inelastic scattering rate  $1/\tau_{ee}(\epsilon)$  within a “Golden rule” approximation. At zero temperature, the result reads (c.f., e.g., [45])

$$\frac{\hbar}{\tau_{ee}(\epsilon)} \sim \int_0^\epsilon d\Omega \int_{-\Omega}^0 d\epsilon' \langle \mathbf{p} | \hat{U} | \mathbf{p} - \mathbf{q} \rangle \langle \mathbf{p}' + \mathbf{q} | \hat{U} | \mathbf{p}' \rangle \delta(\epsilon - \zeta_{\mathbf{p}}) \delta(\epsilon' - \zeta_{\mathbf{p}'}) \delta(\epsilon - \Omega - \zeta_{\mathbf{p}-\mathbf{q}}) \delta(\epsilon' + \Omega - \zeta_{\mathbf{p}'+\mathbf{q}}),$$

where  $\zeta_{\mathbf{p}} \equiv \mathbf{p}^2/2m - E_F$ . Defining the Fourier components of the screened Coulomb interaction  $U_{\mathbf{q}} = 4\pi e^2/(\mathbf{q}^2 + \kappa^2)$  where  $\kappa^{-1}$  represents the screening length, the scattering rate takes the form

$$\begin{aligned} \frac{\hbar}{\tau_{ee}(\epsilon)} &\sim \int_0^\epsilon \Omega d\Omega \int q^{d-1} dq \frac{|U_{\mathbf{q}}|^2}{(qv_F)^2} \\ &\sim \begin{cases} \epsilon^2/E_F & d = 3 \\ \epsilon^2 \ln(\epsilon)/E_F & d = 2. \end{cases} \end{aligned}$$

Here the parameter  $1/qv_F$  can be identified with the typical time scale on which two electrons stay within a radius  $1/q$  and interact.

How do these results change in the presence of disorder? Curiously, several decades of application of Fermi

liquid theory to dirty electron systems passed before this obvious question was seriously addressed for the first time [44]. Yet (albeit with the benefit of hindsight), one should expect the result for the relaxation rate to undergo *qualitative* changes once disorder is present. The reason is that in a disordered medium the relevant time scale to be associated with a characteristic momentum  $q$  is not  $1/qv_F$  but rather the diffusive scale  $\text{Re}[(1/(i\Omega + \hbar D \mathbf{q}^2))]$ . I.e. instead of moving ballistically, the electrons *diffuse* through the interaction zone. It is intuitively clear, that slowing down the kinematics of the particles will lead to an increase of the relaxation rate.

All this is born out of a microscopic calculation [44]. Taking into account the screening of the Coulomb interaction, the energy relaxation rate takes the form

$$\frac{1}{\tau_{ee}(\epsilon)} \propto \frac{\epsilon}{g(L_\epsilon)} \propto \frac{1}{\nu_d L_\epsilon^d}, \quad (19)$$

where  $L_\epsilon = (\hbar D/\epsilon)^{1/2}$  denotes the diffusion length and  $g(L_\epsilon) = \nu_d L_\epsilon^{d-2}$  is the conductance of a system of size  $L_\epsilon$ .

It is instructive to represent the scattering rate of a dirty system in the general “Golden rule form” [46],

$$\frac{1}{\tau_{ee}} = \int_0^\epsilon d\Omega \int_{-\Omega}^0 d\epsilon' M(L, \Omega, \epsilon, \epsilon') \rho(L), \quad (20)$$

where  $\rho(L)$  is the total density of states and  $M(L, \Omega, \epsilon, \epsilon')$  some effective transition matrix element (that encapsulates the full information on the disorder dependent dynamics and on the effective Coulomb interaction.) Assuming that  $M \sim \Omega^x$  depends primarily on the energy *exchange* of the scattering process, we can do the integrals and obtain  $\tau_{ee}^{-1} \sim \epsilon^{x+2}$ . Comparison with (19) then leads to the identification  $x = -2 + d/2$ , i.e. the *effective* matrix element diverges for low energy transfer in dimensions  $d < 4$ ; somehow the disordered system favours *quasi-elastic* interactions processes with vanishingly small energy transfer.

As long as the interest is in ‘high energy’ physics, e.g. the relaxation rate of large energy electrons with  $\epsilon \gg T$ , the infrared singularity of the interaction matrix element is of no real concern. (It is over-compensated by the two extra integrations over  $\epsilon$  and  $\epsilon'$ .) However, it is imperative to ask whether there are circumstances where the low energy behaviour of  $M$  *does* play a role. Indeed, in the context of mesoscopic physics, one is often not so much interested in the dynamical aspects of the interaction process, but rather in the quantum phase decoherence induced by interactions. To understand what is meant by that, let us consider the propagation of a low-energy electron, with characteristic energy  $\epsilon \sim T$ . Suppose at time 0 our electron suffered an inelastic collision with small energy transfer  $\Omega$ . After time  $t$  the quantum phase of the electron will have picked up an extra contribution  $\sim t\Omega$ . If we wait only long enough,  $t \sim \Omega^{-1}$ , even arbitrarily small energy transfers can induce complete “de”phasing of the particle. Processes of this type limit the long range phase coherence in, e.g., weak localization measurements. To get an estimate for the **phase relaxation time**, i.e., the characteristic time scale after which phase coherence is lost due to quasi-elastic electron-electron scattering, we can follow the simple argument [46] (which can be substantiated by microscopic calculation [47]): at finite temperature  $T$ , our low energy electron propagates in the vicinity of a Fermi surface *softened* over a range of  $O(T)$ . The upper cutoff of the integration over  $\epsilon'$  in (20), i.e. the phase volume accessible to the scattered electron, is then set by  $T$ , instead of  $\Omega$ . Replacing in Eq. (19) one power of  $\epsilon$  for  $T$ , we find that  $1/\tau_\phi(\epsilon) \sim T/g(L_\epsilon)$ , where we have identified the quasi-elastic low energy collision rate  $\tau_\phi$  as the relevant time scale for dephazing. This estimate diverges at low energies and can, therefore, not

reflect the full truth. To improve the result, we have to remember that the  $\epsilon$ -powers in the denominator enter the result through  $L_\epsilon$ , i.e. the length scale over which *phase coherent* transport at time scale  $\epsilon^{-1}$  occurs. However, in the present context, phase coherence is limited by the very time scale  $\tau_\phi$ , we wish to compute, i.e. our formula must be replaced by the self consistency relation,

$$\frac{1}{\tau_\phi} \sim \frac{T}{g(L_{\tau_\phi^{-1}})}.$$

Solution of this equation obtains the power law  $\tau_\phi \sim T^{1/(2-d/2)}$ , i.e. a dephazing time that diverges in the low temperature limit.

In a sense, this result forms the basis for the entire field of mesoscopic physics: by cooling a system to ever lower temperature, the spatial extent over which phase coherence phenomena can be observed becomes arbitrarily large. At least in principle. In reality, there are other mechanisms limiting phase coherence, e.g. various types of noise emitted by the measurement apparatus.

This completes our superficial survey of just some of the manifestations of interaction in disordered metallic systems. It is largely included here as a salutary reminder that the experimental environment is often more complex than the models which will address in the following lectures. Indeed, in the majority of the remainder of the course we will neglect the influence of interaction altogether. We remark that there exists a number of reviews on the influence of interaction and disorder including Refs. [48–53].

## D. Impurity Diagram Technique

For completeness, as a footnote to this section, we include a more formal discussion of the “impurity diagram technique” [54,55]. Readers wishing to familiarize themselves on a deeper level with impurity diagrammatics are referred to the review [15]. Here we restrict ourselves to a concise outline of the main concepts that enter the approach. Our aim will be to find formal expressions for the ensemble average of the single-particle and two-particle Green function.

**Single-Particle Green Function:** The starting point of the diagrammatic perturbation theory is the series representation of the single particle Green function, Eq. (5) and its graphic representation Fig. 7 (before averaging) and Fig. 8 (after averaging). For simplicity we assume the scattering potential to be represented by the  $\delta$ - or ‘white noise-’ correlated distribution (6). Separate contributions to the ensemble average can be arranged into reducible and irreducible parts. Diagrams that can be split into two by cutting a single  $G_0$  line are called reducible (see, for example, the last diagram shown in Fig. 8.) Collecting together all the irreducible diagrams, the impurity averaged Green function can be written in the form of a *Dyson equation*

$$\langle \hat{G} \rangle = \hat{G}_0 + \hat{G}_0 \hat{\Sigma} \langle \hat{G} \rangle = \frac{1}{\hat{G}_0^{-1} - \hat{\Sigma}}, \quad (21)$$

where  $\hat{\Sigma}$  denotes the self-energy operator.

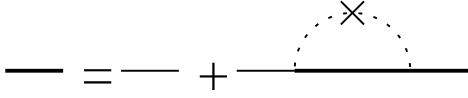


FIG. 23. Diagrammatic representation of the Dyson equation for the ensemble average of the single-particle Green function in the *self-consistent Born approximation (SCBA)*. Here the bold line represents the average Green function while the dotted line indicates a connection to an impurity scattering center represented by a cross. (Higher order contributions to the ensemble averaged Green function involve higher order corrections to the self-energy small in the quasi-classical parameter  $1/k_F\ell$ , where  $k_F = 2\pi/\lambda_F$  represents the Fermi wavevector of the incoming electron.)

An exact evaluation of all diagrams contributing to the self-energy is impossible. However, in the semi-classical limit  $1/k_F\ell \ll 1$ , diagrams with intersecting impurity lines (like, e.g., the fourth contribution to the right hand side of Fig. 8) become negligibly small. (See Ref. [45] for a discussion of this suppression mechanism.) The remaining set of diagrams is formally summed through the reduced Dyson equation displayed in Fig. 23. The self energy operator entering this equation, i.e. a full Green function under a potential contraction is given by

$$\Sigma^\pm(\mathbf{p}) = \int (d\mathbf{q}) V(\mathbf{q}) G^\pm(\mathbf{p} - \mathbf{q}; E \pm i0) V(-\mathbf{q}) =$$

$$P(\mathbf{q}, \Omega) = \int (d\mathbf{p}_1) \int (d\mathbf{p}_2) \int (d\mathbf{p}) \int dE G(\mathbf{p}_1, \mathbf{p} + \mathbf{q}/2; E + \Omega_+) G(\mathbf{p} - \mathbf{q}/2, \mathbf{p}_2; E - \Omega_+),$$

where  $\Omega_+ = \Omega + i0$ . Expanding the Green functions as a diagrammatic series in  $V$  and subjecting the product to an ensemble average, one can identify the dominant contribution as that arising from the connection of the Green function lines by a ladder series (see Fig. 24). More precisely, one finds that

$$\begin{aligned} & \langle G(\mathbf{p}_1, \mathbf{p} + \mathbf{q}/2; E + \Omega_+/2) G(\mathbf{p}_2, \mathbf{p} - \mathbf{q}/2; E - \Omega_+/2) \rangle_c \\ &= \bar{G}(\mathbf{p}_1; E + \Omega_+/2) \bar{G}(\mathbf{p} - \mathbf{q}/2; E - \Omega_+/2) \Pi_D(\mathbf{q}, \Omega) \bar{G}(\mathbf{p} + \mathbf{q}/2; E + \Omega_+/2) \bar{G}(\mathbf{p}_2; E - \Omega_+/2), \end{aligned}$$

where  $\bar{G}(\mathbf{p}; E \pm i0) = \langle G(\mathbf{p} - \mathbf{q}, \mathbf{q}_1; E \pm i0) \rangle = (E - \mathbf{p}^2/2m \pm i/2\tau)^{-1}$  represents the impurity average Green function, and

$$\Pi_D(\mathbf{q}, \Omega) = \frac{1}{2\pi\nu\tau} [1 + \Gamma(\mathbf{q}, \Omega) \Pi_D(\mathbf{q}, \Omega)], \quad \Gamma(\mathbf{q}, \Omega) = \int (d\mathbf{p}) \bar{G}(\mathbf{p} + \mathbf{q}/2, E + \Omega_+/2) \bar{G}(\mathbf{p} - \mathbf{q}/2, E - \Omega_+/2). \quad (23)$$

From this result we obtain  $\Pi_D(\mathbf{q}, \Omega) = (2\pi\nu\tau - \Gamma(\mathbf{q}, \Omega))^{-1}$ . For small  $\mathbf{q}$  and  $\Omega$ ,

$$\Gamma(\mathbf{q}, \Omega) \simeq 2\pi\nu\tau L^d (1 + i\Omega\tau - D\mathbf{q}^2\tau),$$

where  $D = v_F^2\tau/d$  denotes the classical diffusion constant. Altogether, we obtain the diffusion propagator,

$$\Pi_D(\mathbf{q}, \Omega) = \frac{1}{L^d} \frac{1}{2\pi\nu\tau^2} \frac{1}{D\mathbf{q}^2 - i\Omega}.$$

The Cooperon propagator  $\Pi_C$  is calculated in an analogous manner. Expressing the ladder of Fig. 9 (c) in momentum

$$= \frac{1}{2\pi\nu\tau} \int (d\mathbf{q}) G^\pm(\mathbf{p} - \mathbf{q}; E \pm i0),$$

where we have used the shorthand,  $(d\mathbf{q}) = d^d q/(2\pi)^d$ . In the literature, the approximation leading to this form of  $\Sigma$ , i.e. the omission of all diagrams with crossed lines, is referred to as the non-crossing approximation (NCA) or self-consistent Born approximation (SCBA). The real part of the self-energy simply leads to an irrelevant shift in energy, while the imaginary part is given by

$$\text{Im}\Sigma^\pm = \frac{1}{2\pi\nu\tau} \int (d\mathbf{p}) \text{Im}G_0(\mathbf{p}; E \pm i0) = \mp \frac{1}{2\tau}.$$

Substituting the self-energy into the expression for the impurity average Green function (21), we obtain the result

$$\langle G(\mathbf{p}; E_F - i0) \rangle = \frac{1}{E_F + \mathbf{p}^2/2m - i/2\tau} \quad (22)$$

showing that, in real space, the average Green function decays on the length scale of the mean-free path.

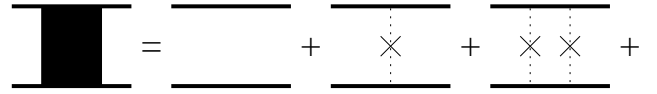


FIG. 24. Diagrammatic representation of the ladder series associated with the average two-particle Green function.

**Two-Particle Green Function:** The transfer probability density involved the two-particle Green function  $P(\mathbf{r}, 0; t) = |G(\mathbf{r}, 0; t)|^2$ . In Fourier space, the latter can be represented as

space, one again arrives at a recursion relation like (23). In the time reversal invariant case, the solution reads

$$\Pi_C(\mathbf{q}, \Omega) = \frac{1}{L^d} \frac{1}{2\pi\nu\tau^2} \frac{1}{D\mathbf{q}^2 - i\Omega},$$

as for the Diffuson. For the case of broken time reversal invariance, see Ref. [15].

Having laid the conceptual foundation for the description of mesoscopic phenomena it is now time to put flesh on these ideas by developing a formal theory. In the previous section, our terminology implied the existence of a diagrammatic perturbation theory whose validity depended on the quasi-classical parameter  $1/k_F\ell \ll 1$ . Indeed, within such an approach, a consistent theory of weak localization and coherence phenomena can be developed. However, the accumulation of quantum interference corrections within the framework of the one-parameter scaling theory, together with the appearance of IR divergences of the diagrammatic perturbation theory hints at the existence of a higher unifying scheme in which the diffusion modes of density relaxation are associated with soft modes of a quantum field theory.

In fact, the coherence properties of weakly disordered conductors can be described within the framework of a statistical field theory in which all the mesoscopic phenomena described in the previous section can be understood. Focusing on the properties of an “ $n$ -orbital” Hamiltonian, Wegner [56] established that the diffusion modes of the diagrammatic perturbation theory were associated with the soft modes of a functional non-linear  $\sigma$ -model. The renormalization properties of this statistical field theory are compatible with diagrammatic perturbation theory and the one-parameter scaling. Within this theory, the breakdown of perturbation theory is understood as a consequence of the proliferation of massless Goldstone modes associated with mechanisms of quantum interference.

With the benefit of hindsight, we can draw a formal analogy between the disordered conductor and the classical O(3) ferromagnet. The classical statistical mechanics of the ferromagnet is also represented by a non-linear  $\sigma$ -model, of the form

$$\mathcal{Z} = \int_{\mathbf{S}^2=1} \exp \left[ - \int K_{\text{sw}} (\partial \mathbf{S})^2 - \mathbf{H} \cdot \mathbf{S} \right], \quad (24)$$

where  $K_{\text{sw}}$  denotes the spin wave stiffness, and  $\mathbf{H}$  represents an external magnetic field. As with the disordered metal, the ferromagnet exhibits a branch of low-lying excitations describing spin wave modes,  $(K_{\text{sw}} \mathbf{q}^2 + H)^{-1}$ . If the magnetic field is strong, a controlled diagrammatic perturbation theory of the ferromagnet can be formally established. At the same time, the renormalization properties of the spin wave stiffness can be developed by studying the influence of spin-wave interactions. However, by diminishing the magnetic field, the spin wave modes become massless and perturbation theory breaks down. Associating the spin wave stiffness  $K_{\text{sw}}$  with the diffusion constant  $D$ , and the magnetic field  $H$  with the frequency scale of the two-particle response  $i\Omega$ , the analogy is complete.

The development of the quantum field theory of disordered conductors has a history dating back to the pioneering work of Wegner [56]. In the following, for reasons that will become clear, we will develop a more recent version of the field theory introduced by Efetov [57]. Our analysis will concentrate on establishing the fundamental principles behind the theory (often at the expense of technical detail). For a more comprehensive discussion the reader is referred to the existing reviews on the subject, particularly those by Efetov [58], and Weidenmüller, Verbaarschot and Zirnbauer [59] as well as the excellent and more modern expositions by Fyodorov [60] and Mirlin [61,62]. The material developed in this section will form the backbone for the remainder of the course.

### A. Derivation of the $\sigma$ -Model Action

As preparation for the formal analysis, we begin by presenting a rough outline of the derivation of the effective field theory. Previously we saw that spectral and transport properties can be expressed through the correlators of the Green function  $\hat{G}(E) = (E - \hat{H})^{-1}$ . The starting point of the field theoretic approach is the representation of the Green function (or rather their product) as a Gaussian functional field integral. When subjected to an ensemble average over configurations of the impurity potential, an interaction amongst the fields is generated. At this stage, a power series expansion of the action in the interaction can be assembled into the diagrammatic perturbation theory described qualitatively in section I. Instead, anticipating the existence of long-range diffusion modes, we will introduce a Hubbard-Stratonovich decoupling of the interaction where the auxiliary fields  $Q$  are associated with the soft modes of the theory.

Again, it is useful to draw a formal analogy, this time with the BCS theory of superconductivity. The quantum partition function of the bare BCS Hamiltonian, is also expressed in terms of an interacting quantum field theory. Anticipating the slow fields of the theory to be associated with the formation of the Cooper pair condensate, the interaction can be decoupled by a Hubbard-Stratonovich transformation involving the BCS order parameter,  $\Delta$ . When subjected to a saddle-point, or mean-field approximation, the action recovers the “Gap equation” for  $\Delta$ . Taking into account fluctuations around the saddle-point, a gradient expansion obtains the familiar Ginzburg-Landau theory. Neglecting the massive fluctuations of the amplitude of the order parameter, the massless phase fluctuations are described by an action of non-linear  $\sigma$ -model type.

In the present case, the saddle-point field configuration of  $Q$  is associated with the self-consistent Born approximation for the average single-particle Green function. As with the superconductor, subjecting the action to a gradient expansion in the vicinity of the saddle-point we

will in turn obtain a non-linear  $\sigma$ -model in which the low-lying modes represent the diffusion modes of the theory.

Finally, before we embark on this program, we should keep in mind that the Ginzburg-Landau theory of superconductivity found its origin in phenomenological considerations. The structure of the theory is fully constrained by the fundamental symmetries of the microscopic Hamiltonian. In principle, identifying the fundamental symmetries, one could legitimately apply the same line reasoning to develop the “Ginzburg-Landau theory” of the disordered conductor. However, for the

sake of clarity, we will stick to the more pedestrian route of presenting a formal derivation of the  $\sigma$ -model action.

### 1. Field Integral

Following the outline above our first task is to represent the Green function of the stochastic Hamiltonian (3) as a Gaussian functional field integral. Applied to the advanced function,

$$G^-(\mathbf{r}, \mathbf{r}'; E_F) \equiv \left\langle \mathbf{r}' \left| \frac{1}{E_F^- - \hat{H}} \right| \mathbf{r} \right\rangle \equiv \sum_{\nu} \frac{\psi_{\nu}(\mathbf{r}')^* \psi_{\nu}(\mathbf{r})}{E_F^- - E_{\nu}} = \frac{i}{\mathcal{Z}} \int D S S(\mathbf{r}) S^*(\mathbf{r}') e^{i \int S^* (\hat{H} - E_F^-) S}$$

where  $\mathcal{Z}[V]$  denotes the constant of normalization,  $E_F^- \equiv E_F - i0$ , and  $\hat{H}$  represents the Hamiltonian (3) of a single particle subject to a weak impurity potential. Here we have deliberately introduced the notation  $E_F$  for the energy to remind us that the *non-interacting* theory developed below is tailored to the consideration of large Fermi energy scales in the disordered electron gas. Applied to a single-particle Hamiltonian, one might wonder why it is necessary invoke a functional field integral as opposed to a Feynman path integral — indeed the latter formed the basis of our conceptual discussions in section I. In fact, while it is possible to reproduce the diagrammatic perturbation theory from ensemble averages of the Feynman path integral, for reasons that will become clear, a trajectory representation seems to be inappropriate as a vehicle to describe the soft modes.

Expressed in this form, the presence of the normalization factor  $\mathcal{Z}[V]$ , which depends explicitly on the impurity potential  $V$ , makes ensemble averaging difficult. The neglect of this dependence leads to unphysical vacuum loops when  $G^-$  is subjected to an ensemble average. To circumvent these difficulties, various “tricks” have been introduced in the literature. Originally conceived to study the classical spin glass, the “Replica Trick” [63,64] exploits the formal identity

$$\ln \mathcal{Z} = \lim_{n \rightarrow 0} \frac{\mathcal{Z}^n - 1}{n}, \quad (25)$$

to express ensemble averages. However, experience has shown considerable difficulty in correctly implementing the analytic continuation  $n \rightarrow 0$  in a way that respects the non-perturbative sector of the theory [65,66]. While very recent advances hint at a resolution of this problem within the framework of “replica symmetry breaking [67,68]”, fortunately, at least for systems which are non-interacting, a second and more reliable approach can be developed.

The “supersymmetry method” exploits properties of the Grassmann algebra to implement a scheme of “book-keeping”. In particular, expressed as a field integral over

two-component superfields  $\psi^T = (S, \chi)$ , the Green function can be expressed as

$$G^-(E_F) = i \int D \psi S S^* e^{i \int \psi^\dagger (\hat{H} - E_F^-) \psi}.$$

Here, exploiting the properties of Gaussian integrals over complex commuting or bosonic (B) variables,  $\int D S e^{-S^* M S/2} = \det M^{-1}$ , and anti-commuting or fermionic (F) variables,  $\int D \chi e^{-\bar{\chi} M \chi/2} = \det M$ , the normalization  $\mathcal{Z} = 1$  is assured. (A comprehensive introduction to superalgebra can be found in Ref. [69].)

A doubling of the field space, allows the representation of *two-point* correlators or response functions to be expressed. More precisely, the product of advanced (A) and retarded (R) Green functions can be expressed as

$$G^-(E_F - \Omega/2) G^+(E_F + \Omega/2) = - \int D \psi S_- S_-^* S_+ S_+^* e^{i \int \bar{\psi} (\hat{H} - E_F + \frac{\Omega^+}{2} \sigma_3^{\text{AR}}) \psi}$$

where  $\Omega^+ \equiv \Omega + i0$  denotes the frequency source, and the field integral involves four-component superfields

$$\psi = \begin{pmatrix} \psi_- \\ \psi_+ \end{pmatrix}_{\text{AR}}, \quad \psi_{\mp} = \begin{pmatrix} S_{\mp} \\ \chi_{\mp} \end{pmatrix}_{\text{BF}}.$$

Setting  $L = \sigma_3^{\text{AR}} \otimes E_{\text{BB}} + \mathbb{1}^{\text{AR}} \otimes E_{\text{FF}}$ , where  $E_{\text{BB}}$  and  $E_{\text{FF}}$  project onto the bosonic and fermionic sector respectively, the superfields have the property  $\bar{\psi} = \psi^\dagger L$ .

Pauli matrices  $\sigma_3^{\text{BF}}$  and  $\sigma_3^{\text{AR}}$  respectively break the symmetry between boson/fermion and advanced/retarded degrees of freedom. Convergence of the field integral determines the form of the metric  $L$  in the BB sector. While the choice in the fermionic sector seems arbitrary, a consideration of the saddle-point manifold of the  $\sigma$ -model determines the form above [59].

Finally, our preliminary discussion in the previous section classified two modes of density relaxation in the disordered metal, Diffusons and Cooperons. Both will be

identified in the analysis that follows. Accordingly, anticipating the structure of the saddle-point action, it is convenient to further double the field space to include complex or time-reversed components,

$$\Psi = \frac{1}{\sqrt{2}} \begin{pmatrix} \psi \\ \psi^* \end{pmatrix}.$$

The elements of the newly defined supervector  $\Psi$  are not independent, but fulfill the “time-reversal” symmetry relation

$$\Psi^\dagger = (C\Psi)^T,$$

where  $C = \sigma_1^{\text{TR}} \otimes E_{\text{BB}} + i\sigma_2^{\text{TR}} E_{\text{FF}}$ . Under the transformation  $\psi \mapsto \psi^*$ , the Hamiltonian maps to the time-reversed counterpart  $\hat{H} \mapsto \hat{H}^T$  ( $\equiv \hat{H}$  in the present time-reversal invariant case). In fact, any discrete symmetry of the microscopic Hamiltonian doubles the number of low-lying modes of density relaxation. In each case, it is convenient to double the field space [70].

Finally, instead of representing each vertex separately, it is often more convenient to introduce a “source term” into the effective action from which arbitrary correlators can be constructed,

$$\mathcal{Z}[J] = \int D\Psi e^{\int [i\Psi(\hat{H} - E_F + \frac{\Omega^+}{2}\sigma_3^{\text{AR}})\Psi + J\Psi + \bar{J}\Psi]}. \quad (26)$$

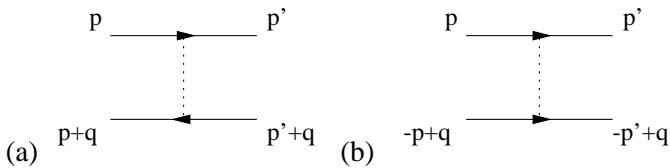
Here the sources  $\bar{J}$  and  $J$  obey the same symmetry properties as  $\bar{\Psi}$  and  $\Psi$ . Hereafter, for the sake of clarity, we will turn off the source (i.e.  $\mathcal{Z}[J=0]$ ), reinstating it only when essential.

## 2. Impurity Averaging

Expressed as a functional field integral involving superfields, the ensemble average over a Gaussian  $\delta$ -correlated impurity distribution

$$\int (\bar{\psi}\psi)^2 \approx \sum_{\mathbf{p}, \mathbf{p}'} \sum_{|\mathbf{q}| \ll \ell^{-1}} [(\bar{\psi}_{-\mathbf{p}'}\psi_{\mathbf{p}})(\bar{\psi}_{-\mathbf{p}-\mathbf{q}}\psi_{\mathbf{p}'+\mathbf{q}}) + (\bar{\psi}_{-\mathbf{p}'}\psi_{\mathbf{p}})(\bar{\psi}_{\mathbf{p}'-\mathbf{q}}\psi_{-\mathbf{p}+\mathbf{q}})]$$

where the first and second terms generate the contributions from the Diffuson and Cooperon respectively, and the summation over  $\mathbf{q}$  is limited to low momentum transfer. Both processes are represented diagrammatically in Fig. 25.



$$P(V)DV = \exp \left[ -\pi\nu\tau \int V^2 \right] DV$$

can be applied straightforwardly. (Here, and henceforth, we set  $\hbar = 1$ .) Applied to the generating function,

$$\langle \mathcal{Z}[J=0] \rangle = \int D\Psi e^{\int [i\bar{\Psi} \left( \frac{\hat{p}^2}{2m} - E_F + \frac{\Omega^+}{2}\sigma_3^{\text{AR}} \right) \Psi - \frac{1}{4\pi\nu\tau} (\bar{\Psi}\Psi)^2]}$$

where  $\langle \dots \rangle = \int (\dots) P(V)DV$  represents the ensemble average. In the absence of the symmetry breaking sources,  $\Omega$  and  $J$ , the total action is seen to be invariant under pseudo-unitary rotations of the fields in superspace,

$$\Psi \longrightarrow U\Psi, \quad U^\dagger L U = L, \quad U \in SU(2, 2|4).$$

At this stage, an expansion of the total action in powers of the field interaction can be assembled into a diagrammatic series expansion from which the *perturbative* results of section I can be established. However, anticipating the dominance of contributions arising from long-range fluctuations of the density, we will instead seek a mean-field decomposition of the action.

## 3. Hubbard-Stratonovich Decoupling

To establish a useful mean-field decoupling of the interaction requires the identification of the soft modes of the theory, i.e. those modes that arise from two-particle channels undergoing multiple scattering with the exchange of momenta smaller than the inverse of the elastic mean-free path,  $\ell = v\tau$ . The isolation of these modes is conveniently performed in the Fourier space. Applied to the interaction of the fields, the relevant contributions arise from the channels

FIG. 25. Diagrammatic representation of the terms in the Hubbard-Stratonovich decoupling that lead to (a) the diffusion mode, and (b) the Cooperon mode.

Introducing the Hubbard-Stratonovich decoupling

$$\exp \left[ -\int \frac{1}{4\pi\nu\tau} \text{str} (\Psi \otimes \bar{\Psi})^2 \right] = \int DQ \exp \left[ -\frac{1}{2\tau} \int (\bar{\Psi} Q \Psi - \frac{\pi\nu}{4} \text{str} Q^2) \right], \quad (27)$$

the contributions to the Diffuson and Cooperon degrees of freedom are accounted for by *slow* fluctuations of the  $8 \times 8$  supermatrix fields,  $Q$ . Here the supertrace oper-

ation is defined by  $\text{str}M = \text{tr}M_{\text{BB}} - \text{tr}M_{\text{FF}}$ . (Note that, as written, the Hubbard-Stratonovich transformation is not exact. If *all* degrees of freedom of  $Q$  (fast and slow) are taken into account, the decoupling (27) involves an over-counting by a factor of 2. This is because the saddle-point corresponding to the Cooperonic sector (i.e. those degrees of freedom which anti-commute with the symmetry breaking matrix  $\sigma_3^{\text{tr}}$ ) can be found in fast fluctuations of the diffuson sector, and *vice versa*.)

Finally, the symmetry properties of the dyadic product  $\Psi \otimes \bar{\Psi}$  are reflected in the symmetry properties of  $Q$  by the constraint

$$Q = CLQ^TLC^T, \quad (28)$$

where the transpose of a supermatrix is defined by

$$M^T = \begin{pmatrix} M_{\text{BB}}^T & M_{\text{FB}}^T \\ -M_{\text{BF}}^T & M_{\text{FF}}^T \end{pmatrix}.$$

Gaussian in the fields  $\Psi$ , the functional integral obtains

$$\langle \mathcal{Z}[0] \rangle = \int DQ \exp \left[ \int \text{str} \left( \frac{\pi\nu}{8\tau} Q^2 - \frac{1}{2} \ln \hat{G}^{-1} \right) \right],$$

where

$$\hat{G}^{-1} = \frac{\hat{\mathbf{p}}^2}{2m} - E_F + \frac{\Omega^+}{2} \sigma_3^{\text{AR}} + \frac{i}{2\tau} Q, \quad (29)$$

represents the supermatrix Green function. In summary, the problem of computing impurity averaged Green functions has been reduced to the consideration of the Euclidean field theory which depends on an  $8 \times 8$  supermatrix field  $Q$ .

#### 4. Saddle-Point Equation

Following the procedure outlined at the beginning of this section, we now subject the field integral to a saddle-point analysis. The legitimacy of such a mean-field decomposition is ensured by the symmetry properties of the Hubbard-Stratonovich fields which were chosen to reflect the soft modes of the disordered Hamiltonian. A variation of the action with respect to  $Q$  generates the saddle-point equation

$$Q_{\text{sp}}(\mathbf{r}) = \frac{i}{\pi\nu} \mathcal{G}(\mathbf{r}, \mathbf{r}). \quad (30)$$

Taking the symmetry breaking sources  $\Omega$  and  $J$  to be vanishingly small, and applying the ansatz that the saddle-point solution  $Q_{\text{sp}}$  is spatially constant, and diagonal in the internal indices, the saddle-point equation (30) takes the form

$$Q_{\text{sp}} = -\frac{i}{\pi\nu} \int d\mathbf{p} \left[ \frac{\mathbf{p}^2}{2m} - E_F + i0 + \frac{i}{2\tau} Q_{\text{sp}} \right]^{-1} = \frac{i}{\pi} \int d\xi \left[ E_F - \xi - \frac{i}{2\tau} Q_{\text{sp}} \right]^{-1}.$$

From this equation, one can attach to  $Q_{\text{sp}}$  the interpretation of the self-energy of the impurity averaged single-particle Green function. Performing the integral over  $\xi$ , we deduce that the elements of  $Q_{\text{sp}}$  take values of  $\pm 1$ . To choose the signs correctly, we note that the expression on the right-hand side of the saddle-point equation relates to the Green function for the disordered system in the self-consistent Born approximation. The disorder preserves the causal (i.e. advanced versus retarded) character of the Green function, therefore the signs of the diagonal elements of  $Q_{\text{sp}}$  must coincide with the sign of the imaginary part of the energy. This singles out the solution  $Q_{\text{sp}} = \sigma_3^{\text{AR}}$ .

In the limit  $\Omega \rightarrow 0$ , the action is invariant under the global transformations  $Q(\mathbf{r}) \mapsto TQ(\mathbf{r})T^{-1}$ , where  $T$  represent pseudo-unitary rotations that are constant in space and compatible with the symmetry properties of  $Q$  (28). This implies that the saddle-point solution spans the non-linear manifold  $Q_{\text{sp}}^2 = \mathbb{1}$  (i.e.  $Q_{\text{sp}} = T\sigma_3^{\text{AR}}T^{-1}$ ). Dividing out rotations that leave  $\sigma_3^{\text{AR}}$  invariant, the degeneracy of the manifold is specified by the coset space  $SU(2, 2|4)/SU(2|2) \otimes SU(2|2)$ .

Substituting  $Q_{\text{sp}}$  into Eq. (29), we obtain the following expression for the supermatrix Green function at the

saddle-point:

$$\mathcal{G}_{\text{sp}}(\mathbf{r}, \mathbf{r}') = -i\pi\nu f_d(|\mathbf{r} - \mathbf{r}'|) Q_{\text{sp}},$$

where defining  $G_0^-(\mathbf{r}) = \langle G^-(\mathbf{r}, 0) \rangle$ ,  $f_d$  denotes the ‘‘Friedel function’’

$$f_d(r) \equiv \frac{\text{Im}G_0^-(\mathbf{r})}{\text{Im}G_0^-(0)} = \Gamma(d/2) \left( \frac{2}{kr} \right)^{\frac{d}{2}-1} J_{\frac{d}{2}-1}(kr) e^{-\frac{r}{2\ell}},$$

which decays on a scale comparable to the mean free path.

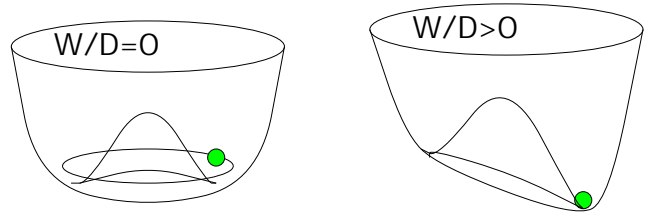




FIG. 26. Schematic diagram showing the structure of the saddle-point manifold. For  $\Omega/\Delta \gg 1$ , there is a unique saddle-point. As  $\Omega/\Delta \rightarrow 0$ , the saddle-point opens to span an entire manifold. Spatial fluctuations around the saddle-point can be classified into a massive and massless sector. The massive sector is controlled by the semi-classical parameter  $1/E_F\tau$ .

### 5. Gradient Expansion

In the semi-classical limit (i.e.  $1/E_F\tau \ll 1$  or, equivalently,  $1/k_F\ell \ll 1$ ) spatial fluctuations in the vicinity of the saddle-point manifold can be separated into a massive and massless sector (see Fig. 26). To leading order in the parameter  $1/E_F\tau$ , the massive fluctuations do not contribute to the low-energy effective action. Instead, we will focus on the low-energy spatial fluctuations which preserve the non-linear constraint  $Q(\mathbf{r})^2 = \mathbb{1}$ . Anticipating that the relevant field configurations  $T(\mathbf{r})$  fluctuate only slowly as a function of  $\mathbf{r}$ , it makes sense to separate the momentum operator into two parts,  $\hat{\mathbf{p}} = \mathbf{p} + \hat{\mathbf{q}}$ , where the operator  $\hat{\mathbf{q}} = -i\partial$  acts exclusively on the fields  $Q(\mathbf{r})$ , while the momenta  $\mathbf{p}$  are associated with the trace. Taking  $\hat{\mathbf{p}}^2/2m \simeq \mathbf{p}^2/2m + \mathbf{p} \cdot \hat{\mathbf{q}}/m$ , an expansion of the action yields

$$S[Q] = \frac{1}{2} \text{str}_{\mathbf{r}, \mathbf{p}} \ln \left[ G_0^{-1} - T^{-1} \left( i\Omega^+ \sigma_3^{\text{AR}} + \frac{1}{m} \mathbf{p} \cdot \hat{\mathbf{q}} \right) T \right]$$

where  $G_0^{-1}(\mathbf{p}) = E - \mathbf{p}^2/2m - i\sigma_3^{\text{AR}}/2\tau$ , and  $\text{str}_{\mathbf{r}, \mathbf{p}}$  denotes a trace over internal indices, and the phase space coordinates.

Taking  $1/E_F\tau \ll 1$  and  $\Delta\tau \ll 1$  an expansion in the ‘slow’ operators  $\hat{\mathbf{q}}$  to lowest non-vanishing order obtains

$$S[Q] \simeq \frac{1}{2} \text{str}_{\mathbf{r}, \mathbf{p}} \left[ G_0 T^{-1} i\Omega^+ \sigma_3^{\text{AR}} T + \frac{1}{2} \left( G_0 T^{-1} \frac{\mathbf{p} \cdot \hat{\mathbf{q}}}{m} T \right)^2 \right].$$

(Note that the term linear in the fast momenta  $\mathbf{p}$  vanishes under the trace.)

To prepare for the tracing out of the fast momenta, we first formulate some useful identities involving the bare average Green function  $G_0$ . All the relations below can be proved straightforwardly by explicitly performing the momentum integrations and using some Pauli-matrix identities.

- ▷ Firstly, in the momentum representation, the Green function can be presented as

$$G_0(\mathbf{p}) = \frac{1}{2} \sum_{s=\pm 1} \frac{1 + s\sigma_3^{\text{AR}}}{E_F - \mathbf{p}^2/2m + is/2\tau}.$$

- ▷ In this form, the trace over internal momentum variables obtains:

$$\int (d\mathbf{p}) G_0(\mathbf{p}) = \text{const.} \times \mathbb{1}^{\text{AR}} - i\pi\nu\sigma_3^{\text{AR}}$$

- ▷ Finally, if operators  $\hat{\mathbf{A}}$  and  $\hat{\mathbf{B}}$  vary slowly in space, then

$$\begin{aligned} & \int (d\mathbf{p}) \text{str} \left[ G_0(\mathbf{p}) \mathbf{p} \cdot \hat{\mathbf{A}} G_0(\mathbf{p}) \mathbf{p} \cdot \hat{\mathbf{B}} \right] \\ &= \frac{m^2}{4} 2\pi D\nu \sum_s \text{str} \left[ (1 + s\sigma_3^{\text{AR}}) \hat{\mathbf{A}} \cdot (1 - s\sigma_3^{\text{AR}}) \hat{\mathbf{B}} \right]. \end{aligned}$$

A straightforward application of these identities to the effective action above leads to the non-linear  $\sigma$ -model action,

$$S[Q] = -\frac{\pi\nu}{8} \int \text{str} \left[ D(\partial Q)^2 + 2i\Omega^+ \sigma_3^{\text{AR}} Q \right]. \quad (31)$$

We have thus succeeded in expressing the average two-particle properties of weakly disordered metallic grains in the form of a functional supersymmetric non-linear  $\sigma$ -model. (Note that the generalization of this formalism to account for higher-point response functions follows straightforwardly.) The derivation of the effective action relies only on the integrity of the semi-classical parameter  $1/E_F\tau$  (c.f. the discussion of section I B 6).

### 6. Magnetic Field

An extension of the present theory to include an external magnetic field introduces a magnetic vector potential into the action,

$$\mathcal{Z}[J=0] = e^i \int \Psi \left[ \frac{1}{2m} \left( \hat{\mathbf{p}} - \frac{e}{c} \sigma_3^{\text{TR}} \mathbf{A} \right)^2 + V - E_F + \frac{\Omega^+}{2} \sigma_3^{\text{AR}} \right] \Psi.$$

The magnetic field breaks time-reversal symmetry and couples to the symmetry breaking matrix  $\sigma_3^{\text{TR}}$ . Treating the magnetic field as a *weak* perturbation (see below), and proceeding as before (i.e. setting  $\hat{\mathbf{q}} \equiv -i\partial - (e/c)\sigma_3^{\text{TR}}\mathbf{A}$ ), it is straightforward to show that the effective action takes the same form as Eq. (31), but where the derivative is replaced by a covariant derivative involving the magnetic vector potential,  $\partial \mapsto \tilde{\partial} \equiv \partial - i(e/c)\mathbf{A}[\sigma_3^{\text{TR}}, \ ]$ .

According to this result, the degrees of freedom of  $Q$  which commute with  $\sigma_3^{\text{TR}}$  remain unperturbed by a *weak* magnetic field, while those degrees of freedom that do not commute acquire a mass. The former denote the diffuson modes while the latter represent the field sensitive Cooperon modes (recall the phenomenological discussion of section I). For strong enough magnetic fields, the influence of the Cooperon modes become negligible and can be neglected. Note that the Cooperon degrees of freedom are coupled to an effective charge of  $2e$  reflecting the two-particle nature of the mode.

The influence of magnetic fields on the phase coherence properties of disordered conductors appears at minute

fields (ca. one flux quantum through the system.) However, if the magnetic length  $L_B = (\phi_0/B)^{1/2}$ , equal to the cyclotron radius, becomes comparable to the mean-free path  $\ell$ , the influence of *orbital* effects becomes significant. In this case we enter the **quantum Hall regime**, a limit to which we will return in section III. For simplicity we will postpone the consideration of this regime and focus on the limit of weak or zero field.

## B. Applications of the $\sigma$ -Model

Having established the basis of the statistical field theory, how can the phenomenology of disordered conductors be recovered. In the twenty years since its construction, the  $\sigma$ -model action has been subject of numerous investigations. In the following we will briefly review just a few of the principle applications from which connections to the conceptual discussions of section I can be drawn.

### 1. Perturbation Theory

To help digest the form of the effective action it is useful to establish contact between the field integral and the phenomenology of the diagrammatic perturbation theory. To do so, we focus on the short-time dynamics limiting our considerations to frequency scales  $\Omega$  large as compared to the inverse transport or diffusion time  $E_c = D/L^2$  — i.e. the diffusive regime. In this case, the functional integral is dominated by field configurations of  $Q(\mathbf{r})$  which deviate little from the global saddle-point,  $\sigma_3^{\text{AR}}$ . (c.f. the spin wave expansion of the ferromagnet.)

With the parameterization  $T = e^{-W/2}$ , where the generators obey the constraint  $[W, \sigma_3^{\text{AR}}]_+ = 0$ , an expansion of the effective action obtains

$$S_0[W] = -\frac{\pi\nu}{8} \int \text{str} W \hat{\Pi}^{-1} W + O(W^4),$$

where  $\hat{\Pi}^{-1} = -D\partial^2 + i\Omega^+$ . As anticipated, the slow modes of density relaxation are associated with diffusion modes. More precisely, the components of  $W$  which commute with  $\sigma_3^{\text{AR}}$  represent the diffuson modes while those which do not acquire a mass in the presence of a weak magnetic field, and represent the Cooperon modes. At zero magnetic field, both are controlled by the same propagator. Corrections to the action higher order in  $W$  induced by the non-linear constraint  $Q^2 = \mathbb{1}$  describe interactions of the diffusion modes, and reflect different mechanisms of quantum interference.

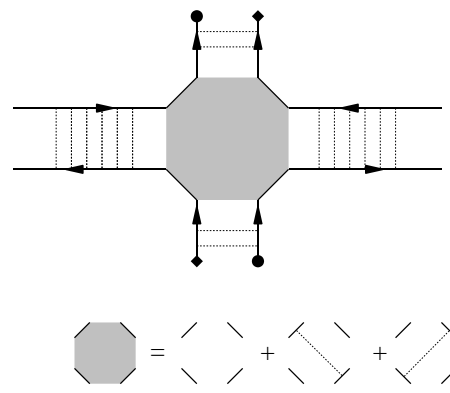


FIG. 27. Diagram contributing to the weak localization correction to the diffusion constant at one loop. The two diamonds should be imagined as connected by a Green function line, the same for the two circles. The shaded area represents the Hikami box, i.e. the sum of the three single impurity insertions indicated at the bottom of the figure.

### 2. Weak Localization, Scaling and the RG

As with the  $O(3)$   $\sigma$ -model for the ferromagnet, the action (31) can be subjected to a  $2 + \epsilon$  perturbative renormalization group analysis. Separating slow from fast degrees of freedom, an application of the momentum shell RG to one loop order obtains the renormalization,

$$D \mapsto D' = D \left[ 1 - \frac{(2 - \beta)}{\pi\nu} \Pi(0, 0) \right],$$

where  $\beta = 1$  or  $2$  according to whether or not the Hamiltonian is invariant under time-reversal. A diagrammatic representation of this correction is shown in Fig. 27. This contribution represents just the first order correction to an infinite series which forms the one parameter scaling of the diffusion constant, or equivalently, of the conductivity.

This result, which predicts a quantum correction to the conductivity of  $\delta\sigma/\sigma = -(2 - \beta)\Pi(0, 0)/\pi\nu$ , is consistent with the estimate of the weak localization made in section I. (Note that, while the leading order weak localization correction is cancelled by a weak magnetic field, higher order contributions from diffusons alone, lead to a renormalization of the diffusion constant even in the unitary ensembles.)

Let us digress for a moment from the construction of the field theory and comment on some *technical* aspects of perturbative approaches to computing Green function correlators in mesoscopic systems. Broadly speaking, three principal perturbative schemes exist: diagrammatic perturbation theory, as discussed in section ID, perturbative evaluation of fluctuations around the mean field of the nonlinear  $\sigma$ -model, and semi-classical schemes aiming at identifying relevant contributions to the Green function *path* integral.

The principal difficulty of including higher order quantum interference corrections into diagrammatic summations is that

the ‘junction’ between ladder diagrams usually needs to be dressed by a number of single impurity lines. This is illustrated in Fig. 27, where the shaded junction, i.e. the Hikami box, includes three sub-diagrams differing by a single line. The proper identification of all those vertex corrections is an art by itself and any mistake is penalized heavily. Which is to say that incorrect account for vertex corrections leads to violations of the unitarity of the theory and, therefore, to non-sensical results. In principle, it is possible to check the validity of diagrammatic expansions by confirming compatibility with various conservation laws, Ward identities etc. However, the issue remains subtle enough and is responsible for a large number of serious errors in the literature.

The problem arises in a sharpened form within semi-classical schemes, based on the path integral. The semi-classical analog of the junction between a Diffuson and a Cooperon is a region where a pair of quantum amplitudes splits and later recombines (c.f. Fig. 10.) It has, so far, been impossible to identify and include the analog of the Hikami box correction into semi-classical path counting schemes. This means that the computation of even first order weak localization corrections is beyond present day semi-classics.

It is one of the principle advantages of the field theory scheme, that the aforementioned difficulties do not arise. Within the field theory approach, unitarity is conserved as long as the action remains invariant under the action of the symmetry manifold  $SU(2, 2|4)$  (see [59] for a detailed discussion of this point). Since all manipulations done in extracting the low energy action carefully respect this invariance property, all ‘single impurity corrections’ needed to guarantee unitarity of the theory are automatically included, to all orders in perturbation theory! This makes the field theory approach an ideal tool for solving problems that require large order perturbative summations.

### 3. Level Statistics

As a second application, let us consider the two-point correlator of DoS fluctuations  $R_2(\Omega)$ . In the  $\sigma$ -model representation, the latter is expressed in terms of the correlator

$$R_2(\Omega) = \frac{1}{64} \left\langle \left[ \int \frac{d\mathbf{r}}{L^d} \text{str}(\sigma_3^{\text{AR}} \otimes \sigma_3^{\text{BF}} Q(\mathbf{r})) \right]^2 \right\rangle_Q - 1.$$

To leading order, an expansion in terms of the generators obtains  $R_2(\Omega) = \langle [\int \text{str}(\sigma_3^{\text{BF}} W^2)]^2 \rangle_W / 256$ , where  $\langle \dots \rangle_W = \int DW \dots e^{-S_0[W]}$  and the generators

$$W = \begin{pmatrix} & B \\ \bar{B} & \end{pmatrix},$$

are block off-diagonal in AR-space. Focusing on the unitary symmetry class,  $[Q, \sigma_3^{\text{TR}}] = 0$ , and making use of the contraction rules [58, 72],

$$\begin{aligned} \langle \text{str}[B(\mathbf{r})P\bar{B}(\mathbf{r}')R] \rangle_B &= \Pi(\mathbf{r}, \mathbf{r}') \text{str} P \text{str} R, \\ \langle \text{str}[B(\mathbf{r})P] \text{str} [\bar{B}(\mathbf{r}')R] \rangle_B &= \Pi(\mathbf{r}, \mathbf{r}') \text{str} [PR], \end{aligned}$$

we recover the perturbative result of Eq. (13)

$$R_2(\Omega) = \frac{\Delta^2}{2\pi^2} \text{tr} \hat{\Pi}^2. \quad (32)$$

Formally, in the language of diagrammatics, this contribution is associated with the exchange of two diffuson ladders between two closed loops (see Fig. 14). Performing the trace we find that, for  $\Omega \gg E_c = D/L^2$ ,  $R_2(\Omega) \simeq g^{-d/2} (\Delta/\Omega)^{2-d/2}$ . In the zero-dimensional limit this result recovers the perturbative random matrix limit. Interestingly, in two-dimensions, the constant of proportionality identically vanishes, and a non-trivial dependence of  $R_2$  on  $\Omega$  only emerges from higher order weak localization corrections [?].

### 4. Zero-Mode

Having examined the short-time perturbative dynamics, we now switch attention to consider the low energy quantum regime where diagrammatic analysis fails. Taking  $\Omega \ll E_c$ , contributions to the effective action involving spatial fluctuations of  $Q$  are strongly suppressed. In this limit, the contribution at leading order in  $1/g$  is dominated by the spatially uniform zero-mode configuration  $Q(\mathbf{r}) = Q_0$ . In this case, the effective action takes the universal form

$$S[Q_0] = i \frac{\pi \Omega^+}{4\Delta} \text{str}(\sigma_3^{\text{AR}} Q_0), \quad (33)$$

independent of dimensionality, the value of the diffusion constant, or geometry of the system. In fact, as will be shown below, Eq. (33) is an exact representation of statistical correlators of the corresponding random matrix ensembles.

Although the zero mode integration is definite, its evaluation relies on finding an explicit parameterization for the  $Q$  matrix. While straightforward in principle, the practice is somewhat involved. As such, the detailed parameterization of the zero-dimensional  $Q$  matrix has been included only as a footnote to this section. Qualitatively, parameterizing  $Q_0$  through the pseudo-unitary transformations which bring it to diagonal form, an expression for  $R_2$  can be given in terms of eigenvalue integrations,

$$R_2(\Omega) = \frac{1}{2} \text{Re} \int_1^\infty d\lambda_1 \int_{-1}^1 d\lambda e^{i \frac{\pi \Omega^+}{\Delta} (\lambda_1 - \lambda)}. \quad (34)$$

Explicit integration over the eigenvalues  $\lambda, \lambda_1$  [58] recovers the random matrix result (17).

In conclusion, we have demonstrated that, by exploiting the ensemble average, an effective field theory can be developed which is capable of describing the response of disordered conductors from time scales short as compared to the typical transport or diffusion time, to times in excess of the Heisenberg time  $t_H = 1/\Delta$  where properties become universal. As an appendix to this section,

we will employ the same supersymmetry approach to exemplify that the zero-dimensional  $\sigma$ -model produces the correlators of random matrix ensembles.

### C. Zero-Mode Integration

The evaluation of the zero mode integrations is most readily performed by finding a convenient parameterization of the  $Q_0$  matrix. For this purpose we adopt a parameterization which separates the degrees of freedom into eigenvalues and pseudo-unitary rotations. For the unitary ensemble, the parameterization takes the form [58]

$$Q_0 = UH\bar{U},$$

where matrices  $H$  and  $U$  have the block structure

$$H = \begin{pmatrix} \cos \hat{\theta} & i \sin \hat{\theta} \\ -i \sin \hat{\theta} & -\cos \hat{\theta} \end{pmatrix}_{\text{AR}}, \quad U = \begin{pmatrix} u_1 u_2 & 0 \\ 0 & v \end{pmatrix}_{\text{AR}}.$$

These matrices are further separated into components

$$\begin{aligned} \hat{\theta} &= \begin{pmatrix} i\theta_1 & 0 \\ 0 & \theta \end{pmatrix}_{\text{BF}} \otimes \mathbb{1}^{\text{TR}}, \quad \theta_1 > 0, \quad 0 < \theta < \pi, \\ u_1 &= \exp \begin{bmatrix} 0 & -2i\eta \\ 2i\eta & 0 \end{bmatrix}_{\text{BF}}, \quad \eta = \begin{pmatrix} \eta_1 & 0 \\ 0 & -\eta_1^* \end{pmatrix}_{\text{TR}}, \\ u_2 &= \begin{pmatrix} e^{i\chi\sigma_3^{\text{TR}}} & 0 \\ 0 & e^{i\phi\sigma_3^{\text{TR}}} \end{pmatrix}_{\text{BF}}, \\ v &= \exp \begin{bmatrix} 0 & -2i\kappa \\ 2i\kappa & 0 \end{bmatrix}_{\text{BF}}, \quad \kappa = \begin{pmatrix} \kappa_1 & 0 \\ 0 & -\kappa_1^* \end{pmatrix}_{\text{TR}}, \end{aligned}$$

where  $\bar{u}_i \equiv u_i^\dagger$ ,  $\bar{v} \equiv \sigma_3^{\text{BF}} v^\dagger \sigma_3^{\text{BF}}$ . Here the coordinates  $\theta_1$  and  $\theta$  represent the eigenvalues of the non-compact bosonic and compact fermionic sector respectively.

Employing this parameterization we find

$$\begin{aligned} \text{str} [\sigma_3^{\text{AR}} Q_0] &= 4(\lambda - \lambda_1), \\ \text{str} [\sigma_3^{\text{FB}} \otimes \sigma_3^{\text{AR}} Q] &= 4(\lambda_1 + \lambda) - 16(\lambda_1 - \lambda)[\eta_1^* \eta_1 - \kappa_1^* \kappa_1], \end{aligned}$$

where  $\lambda = \cos \theta$ ,  $\lambda_1 = \cosh \theta_1$ ,  $\mu = (1 - \lambda^2)^{1/2}$ , and  $\mu_1 = (\lambda_1^2 - 1)^{1/2}$ . Finally, taking into account the invariant measure,

$$dQ_0 = \frac{1}{128\pi^2} \frac{\mu\mu_1}{(\lambda_1 - \lambda)^2} d\theta d\theta_1 d\phi d\chi d\eta_1^* d\eta_1 d\kappa_1^* d\kappa_1,$$

and integrating over the Grassmann and auxiliary bosonic variables, we obtain Eq. (34).

### D. Random Matrix Theory

To make explicit the connection between the long-time dynamics of disordered conductors and the properties of random matrix ensembles we can quickly repeat the construction of the  $\sigma$ -model action, now for the Green functions of a random matrix Hamiltonian [74]. In particular, following the classification scheme of section IB 6, the

application of the field integral technique to a Gaussian distribution of  $N \times N$  random matrices,

$$P(H)dH \propto \exp \left[ -\frac{N\beta}{\lambda^2} \text{tr} H^2 \right] dH,$$

where  $\beta$  indicates the corresponding symmetry class, an ensemble average of the generating function leads to the expression

$$\langle \mathcal{Z}[0] \rangle = \int d[\Psi] e^{-i\Psi \left( E + \frac{\Omega^+}{2} \sigma_3^{\text{AR}} \right) \Psi - \frac{\lambda^2}{N} (\Psi \Psi)^2},$$

where  $\Psi$  represents  $8 \times N$  component supervectors.

The interaction of the supervectors generated by the ensemble average can be decoupled with the introduction of zero-dimensional  $8 \times 8$  supermatrices with the symmetry properties shown in Eq. (28). Integrating out the supervectors obtains

$$\langle \mathcal{Z}[0] \rangle = \int d[Q] \exp \left[ \text{str} \left( \frac{N}{4} Q^2 - \frac{1}{2} \ln \mathcal{G}^{-1} \right) \right]$$

where  $\mathcal{G}^{-1} = -E + \Omega^+ / 2\sigma_3^{\text{AR}} + i\lambda Q$ .

A variation of the action with respect to fluctuations of  $Q$  obtains the saddle-point equation  $Q_{\text{sp}} = i\lambda \mathcal{G}$  from which we obtain the solution

$$Q_{\text{sp}} = -\frac{i}{2\lambda} E + \left( 1 - \frac{E^2}{4\lambda^2} \right)^{1/2} \sigma_3^{\text{AR}}.$$

Applied to the average DoS, the saddle-point solution recovers the semi-circular Wigner distribution  $\langle \nu(E) \rangle = (N/\pi\lambda)(1 - (E/2\lambda)^2)^{1/2}$ . Finally, taking the energy at the center of the band,  $E = 0$ , and expanding to leading order in  $N$ , we obtain the zero-dimensional non-linear  $\sigma$ -model (33).

To summarize, the correspondence between the zero-dimensional field theories of the disordered metal and random matrix ensembles establishes universality of low-energy spectral correlations. I.e. when rescaled by the average energy level spacing  $\Delta = 1/\nu L^d$ , statistical correlations of the energy levels,  $\epsilon_i = E_i/\Delta$ , become independent of the detailed properties of the system. In fact, universality can be extended to include the response of energy levels to an arbitrary external perturbation such as a magnetic field. Characterizing the field strength by some parameter  $X$ , when subjected to the rescaling

$$C(0) = \left\langle \left( \frac{\partial \epsilon_i(X)}{\partial X} \right)^2 \right\rangle, \quad x = \sqrt{C(0)} X, \quad (36)$$

the statistical properties of the entire random functions  $\epsilon_i(x)$  becomes universal [75,76].

The intuition afforded by the random matrix theory has proved to be of considerable use both qualitatively and quantitatively. As well as providing a complete description of the universal properties associated with energy level, the statistics of wavefunctions is also provided by the random matrix theory.

Let us conclude this more methodologically oriented section with a brief survey of theories of mesoscopic systems. Broadly speaking, there are five theoretical streamlines that have been applied to the analysis of quantum phase coherence in mesoscopic environments: random matrix theory, semi-classics, diagrammatic perturbation theory, the so-called DMPK-transfer matrix approach, and field theory. Although the emphasis of the present text is on field theoretical methods, more will be said about the complementary theories later on.

However, one important theoretical approach will not be discussed any further in this course, the **DMPK transfer matrix** formalism. For completeness, let us at least try to formulate the basic idea of this extraordinarily powerful approach.

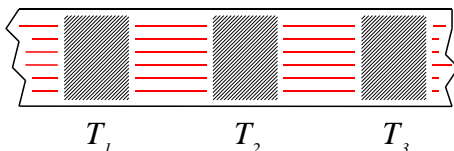


FIG. 28. The idea of the transfer matrix approach. Disorder scattering of transverse momentum modes (the horizontal lines) is represented through a sequence of black box scatterers (the shaded areas). The information on the scattering processes (i.e. the set of inter-mode scattering matrix elements) is held by transfer matrices  $T_i$ , one for each scatterer. The total transfer matrix obtains as the product over all  $T_i$ .

The transfer matrix approach is specific to quasi one-dimensional systems. A quasi one-dimensional wire can be imagined as a set of transverse momentum channels (or “modes”) which scatter off static disorder. Appealing to the general concept of universality and insensitivity to microscopic details of the disorder the latter can be modeled as a set of spatially separated black boxes which scatter between different modes (see Fig. 28.) Technically speaking, each box is described by an  $S$ -matrix, i.e. a code that relates the set of incoming wave amplitudes to the outgoing ones. However, sometimes it is more convenient to encode the scattering information into a transfer-, or  $T$ -matrix, i.e. a matrix that relates the wave amplitudes to the right of a scattering block to the amplitudes on the left. Of course, both descriptions are equivalent, i.e.  $S$ - and  $T$ -matrix carry the same information. However, the  $T$ -matrix formulation has one big advantage, viz. it can straightforwardly be iterated to yield the scattering profile of *extended* regions. E.g., it is intuitively clear that the  $T$ -matrix of a composite set of two scatterers 1 and 2 obtains as a convolution over all scattering states connecting 1 and 2, i.e. as the product of the two individual transfer matrices:  $T = T_1 T_2$ . Building on this observation, the basic idea of the general  $T$ -matrix approach is ask how much the total transmission through a one-dimensional structure of  $K$  scatterers changes when one more scatterer is added. In the limit  $K \gg 1$ , the answer can

be formulated in terms of a Fokker-Planck type differential equation, known as the **DMPK-equation** (after Dorokhov-Mello-Pereyra-Kumar [77,78]). The DMPK-approach has proven enormously successful in the analysis of transport characteristics of quasi one-dimensional structures. A comprehensive up to date review of the subject can be found in [79].

The table below gives a broad and necessarily superficial survey of the suitability of each theory to certain common applications. Notice that the table does not say anything about the actual *efficiency* of a given approach. E.g. non-interacting quasi one-dimensional systems can be described in terms of both field theory and DMPK-transfer matrix methods. However, the DMPK-formulation, tailor-made to one dimension, turns out to the more powerful tool. Similarly one would think twice before constructing a field theory model of a zero-dimensional quantum dot when the alternative is to employ a simple random matrix model.

Theory	$d$	non-pert.	$e - e$	clean/weak dis.
RMT	0	+	+	$o^1)$
DMPK	1	+	—	—
semi-classics	arb.	$-/o^2)$	—	+
diagrammatics	arb.	—	+	—
field theory	arb.	+	$+^3)/-^4)$	$o^5)$

FIG. 29. Application areas of various theories of mesoscopic systems. The column “non-pert.” indicates the possibility to address problems of non-perturbative nature; “ $e - e$ ” stands for electron-electron interactions and “clean-weak dis.” for the possibility to describe weakly disordered (i.e. non-diffusive) or even clean systems. A ‘+’ sign indicates that an approach is well suited while a ‘—’ stands for a no-go situation or, at least, for severe difficulties. A ‘o’-symbol indicates an ambivalent status. 1) See the discussion of section III A 4; 2) For attempts to apply semi-classical methods in non-perturbative regimes, see Ref. [80]; 3) Replica- or Keldysh-field theory, 4) Supersymmetry; 5) See section III C.

Further detail of the field theoretic approach can be found in the followings reviews: Ref. [58–62].

### III. QUANTUM CHAOS

In the previous section a statistical field theory of weakly disordered metallic systems was established. The non-linear  $\sigma$ -model (31) provided a formal framework from which the phenomenology of section I could be developed: Weak Localization, Scaling, Universality, and the Random Matrix Theory. In this section, we will explore generalizations of the statistical approach which account firstly for the quantum properties of systems whose

classical counterparts are *chaotic* (but not necessarily disordered.)

The derivation of the low-energy effective action for the disordered conductor specifically involved the consideration of a single-particle Hamiltonian in which the random impurity potential was drawn from a Gaussian  $\delta$ -correlated white-noise distribution. However, in the spirit of the Ginzburg-Landau phenomenology, we would expect the domain of applicability of the low-energy effective action to be much wider. In particular, for any model in which the long-time classical dynamics is fundamentally diffusive, one would expect the non-linear  $\sigma$ -model to apply. For example, a particle subject to a random “classical” potential (i.e. one on which the scale of variation is greatly in excess of the Fermi wavelength) is expected to be described by the same diffusive  $\sigma$ -model on time scales in excess of the corresponding transport mean free time (i.e. the typical time scale on which the momentum of a particle becomes randomized). Yet, such a model, which has a well defined classical limit, belongs to the wider class of systems which are *chaotic*. Does the field theory tell us something about chaotic quantum structures?

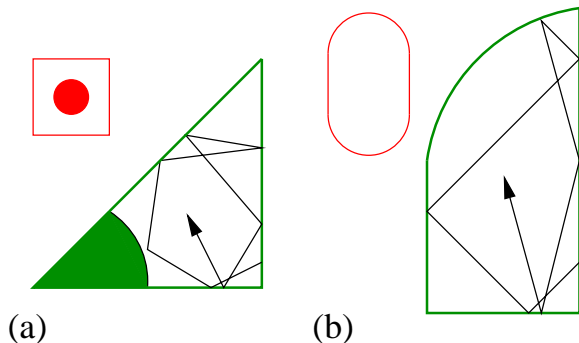


FIG. 30. (a) Sketch of the chaotic “stadium” billiard, and (b) the Sinai billiard.

According to the laws of classical Hamiltonian dynam-

ics, a system in which the number of degrees of freedom exceed the number of constants of motion is chaotic. In the simplest cases, the only constant of motion is the energy. For strongly chaotic systems, the fundamental non-integrability of the Hamiltonian is reflected in an exponential sensitivity of the classical dynamics to the initial boundary condition. (i.e. a classical path in phase space separates exponentially fast from an initially neighboring classical path.) Such systems are known as “Axiom A” or “uniformly hyperbolic”. More generally, chaotic structures usually exhibit a mixed phase space in which chaotic regions are intersected by islands of integrability.

The quantum description of systems which are chaotic in their classical limit is the subject of “Quantum Chaos” [81]. A wide variety of physical systems fall into this category. Amongst those most commonly studied are models of particles confined to irregular potentials, the so-called “Quantum Billiards” (see Fig. 30), resonances of microwave cavities, and Rydberg atoms in strong magnetic fields. While much of the on-going research in quantum chaos is theoretical, or even mathematical, quite a few system classes have been the subject of experimental investigations. We begin our survey of quantum chaos with a brief (and incomplete) review of these activities:

Our first example is the hydrogen atom subject to a strong magnetic field (for a review see, e.g., Ref. [82]). The corresponding non-relativistic Hamiltonian is specified by (in atomic units)

$$\hat{H} = \frac{p^2}{2} - \frac{1}{r} + \frac{B}{2}m + \frac{B^2}{8}(x^2 + y^2).$$

The third term describes the Zeeman splitting separating levels according to the conserved  $z$ -component of angular momentum,  $m$ . This, together with the parity represent the only good quantum numbers. The final diamagnetic term prevents the usual separation of variables and is responsible for non-integrability. For highly excited states, the diamagnetic energy can become comparable to the Coulomb energy at which point the classical dynamics becomes fully chaotic (see Fig. 31).

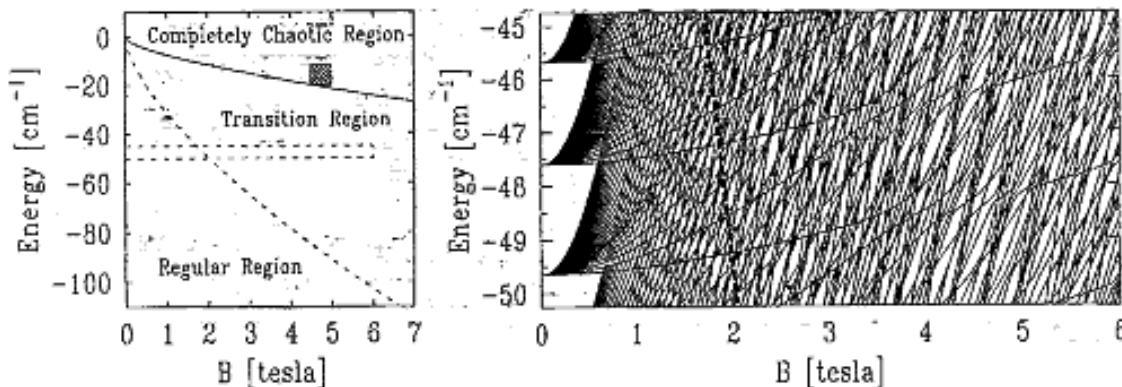


FIG. 31. Typical section of the spectrum of the diamagnetic hydrogen atom spanning a region in which the phase space is mixed (shown dotted). The shaded region lies in a domain in which the classical dynamics is fully chaotic. Here the spectral correlations are universal.

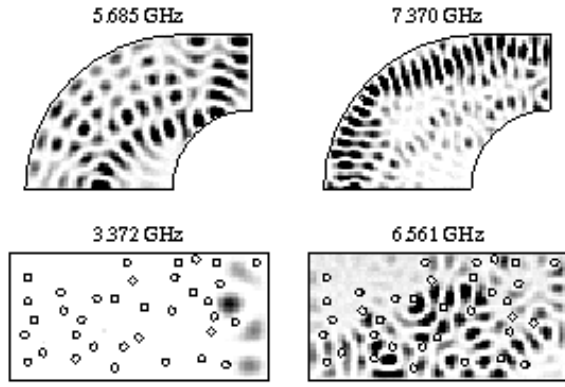


FIG. 32. Measurements of the typical wavefunction amplitude of a “Sinai stadium” billiard and an array of scatterers courtesy of Ref. [83].

The second experimental system which has been the subject of investigation are the stationary modes of a microwave cavity. In particular, exploiting the equivalence of the Maxwell equation for the stationary TM modes of a two-dimensional cavity with a Schrödinger equation,  $(\nabla^2 + k^2)\psi = 0$ , the eigenfunctions and eigenspectra of chaotic “billiards” have been investigated. Fig. 32 shows typical eigenfunctions for modes of a “Sinai stadium” billiard, together with a device involving a disordered array of scatterers.

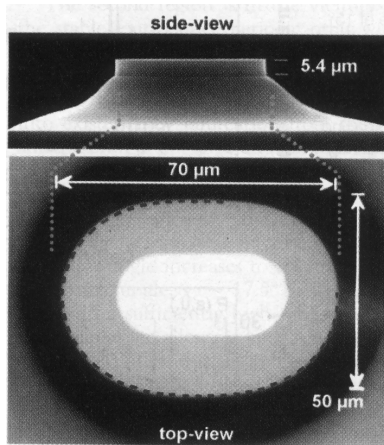


FIG. 33. Scanning electron microscope image of a deformed cylindrical semiconductor resonator. The laser active material is contained in the disk (of thickness  $5.4 \mu\text{m}$ ) sitting on top of an *InP* pedestal. Light emission occurs in the plane of the disk. Taken from Ref. [84].

While research on the aforementioned systems has largely been motivated by fundamental science, recent

experimental findings have led to the perspective of concrete *technological* applications of quantum chaos: recent technological advances have made possible the fabrication of semiconductor micro-lasers with arbitrarily shaped cavity geometry. Basically, such a device consists of a GaInAs/AlInAs heterostructure grown by molecular beam epitaxy onto a substrate [84] (see Fig. 33.) The quasi two-dimensional core of the structure (i.e. the ‘stadium’ shaped structure shown in Fig. 33 bottom) contains a laser-active material; light is internally reflected off the boundaries of the structure and emitted in the plane of the disk. Due to their smallness, a natural problem with these lasers is emission power. For example, in a regular, circular shaped geometry, internally reflected light propagates along ‘whispering gallery’ trajectories (see Fig. 34, left). Light is then emitted uni-directionally, at average low intensity. Interestingly, much higher emission intensities can be achieved [84] with deformed cavity geometries. This is illustrated in Fig. 34, right for the example of a ‘stadium’ type geometry. The classical dynamics of a stadium is chaotic. However, the system supports a number of stable periodic orbits, i.e. solutions of the classical equations of motion that are periodic. (A ‘bow-tie’ shaped example of such an orbit is displayed in the figure.) In the stadium laser, such orbits identify long-lived resonator modes, i.e. modes of anomalously large photon intensity. This is illustrated in the contour plot of Fig. 35, left bottom. Bright areas identify regions of large field intensity, both in the internal geometry of the cavity and in the far field region. This plot has been obtained by numerical solution of the Helmholtz equation defining the optical problem. The experimentally observed angle-resolved intensity pattern is displayed in the left part of the figure. Notice that the maximum intensity of the chaotic cavity exceeds that of the regular one by orders of magnitude!

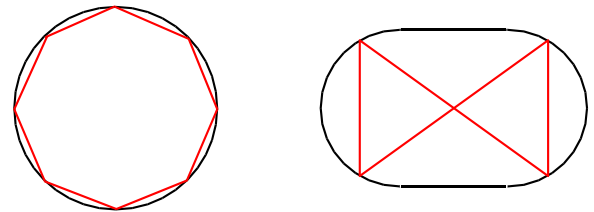


FIG. 34. Left: schematic plot of circular laser structure. The internal line indicates a whispering gallery type trajectory traced out by the photon beam. Light emission is uni-directional. Right: strongly deformed cavity geometry. The system supports a stable periodic orbit of ‘bow-tie’ geometry which identifies a region of strongly enhanced light intensity. The strongest light emission occurs in the direction of the four segments defining the orbit.

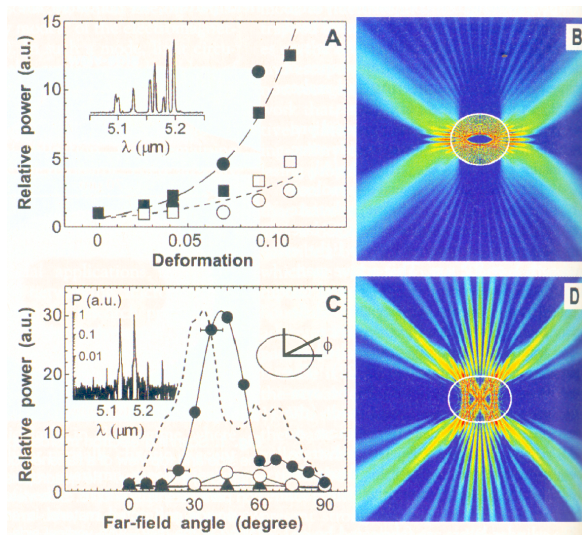


FIG. 35. Upper left: Intensity of a deformed laser cavity in direction 0deg (open symbols) and 90deg (full symbols) as a function of the degree of deformation. Here lasing is due to several whispering gallery modes. Deformation leads to a ‘bundling’ of the emission pattern and, therefore, to an increase of the field intensity along the principal axes of the geometry. Upper right: Numerically obtained contour plot of the intensity pattern of a moderately deformed cavity. Lower left: Angle resolved emission pattern of a massively deformed cavity (circular symbols) as compared to the emission of a circular cavity (triangles). Lower right: the contour plot clearly identifies the stable bow-tie mode responsible for the  $\simeq 45$ deg emission peak observed in experiment. Taken from Ref. [84].

Over the years, the general properties of these and many other chaotic quantum structures have come under intense scrutiny from both mathematicians and physicists alike. All have been motivated in part by the question: what are the manifestations of chaotic dynamics in the quantum properties of classically non-integrable structures? We begin our investigation with a brief review of the important milestones that have helped to shape the general field of quantum chaos.

## A. Spectral Statistics: A Brief History

### 1. Wigner Surmise

Perhaps the earliest investigation of the statistical properties of complex quantum systems began with the pioneering work of Wigner in the late '40's and early '50's. Guided by the very complexity of the system, Wigner introduced a statistical ansatz to explain strong level correlations observed in the resonance spectra of complex nuclei [85,86]. Taking matrix elements to be statistically uncorrelated Wigner obtained, within a two-level approximation, an estimate of the distribution of

neighbouring level spacings known as the Wigner surmise,

$$P(S) = \langle \delta(S - (E_{i+1} - E_i)) \rangle \sim \frac{\pi S}{2 \Delta} \exp \left[ -\frac{\pi S^2}{4 \Delta^2} \right],$$

where, as usual,  $\Delta = \langle E_{i+1} - E_i \rangle$  denotes the average level spacing. Qualitatively, this law expresses the fact that two levels which are correlated (coupled through some kind of matrix element) will not cross, an ubiquitous feature shown by the spectra of large nuclei, and other chaotic systems. More accurately, according to the statistical Ansatz, the spectral properties of complex nuclei coincides with those of (time-reversal invariant) random matrix ensembles.

Thus, by surrendering information specific to each individual system, Wigner was able to quantitatively account for the characteristic level repulsion observed in experiment. Forty years on, similar considerations are now frequently given to explain the ground state properties of artificial atoms, or quantum dots [7] (with so far only limited success!).

### 2. Gor'kov-Eliashberg Theory

While successfully studied and applied to the physics of complex nuclei, it was not until almost twenty years later that similar ideas were applied to the study of the quantum properties of weakly disordered metallic grains. By identifying spectral correlations of the grains with those of random Hermitian matrix ensembles, Gor'kov and Eliashberg investigated the dielectric response of metallic grains embedded in an insulating matrix [87]. Although often neglected in the more recent literature, this early work anticipated applications of random matrix theory to the field of mesoscopic physics by two decades.

As confirmation of the random matrix hypothesis for disordered metallic grains, Fig. 36 shows the distribution of neighboring level spacings  $P(s)$  for an ensemble of tight-binding models with on-site disorder belonging to the unitary ensemble. The results compare favourably with the universal formula for the Wigner surmise.



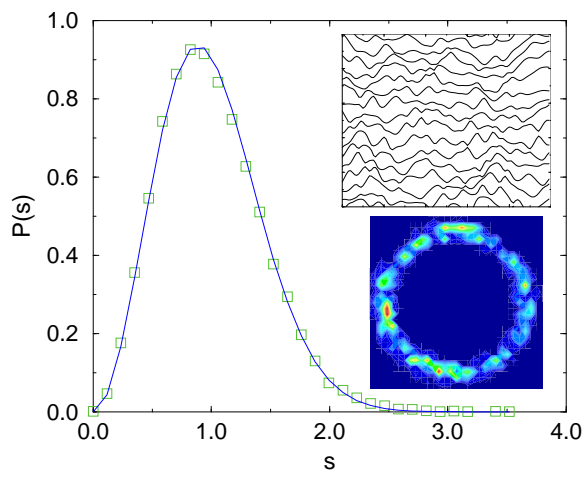


FIG. 36. The distribution of level spacings for a tight-binding impurity Hamiltonian subject to a quasi-periodic boundary conditions. The estimate from the Wigner surmise ( $P(s) = 32s^2 \exp[-4s^2/\pi]/\pi^2$  for unitary ensembles) is shown for comparison. Inset, a typical set of levels is shown as a function of the changing quasi-periodic boundary condition. Also shown is are the Fourier components of a typical high energy wavefunction. The bulk of the weight lies around the energy shell  $E = \mathbf{p}^2/2m$ .

### 3. Supersymmetry: Efetov's Non-linear $\sigma$ -Model

Belonging to a statistical ensemble, average properties of disordered quantum systems are more susceptible to analytical investigation than individual systems. As we have seen, providing the statistical average of an individual system (for example, over a range of energy levels) is statistically equivalent to an average over an ensemble of similar systems, analytical results can be obtained systematically and rigorously.

Relying on such an *ergodicity hypothesis*, Efetov developed a statistical field theory of level correlations in weakly disordered metallic grains [58]. As we have seen in section II, building upon the seminal work on Anderson localization by Wegner [56] and others [88–93], Efetov provided a rigorous mathematical foundation for the random matrix hypothesis introduced by Gor'kov and Eliashberg. However, perhaps more importantly, Efetov's approach provided a systematic way in which non-universal properties reflecting the intrinsic diffusive dynamics of the system could be studied.

### 4. Bohigas-Giannoni-Schmidt Conjecture

Until the early '80's, the application of random matrix theory had been largely limited to the study of complex many-body or disordered quantum systems. However, an extension of these ideas to a wider class of structures was suggested by Bohigas, Giannoni and Schmidt [94].

Based on an extensive numerical investigations the following conjecture was proposed:

- ▷ The spectral statistical properties of quantum systems which are chaotic in their classical limit (even those with few degrees of freedom) are UNIVERSAL, independent of material properties of the system, and coincide with those of random matrix ensembles.

(Being, in general, unable to define an ensemble, the statistics are assumed to involve averaging over a suitably wide range of states.) This conjecture is now acknowledged as a milestone in the phenomenology of quantum chaos. It suggested a common thread which united a whole class of qualitatively different systems, and lay down a gauntlet to mathematicians to establish a proof. So far, very few exceptions to this rule have been identified. Importantly, for those that have, it is usually simple to understand why they lie outside the present scheme. However, despite more than fifteen years of intense study, and the accumulation of a wealth of supporting data, this conjecture still awaits a rigorous mathematical proof.

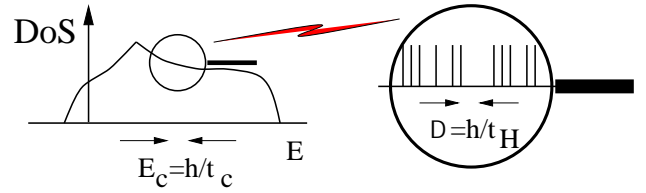


FIG. 37. Time scales over which response functions such as  $R_2(\Omega)$  are universal.

Although compelling in its simplicity, the conjecture of Bohigas, Giannoni and Schmidt begs the question: which properties are universal and, perhaps more importantly, *which are not*? Empirically, the study of spectral statistics typically shows level correlations to be universal on low energy scales comparable with the average energy level spacing  $\Delta$  (see Fig. 37). However, universal correlations are typically observed to break down at some non-universal large energy scale, or equivalently, some short-time scale  $E_c = 1/t_c$ . With this observation, one can ask:

- ▷ What, in general, sets the range of universal correlations?
- ▷ How is chaos reflected in the statistics of the non-universal interval?

To address these questions and identify others we can gain useful insight by drawing on the statistical properties of weakly disordered conductors. There we saw that the low-energy response of spectral correlators were governed by the low-lying modes of density relaxation as specified by the non-linear  $\sigma$ -model action (31). On energy scales  $\Omega$  in excess of the Thouless energy  $E_c$ , the

inverse diffusion time across the system  $t_D = L^2/D$ , the spectral properties depend sensitively on the spectrum of the diffusion modes. While on energy scales  $\Omega < E_C$  spectral correlations become universal, independent of the particular geometry or morphology of the system. Within this ergodic regime, the statistical properties of the spectrum and wavefunctions become indistinguishable from those of random matrix ensembles.

Does an analogous scenario describe the spectral response of, say, an irregular or chaotic cavity (a quantum billiard) without impurities? In such systems there too exists some ergodic energy scale below which properties of the system become universal. How is the unstable nature of the classical dynamics reflected in the large energy scales properties? More precisely,

- ▷ What plays the role of diffusion in describing the low-lying relaxational degrees of freedom in general chaotic quantum systems?
- ▷ What is the analogue of *weak localization* and how are such quantum coherence effects manifest in experiment?
- ▷ What determines the domain of universality?

In the following, we will introduce a statistical field theory which provides a solid framework in which these questions can be answered (at least in principle). However, to motivate the form of the effective action, (and, indeed, to answer the first of the questions above) we will begin with a semi-classical analysis based on the Feynman path integral. Here we will exploit ideas similar to the phenomenology discussed in section I.

## B. Semi-classics and the Trace formula

As with the disordered conductors, expressed as the trace of the propagator, we can gain some intuition into spectral properties of chaotic structures by representing the DoS as a Feynman path integral. In the semi-classical limit ( $\hbar \rightarrow 0$ ), this representation identifies the special role played by closed (i.e. periodic) classical trajectories. (Recall  $\nu(\epsilon) = \text{tr} \text{Im} G(\epsilon - i0)/\pi$ .) Taking into account the dominant contribution to the Feynman propagator, the (local) DoS assumes the form [81,95–97]

$$\frac{\nu(E)}{\nu} = 1 + \text{Re} \frac{\Delta}{\pi \hbar} \sum_p T_p \sum_{r=1}^{\infty} \frac{e^{iS_p(E)r/\hbar - i\nu_p r}}{|\det(M_p^r - \mathbb{1})|^{1/2}}, \quad (37)$$

where  $p$  labels a primitive orbit with a period  $T_p \equiv \partial S_p(E)/\partial E$ , action  $S_p(E)$ , and Maslov phase  $\nu_p$ . (Here the first uniform contribution (known as the Weyl term) depends only on the phase space volume and derives from very short (non-classical) Feynman trajectories.) The sum over  $r$  accounts for repetitions of the classical periodic trajectory. Finally the prefactor takes into account

the leading fluctuations around the classical paths and involves the stability or *monodromy matrix*  $M_p$  associated with the linearized dynamics on the Poincaré section perpendicular to the orbit  $p$  (see Fig. 38). Crucially, this expression identifies the local DoS with a sum over classical periodic orbits weighted by a phase which depends sensitively on the orbit.

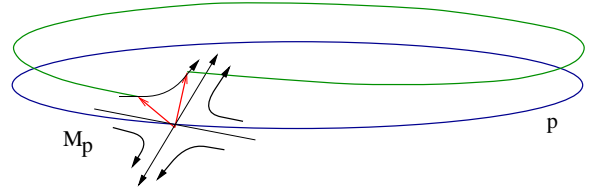


FIG. 38. Schematic diagram showing the meaning of monodromy matrix. Specifically, the monodromy matrix  $M_p$  here describes the linearized mapping of a vector on the Poincaré surface of section to another under a cycle of a periodic orbit  $p$ .

Now, as with the disordered conductor, when subjected to an average over a range of energies greatly in excess of the average level spacing, the incoherent superposition of the phase associated with different classical paths removes the second contribution. However, applied to the two-point function, the average preserves a long-range phase coherent contribution. More precisely, substituting Eq. (37) into Eq. (11), the two-point correlator of DoS fluctuations is expressed as a double sum over periodic orbits. A random phase cancellation of long trajectories identifies the “diagonal contribution” as dominant. Taking this contribution alone, and expanding  $S_p(E + \Omega) \simeq S_p(E) + T_p \Omega$ , we obtain

$$R_2(\Omega) = \text{Re} \frac{\Delta^2}{2\pi^2 \hbar^2} \sum_p T_p^2 \sum_{r=1}^{\infty} \frac{e^{i\Omega T_p r/\hbar}}{|\det(M_p^r - \mathbb{1})|}. \quad (38)$$

In the disordered metal, the diagonal contribution to the two-point function was identified with the exchange of diffusion modes. To identify the physical relaxation mode to which the diagonal sum (38) corresponds we first consider the propagator of classical phase space density, the Liouville operator. Formally, the latter is defined by

$$\rho(\mathbf{x}, t) = e^{\{H, \}_t} \rho(\mathbf{x}, 0) = \int d\mathbf{x}' \delta^{2d}(\mathbf{x} - \mathbf{u}(\mathbf{x}'; t)) \rho(\mathbf{x}', 0)$$

where

$$\{H, \}_t = \partial_{\mathbf{r}} H \cdot \partial_{\mathbf{p}} - \partial_{\mathbf{p}} H \cdot \partial_{\mathbf{r}}$$

denotes the classical Poisson bracket,  $\mathbf{x} = (\mathbf{r}, \mathbf{p})$  represent phase space coordinates, and  $\mathbf{u}(\mathbf{x}; t)$  denotes the solution of the classical equations of motion of a particle starting at a position  $\mathbf{x}$  after a time  $t$ .

From this definition, it is straightforward to obtain the following expression for the trace [98],

$$\text{tr } e^{\{H, \}t} = \sum_p T_p \sum_r \frac{\delta(t - rT_p)}{|\det(M_p^r - \mathbb{1})|}.$$

The  $\delta$ -function is associated with the constraint on the period of the orbit, while the prefactor involving the Monodromy matrix is associated with the Jacobian of the  $\delta$ -function in the phase space directions transverse to the periodic orbit. Comparing this expression to Eq. (38), and *neglecting repetitions*, i.e. the contribution of short periodic orbits that are traversed repeatedly, we obtain [99]

$$\begin{aligned} R_2(\Omega) &= \frac{\Delta^2}{2\pi^2\hbar} \text{Re} \frac{\partial}{\partial(i\Omega)} \int_0^\infty dt e^{i\Omega^+ t/\hbar} \text{tr } e^{\{H, \}t} \\ &= \frac{1}{2\pi^2} \text{Re} \sum_\mu \frac{\Delta^2}{(-i\Omega^+ + \hbar\gamma_\mu)^2}, \end{aligned}$$

where the second equality is based on  $\text{tr } e^{\{H, \}t} = \sum_\mu \exp(t\gamma_\mu)$ ,  $\{\gamma_\mu\}$  being the eigenvalues of the classical evolution operator. This result compares to Eq. (13) (with  $\gamma_\mu \rightarrow D\mathbf{q}^2$ ), and suggests that the soft modes of density relaxation in a general chaotic structure are associated with the modes of the classical evolution operator.

But, if this identification is correct, do the modes of the Liouville operator relax? And how can we account for mechanisms of weak localization, and account for corrections non-perturbative in  $\Delta/\Omega$ ? These questions can not be answered with the framework of the diagonal approximation. Recent attempts to go beyond this approximation within the framework of periodic theory have met with some limited success [100]. However, these studies have, as yet, failed to identify weak localization corrections (see Ref. [101] and the remarks made at the end of section I B 7.) Instead, motivated by this finding, we will employ a different approach based on a non-perturbative field theory. Let us mention right away that, far from being completely developed, the field theory approach to quantum chaos does not yet provide conclusive answers to the questions brought up above, and perhaps never will. However, it represents a fresh, and from our subjective point of view quite promising approach that calls for further investigation.

### C. Ballistic $\sigma$ -Model

The analysis of the trace formula above suggests that the analogy between weakly disordered conductors and the general class of chaotic quantum systems is not superficial. In fact, a very close correspondence between the phase coherence phenomena which characterize mesoscopic structures and those observed in quantum chaos can be (at least phenomenologically) established through a generalization of the statistical field theory.

The first suggestion that such a description was possible came in an insightful work by Muzykantskii and

Khmel'nitskii [102]. Guided by the quasi-classical Boltzmann description of density relaxation in ballistic transport, they proposed a natural generalization of the diffusive  $\sigma$ -model in which the diffusive character of the action is replaced by a kinetic dependence,

$$S = i \frac{\pi}{2\Delta} \int \text{str} [\Omega^+ \sigma_3^{\text{AR}} Q - 2i\hbar T^{-1} \sigma_3^{\text{AR}} \{H, T\}], \quad (39)$$

where, in this case, the supermatrix fields  $Q = T\sigma_3^{\text{AR}}T^{-1}$  depend on the  $2d-1$  phase space coordinates parameterizing the constant energy shell,  $\mathbf{x}_\parallel = (\mathbf{r}, \mathbf{p})_{2d-1}$ . (With this definition the integration measure is normalized such that  $\int \equiv \int d\mathbf{x}_\parallel = 1$ .) Although still phenomenological, as we shall see below, their “ballistic action” establishes a crucial bridge between the semi-classical description of level statistics based on the Trace formula above, and the universal random matrix theory.

After its introduction, the phenomenology of Muzykantskii and Khmel'nitskii found further support in the work of Andreev, Simons, Agam, and Altshuler [103]. Specifically, recognizing that the spectrum of an individual system provides a statistical ensemble over which an average can be performed, an explicit derivation of the ballistic action was proposed. Yet, it should be noted that the formal derivation of the action is flawed. In particular, the formal derivation of Ref. [103] assumes that fluctuations of the matrix degrees of freedom perpendicular to the constant energy shell are suppressed. However, the mechanism by which the matrix degrees of freedom become “locked” remains obscure, and has become the subject of some controversy in the literature (see e.g. [104,105]). Furthermore, the construction of Refs. [102,103] implicitly assumes that the low energy configurations of the field theory are smoothly fluctuating functions over phase space. This presumption stands in marked contrast to the fact that for chaotic systems the eigenfunctions of ‘kinetic energy operator’ of the field theory, the Liouville operator, are highly singular. This means that the field theory needs regularization. However, the *practical* implementation of a regularization scheme represents a subject of on-going and controversial research, to be reviewed in the next section.

### D. Perturbation Theory

Leaving aside the difficulties in deriving the ballistic action, there are separate problems in understanding its behavior. Indeed, to make sense of the functional integral (39) we must identify the low-lying modes of the action. To do so, we adopt a perturbative expansion of the effective action around the high-energy saddle-point  $\sigma_3^{\text{AR}}$ . Employing the parameterization  $T = e^{-W/2}$ , an expansion of the action leads to

$$S[W] = -\frac{\pi}{8\Delta} \int \text{str} [W \hat{\Pi}^{-1} W] + O(W^4) \quad (40)$$

where  $\hat{\Pi}^{-1} = -\hbar\sigma_3^{\text{AR}}\{H, \cdot\} + i\Omega^+$  shows the low-lying modes of density relaxation are described by modes of the classical evolution operator — a result compatible with that obtained in the analysis of the Trace formula. However this identification deserves some qualification.

As with any functional integral there is a need to define an appropriate regularization. For example the functional integral (39) may be understood as the limit  $a \rightarrow 0$  of a product of definite integrations over a discretized space, where  $a$  denotes the discretization cell size. This admits to functions  $T(\mathbf{x}_{||})$  which are *smooth* and square integrable. In seeking such a basis, the eigenfunctions of the classical evolution operator seem to be the natural choice. However, the intricate nature of chaotic classical evolution cause these eigenfunctions to lie outside the Hilbert space: the chaotic dynamics of probability densities involves contraction along stable manifolds, together with stretching along unstable ones (see Fig. 39). Thus, in the course of time, an initially non-uniform distribution turns into a singular function on the unstable manifold, which in turn covers the whole energy shell densely. Therefore the eigenfunctions of  $\hat{\Pi}$  are not square integrable and their contribution to the functional integral cannot be directly recovered by the discretization procedure involved in evaluating the functional integral.

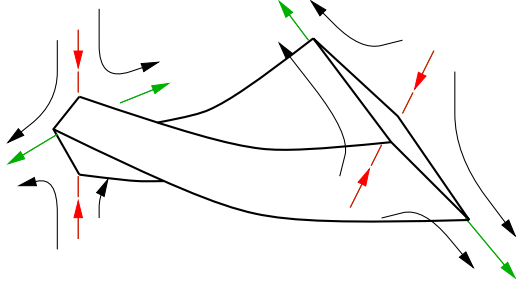


FIG. 39. Schematic diagram showing the tendency for a hyperbolic system to stretch exponentially rapidly along the unstable direction and contract along the stable direction.

Thus, in choosing a convenient basis one has to take account of the regularization. Its primary effect is to truncate the contraction along the stable manifold and thereby render the classical evolution *irreversible*. It is the eigenfunctions of this regularized classical evolution operator that serve as a suitable basis for the quantum mechanical correlator. As mentioned above, the actual implementation of a regularization scheme represents a matter of current research. E.g. one may ask whether a classically vanishing regulator strength (by which we mean a regulator strength that vanishes in the limit  $\hbar \rightarrow 0$ ) suffices to render the theory non-singular, or whether a regulator non-vanishing in the classical limit must be chosen. Equally important, concrete implementations of a regularizing operator, i.e. some *second* order positive differential operator acting on the field configurations, have to be identified. For further discussion of

these points, we refer the interested reader to the literature [104–106].

Remarkably, as the strength of the regulator is taken to zero, the spectrum,  $\{\gamma_n\}$ , of the resulting operator, known in the literature as the Perron-Frobenius operator, reflects intrinsic irreversible properties of the *purely classical dynamics* [107–111].

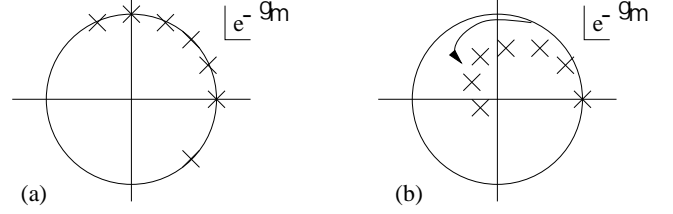


FIG. 40. (a) Formal representation of the eigenvalues of the reversible evolution operator which lie on the unit circle. In non-integrable systems, the eigenvalues form an infinitely degenerate and dense set. (b) Poles or resonances of the coarse-grained, regularized Perron-Frobenius operator. In systems which are uniformly hyperbolic, all resonances lie within the unit circle (apart from the zero mode), and correspond to modes of density relaxation.

In ergodic systems, the leading eigenvalue  $\gamma_0 = 0$  is non-degenerate, and manifests the conservation of probability density. Thus any initial density relaxes, in the course of time, to the state associated with  $\gamma_0$ . If, in addition, this relaxation is exponential in time, then the Perron-Frobenius spectrum has a gap associated with the slowest decay rate. Thus, the first non-zero eigenvalue has the property  $\gamma'_1 \equiv \text{Re}(\gamma_1) > 0$ . This gap sets the ergodic time scale,  $t_e = 1/\gamma'_1$  over which the classical dynamics relaxes to equilibrium. In the case of disordered metallic grains it coincides with the transport time,  $t_D$ , while in ballistic systems or quantum billiards it is of order of the flight time across the system.

In the limit  $\Omega \gg \hbar\gamma'_1$  the perturbative expansion (40) is justified, and  $R_2$  takes the form of Eq. (32) but where the diffusion operator is replaced by the Perron-Frobenius operator. This result coincides with that obtained within the “diagonal approximation” of periodic orbit theory [99] thereby establishing a direct correspondence of the field theoretic and semi-classical approaches. In the limit  $\Omega \ll \hbar\gamma'_1$  the dominant contribution to the semi-classical action (39) arises from the ergodic classical distribution, the zero-mode  $\{H, T\} = 0$ . Taking this contribution alone, the action coincides with the *universal* action (33) from which one can deduce that correlations coincide with those of random matrix ensembles.

Although much attention has been paid to the spectral properties of the Perron-Frobenius operator, still little is known about the resonance spectra in dynamical systems. Uniformly hyperbolic (the so-called axiom A) systems, such as billiards with constant negative curvature, are characterized by exponential decay of classical correlation functions — i.e. the resonance spectrum of the

Perron-Frobenius operator has a gap. Irregular boundary scattering in two-dimensional billiards on flat surfaces is, instead, characterized by isolated resonances together with gapless modes (of low spectral weight) associated with weakly unstable periodic orbits.

Finally, although the resonance spectra of the Perron-Frobenius operator are well defined, the eigenstates associated with the resonances are themselves singular. This has important implications on the role of quantum “weak localization” corrections which are beyond the scope of these lectures. On this point we refer the interested reader to the insightful work of Aleiner and Larkin [112]

In conclusion, we have argued that the quantum statistical properties of chaotic structures are expressed in terms of a ballistic non-linear  $\sigma$ -model. Yet, although this model is a triumph of phenomenology, its formal derivation, as well as its properties are by no means fully understood. As such, it represents one of the many important areas of research discussed in these lectures which are still very much in a stage of early development.

To close this section we will leave behind the subject of quantum chaos, and explore the connection between the ballistic and diffusive action. In order to more selectively probe aspects of the kinematics we will couple our single particle Hamiltonian to a strong magnetic field. This directly leads to the physics of the

### E. Quantum Hall Effect

A particle moving in a random impurity potential and subject to a homogeneous weak magnetic field is specified by the Hamiltonian

$$\hat{H} = \frac{1}{2m} \left( \hat{\mathbf{p}} - \frac{e}{c} \mathbf{A} \right)^2 + V(\mathbf{r})$$

where  $V(\mathbf{r})$  is drawn from some short-ranged impurity distribution, and  $\mathbf{B} = \partial \times \mathbf{A}$ . Previously, we have studied the influence of a *weak* magnetic field on coherence phenomena in the disordered conductor. In the following, we wish to study the influence of a *strong* magnetic field where the kinematic effects become significant. To account for the latter we will make use of the ballistic formalism developed above.

Before turning to the formal analysis, we begin with some qualitative considerations concerning the clean system. Firstly, according to the classical theory of transport, an electron subject to a uniform magnetic field obeys the equation of motion

$$m\dot{\mathbf{v}} = -e\mathbf{E} - e\mathbf{v} \times \mathbf{B} - \frac{m}{\tau}\mathbf{v}.$$

Evaluating the current density  $\mathbf{j} = -en\mathbf{v}$  for a stationary solution (i.e.  $\dot{\mathbf{v}} = 0$ ), one obtains the following formulae for the longitudinal and transverse conductivity

$$\sigma_{xx} = \frac{\sigma}{1 + (\omega_c\tau)^2}, \quad \sigma_{xy} = \omega_c\tau\sigma_{xx},$$

where  $\omega_c = eB/mc$  denotes the cyclotron frequency, and  $\sigma = ne^2\tau/m$  represents the zero-field Drude conductivity. Finally, an inversion of the conductivity tensor reveals that

$$\rho_{xx} = \frac{1}{\sigma}, \quad \rho_{xy} = \frac{1}{\nu_F} \frac{h}{e^2},$$

where the “filling factor”, which measures the ratio of the number of electrons to the total flux through the system, is connected to the electron density by the relation  $\nu_F = 2\pi L_B^2 n$ , with  $L_B = \sqrt{\hbar c/eB}$  defining the magnetic length. Classically, the Hall resistivity scales linearly with the magnetic field.

Quantum mechanically, the situation is found to be quite different: instead the Hall resistivity is found to be constant

$$\rho_{xy} = \frac{1}{i} \frac{h}{e^2}, \quad i = 1, 2, \dots$$

within a certain range around each integer value of the filling factor  $\nu_F$  (see Fig. 41). At the same time, the longitudinal resistivity is found to be vanishing in these ranges so that

$$\sigma_{xx} = 0, \quad \sigma_{xy} = i \frac{e^2}{h}, \quad i = 1, 2, \dots$$

The discovery of this remarkable and unexpected phenomenon [113] earned von Klitzing a Nobel prize in 1985.

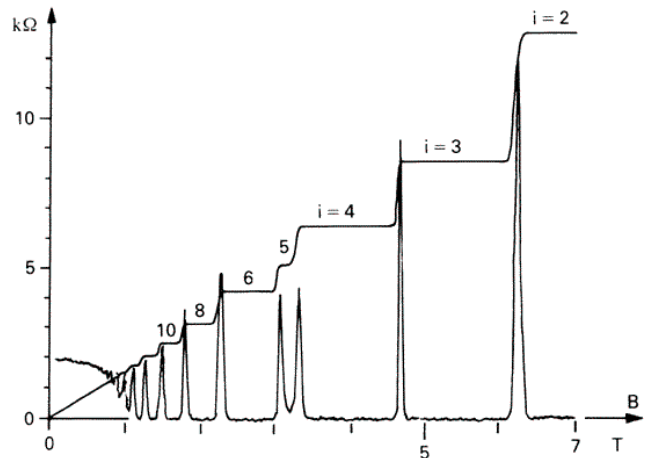


FIG. 41. The change of longitudinal  $R_{xx}$  and Hall resistance  $R_{xy}$  as a function of magnetic field. The Hall resistance varies stepwise with changes in magnetic field  $B$ . The step height is given by the constant of resistance  $h/e^2$  (ca. 25k $\Omega$ ) divided by an integer  $i$ . The figure clearly shows plateaus for  $i = 2, 3, 4, 5$ , and 6 (courtesy of Ref. [114]).

To discover the origin of the quantum Hall effect and to understand how it fits into the framework of the statistical field theory of disordered conductors, we must recall some elementary facts about the influence of a strong magnetic field on the dynamics of electrons. In the absence of disorder, the spectrum of a (spinless) electron confined to two-dimensions and subject to a strong uniform perpendicular magnetic field collapses into highly degenerate Landau levels separated in energy by  $\hbar\omega_c$ . Each Landau level is associated with an electron density of  $n = 1/2\pi L_B^2$  (i.e. a filling factor  $\nu_F = 1$  corresponds to the lowest Landau level being completely filled). When subjected to a weak random impurity potential, the degeneracy of each Landau level is lifted.

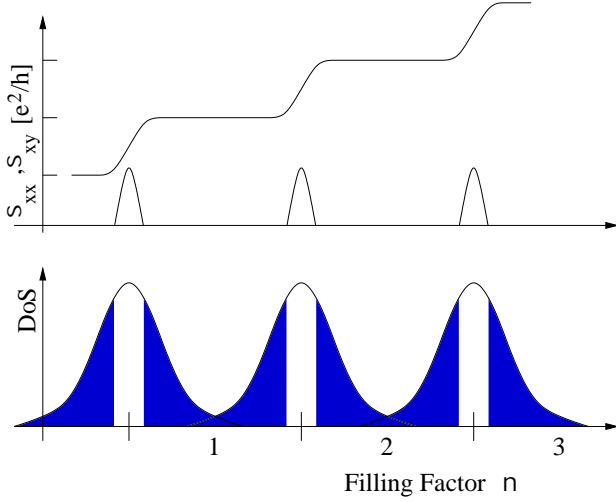


FIG. 42. Schematic diagram showing the broadening of the lowest three Landau levels due to disorder. A mobility edge is indicated separating a region of extended states at the band center, from a region of localized states (shaded) at the band edges.

Now, according to the phenomenology of the one-parameter scaling theory of localization, the eigenstates of a quantum particle confined to two-dimensions and subject to a weak impurity potential are localized. However, in the presence of a strong magnetic field, the localization length is seen to diverge on approaching the center of the Landau band. In a finite system, a region of extended states around the band center is separated from a region of localized states at the band edge by a sharp mobility edge (see Fig. 42). In the thermodynamic limit, this region shrinks leaving behind a single delocalized state at the band center.

Dissipative electric currents are due to transitions of charge carriers from occupied to empty states. At zero temperature, only states at the Fermi energy contribute to the conductivity. Therefore, when the Fermi energy lies in a region of localized states, the longitudinal conductivity  $\sigma_{xx}$  vanishes, while in the region of extended states, the conductivity assumes some non-zero value. By contrast, *every* occupied delocalized state contributes to the non-dissipative Hall current. Therefore, once in the region of delocalized states, the Hall conductivity  $\sigma_{xy}$  assumes a *constant* value. The value of the constant can be determined by invoking arguments of adiabatic continuity. In the clean system, the Hall conductivity associated with a filled Landau level is quantized in units of  $e^2/h$ . Adiabatically increasing disorder, the value of this Hall conductivity at each plateau remains at the same quantized value.

With this preparation, we now ask how this qualitative picture fits within the framework of the statistical field theory of the disordered conductor. To account for the orbital effects associated with the strong magnetic field, we will turn to the ballistic action (39). However, before we can import the field theory proposed above, we must first learn how to deal with the quantum nature of the short-ranged scattering potential  $V(\mathbf{r})$  due to the impurities. As with a Boltzmann equation, a quantum scattering potential can not be treated entirely within the framework of a kinetic action (39). Instead, one must explicitly take into account *irreversible* scattering processes. In such cases, a careful derivation of the effective action obtains an additional term which takes the form of a “collision integral” [102,104]. Taking the energy shell to be specified by the condition  $E_F = p_F^2/2m$ , the latter takes the form

$$S_{\text{qu.}} = -\frac{\pi^2}{\Delta^2} \int \frac{d\mathbf{r}}{L^d} \int \frac{d\mathbf{n}d\mathbf{n}'}{S_d^2} |V(\mathbf{n} - \mathbf{n}')|^2 \text{str}[Q(\mathbf{n})Q(\mathbf{n}')],$$

where  $\mathbf{n} = \mathbf{p}/p_F$  denotes the unit momentum vector,  $S_d$  represents the total  $d$ -dimensional solid angle, and  $V(\mathbf{n} - \mathbf{n}')$  represents the Fourier elements of the scattering potential.

In the presence of a strong magnetic field, the Cooperon degrees of freedom acquire a large mass and can be safely neglected. In this case we may focus on the reduced action for the Diffuson modes — the unitary model. Applied to a Gaussian  $\delta$ -correlated white-noise impurity potential (6), taking into account the Lorentz force due to the strong magnetic field, the total ballistic action takes the form [102,103]

$$S = i \frac{\pi}{2\Delta} \int \frac{d\mathbf{r}}{L^d} \int \frac{d\mathbf{n}}{S_d} \text{str} \left[ \Omega_+ \sigma_3^{\text{AR}} Q + 2i\hbar \sigma_3^{\text{AR}} T^{-1} \left( \mathbf{v} \cdot \partial_{\mathbf{r}} - \frac{e}{c} \mathbf{v} \times \mathbf{B} \cdot \partial_{\mathbf{p}} \right) T \right] + \frac{\pi\hbar}{4\tau\Delta} \int \frac{d\mathbf{r}}{L^d} \int \frac{d\mathbf{n}d\mathbf{n}'}{S_d^2} \text{str}[Q(\mathbf{n})Q(\mathbf{n}')],$$

where  $\mathbf{v} = \mathbf{n}p_F/m$ .

By analogy with the Boltzmann equation, for  $\Delta\tau \ll \hbar$  the ballistic action is easily converted to a diffusive form. To obtain the diffusive action we follow an approach similar to that employed by Muzykantskii and Khmel'nitskii [102].

Anticipating a rapid relaxation of the momentum dependent degrees of freedom of  $Q$  on the energy shell, and a slow variation of the spatial modes, we introduce a parameterization which involves the moment expansion  $T(\mathbf{r}, \mathbf{n}) = [\mathbb{1} + i\mathbf{n} \cdot \mathbf{W}(\mathbf{r})]T_0(\mathbf{r})$ , where  $[\sigma_3^{\text{AR}}, W]_+ = 0$ . Expanding the action to second order in  $\mathbf{W}$  and performing integrals over  $\mathbf{n}$  we obtain

$$S[Q] = \pi\nu \int d\mathbf{r} \text{str} \left[ i\frac{\Omega^+}{2}\sigma_3^{\text{AR}}Q - \frac{i\hbar|\mathbf{v}|}{3}\mathbf{W} \cdot T_0(\partial_{\mathbf{r}}Q)T_0^{-1} - \frac{\omega_c}{3}\sigma_3^{\text{AR}}\mathbf{W} \times \mathbf{W} - \frac{\hbar}{3\tau}\mathbf{W}^2 \right],$$

where  $Q(\mathbf{r}) = T_0(\mathbf{r})\sigma_3^{\text{AR}}T_0^{-1}(\mathbf{r})$ , and  $\omega_c = eB/mc$  denotes the cyclotron frequency. Finally, performing the Gaussian integration over  $\mathbf{W}$ , and treating the term arising from the Lorentz force perturbatively, we obtain the effective unitary action

$$S = \frac{\pi\nu}{2} \int d\mathbf{r} \text{str} [2i\Omega^+\sigma_3^{\text{AR}}Q + D_{xx}(\partial Q)^2 + D_{xy}\epsilon_{\mu\nu}Q(\partial_{r_\mu}Q)(\partial_{r_\nu}Q)] \quad (41)$$

where  $D_{xx} = v_F\ell/d$  and  $D_{xy} = D_{xx}\omega_c\tau$  represent the classical longitudinal and transverse diffusion constant.

From this result, we find that, in the presence of a strong magnetic field, the conventional diffusive action is modified by a topological or boundary contribution which strongly modifies the renormalization properties of the model. In this context, the renormalization properties have been first considered by Pruisken and collaborators [115] within the framework of a replica field theory. These investigations were in qualitative agreement with the phenomenology of a two-parameter scaling theory proposed by Khmel'nitskii [116]. The latter, which can be viewed as a natural generalization of the one-parameter scaling theory, implies that both the longitudinal and transverse components of the conductivity obey renormalization group equations

$$\frac{d \ln \sigma_{xx}}{d \ln L} = \beta_1(\sigma_{xx}, \sigma_{xy}), \quad \frac{d \ln \sigma_{xy}}{d \ln L} = \beta_2(\sigma_{xx}, \sigma_{xy}).$$

In two-dimensions, these equations exhibit a non-trivial fixed point at  $\sigma_{xx} = e^2/2h$  and  $\sigma_{xy} = (n + 1/2)e^2/h$  (see Fig. 43). (Note that the nature of the topological term places the constraint that the RG flow diagram must be periodic in  $\sigma_{xy}$ .)

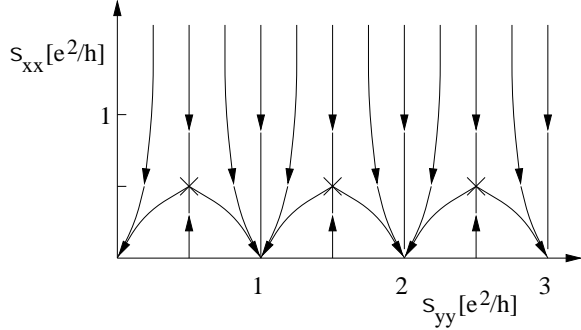


FIG. 43. The two-parameter scaling flow diagram of the integer quantum Hall effect.

Focusing on the lowest Landau level, the two-parameter scaling picture is in accord with the qualita-

tive discussion above. For an electron density less than  $\nu_F = 1/2$ , an increase of the system size leads to a renormalization of the longitudinal and Hall conductivities to zero. At a filling factor of  $1/2 < \nu_F < 1$ , the longitudinal conductivity flows to zero, while the transverse part flows to  $e^2/h$ . Finally, at  $\nu_F = 1/2$ , the system flows towards an unstable fixed point at a critical value of the longitudinal and Hall conductivity.

The success of the two-parameter scaling theory has been recorded in a number of papers including Ref. [117]. On the theoretical side, very recent investigations of the supersymmetric version of the action by Zirnbauer [118] have claimed to identify the conformal field theory governing the transition between quantized Hall plateaus of a disordered non-interacting 2d electron gas. For a review of the general field, we refer to Refs. [119,120].

#### IV. COULOMB INTERACTION PHENOMENA

In section I we saw that many of the coherence phenomena that characterize mesoscopic structures can be understood within the framework of a non-interacting theory. However, experiments both on quantum dots as well as extended semi-conducting electron heterostructures show that Coulomb interaction effects are by no means small. Indeed, dramatic manifestations of Coulomb interaction are seen in both confined and extended structures. Examples include Coulomb Blockade phenomena, low energy anomalies in transport and thermodynamic coefficients, non-Fermi liquid effects in effectively one-dimensional structures, various manifestations of the Kondo effect, the fractional Quantum Hall effect, and more. Given the vast extent of the literature on interaction phenomena in mesoscopic structures, we will not even attempt a complete survey of the field. Instead, staying within the streamline of these notes, we will ask whether the effects of Coulomb interaction be assimilated into the existing field theory. And if so, how would that approach connect to more conventional perturbative schemes and what kind of new information can be obtained?

The full statistical field theory describing the interplay of disorder and interaction contains many elements. We have already seen that, in a non-interacting time-reversal invariant system, at least two soft relaxation modes operate, the Diffuson and Cooperon. When combined with the spin singlet and triplet channels associated with the Coulomb interaction, a complete theory is likely to become unwieldy. To keep our discussion of the influence of Coulomb interaction pedagogical, we will therefore focus on a limited scenario restricting attention to a fictitious gas of spinless electrons interacting via a Coulomb interaction and subject to a weak (time-reversal symmetry breaking) magnetic field. (I.e. we shall not consider orbital effects associated with strong magnetic fields.) In focusing on spinless electrons, exchange effects associated with the electronic degrees of freedom do not arise.

Although the framework developed below is quite general, as a particular goal we will explore the phenomena of the zero-bias anomaly seen in the tunneling conductance measurements in a disordered metal (and described in chapter I). However, our aim is more ambitious. In studying this particular problem, we hope to address the wider phenomenology of electron dynamics in a disordered environment. We will see that the influence of electron interaction effects are strongly enhanced by the slow diffusive dynamics due to the impurity potential.

The starting point for our analysis is the microscopic many-body Hamiltonian  $\hat{H} = \hat{H}_0 + \hat{H}_C$ , where

$$\begin{aligned}\hat{H}_0 &= \int d\mathbf{r} c^\dagger(\mathbf{r}) \left[ \frac{1}{2m} \left( \hat{\mathbf{p}} - \frac{e}{c} \mathbf{A} \right)^2 + V(\mathbf{r}) \right] c(\mathbf{r}) \\ \hat{H}_C &= \frac{1}{2} \int d\mathbf{r} \int d\mathbf{r}' c^\dagger(\mathbf{r}) c^\dagger(\mathbf{r}') \frac{e^2}{|\mathbf{r} - \mathbf{r}'|} c(\mathbf{r}') c(\mathbf{r}),\end{aligned}$$

$c^\dagger(\mathbf{r})$  and  $c(\mathbf{r})$  represent the particle creation and annihilation operator, and, as usual,  $V(\mathbf{r})$  represents a Gaussian  $\delta$ -correlated impurity potential.

Our aim is to establish a statistical field theory describing the thermodynamic properties of the electron system: i.e. to determine the ensemble average free energy  $\langle F \rangle = -kT \langle \ln \mathcal{Z} \rangle$  of the electron gas. For this purpose we invoke the Replica field theory approach representing the free energy as the analytic continuation  $\ln \mathcal{Z} = \lim_{n \rightarrow 0} (\mathcal{Z}^n - 1)/n$ . Note that the Fermionic nature of the particles prohibits a supersymmetric formulation of the problem. Therefore, it is pertinent to ask whether we are equipped to deal properly with the analytic continuation  $n \rightarrow 0$ .

Indeed this issue has become the subject of some controversy in the literature. Broadly speaking, the state of affairs can be summarized as follows: as long as the field theory is evaluated perturbatively, the replica formalism stands on safe ground; the replica index then merely serves as a book-keeping index identifying disconnected, or vacuum contributions to the functional integral [121]. However, going beyond perturbation theory is problematic [122], inasmuch as the analytic continuation  $n \rightarrow 0$  becomes ill-founded and, when carried out

casually, may lead to incorrect results. Recently, ideas have been formulated [67,68], whereby the replica scheme is combined with an extended saddle point analysis of the  $\sigma$ -model, i.e. an approach that accounts for *all* stationary phase configurations of the model (including those that are perturbatively inaccessible from the ‘trivial saddle point’  $\sigma_3^{\text{AR}}$  discussed above.) Application of this approach to the *non-interacting* problem has correctly produced the large energy asymptotics of the two point correlation functions describing spectral correlations. (Here ‘large energies’ means energetic structures in access of the single particle level spacing.) Whether or not the scheme may be extended down to low energies (where the saddle point scheme becomes questionable) is the subject of some debate [66].

For completeness, we remark that a separate field theoretic approach has been developed which circumvents the explicit need for replicas. The latter, which is based on a technique due to Keldysh [123], has been introduced by Horbach and Schön [124] and developed further by Kamenev and Andreiev [125]. Application of methods similar to generalized saddle point scheme mentioned above [126] led to the correct form of spectral correlators. Summarizing, in any situation where the focus is on energy scales in access of the single particle level spacing, both the replica and Keldysh version of the nonlinear  $\sigma$ -model stand on safe ground and can be applied to the analysis of perturbative and non-perturbative problems.

### A. Matsubara Field Integral

To gain some confidence in the replica approach applied to a many-body Hamiltonian, we begin by focusing attention on the purely *non-interacting* model  $\hat{H}_0$ . Starting with the coherent state path integral, the replicated quantum partition function for a weakly disordered metallic conductor is given by

$$\mathcal{Z}_0^n = \int D[\bar{\psi}, \psi] e^{-\int_0^\beta d\tau \int \bar{\psi}_\alpha \left[ \partial_\tau + \frac{1}{2m} \left( \hat{\mathbf{p}} - \frac{e}{c} \mathbf{A} \right)^2 + V - E_F \right] \psi_\alpha}$$

where  $\psi_\alpha(\mathbf{r}, \tau)$  represent a set ( $\alpha = 1, \dots, n$ ) of Grassmann fields. Here the sum over repeated replica indices is assumed. (In the following, for simplicity, we will avoid explicitly writing out the replica indices.) Note that, were the Hamiltonian invariant under time-reversal, a further doubling of the field space would be necessary.

Switching to the Matsubara representation  $\psi(\tau) = (1/\sqrt{\beta}) \sum_{\epsilon_n} e^{i\epsilon_n \tau} \psi_{\epsilon_n}$ , where  $\epsilon_n = \pi(2n+1)/\beta$  denote Fermionic frequencies, the ensemble average over the Gaussian  $\delta$ -correlated impurity potential (6) generates a quartic interaction of the fields. Following our experience with the non-interacting theory, the latter are decoupled with the introduction of matrix fields non-local in time,

$$\begin{aligned}& \exp \left[ \int \frac{1}{4\pi\nu\tau_{\text{tr}}} \text{tr} (\psi \otimes \bar{\psi})^2 \right] \\ &= \int DQ \exp \left[ \frac{1}{2\tau_{\text{tr}}} \int \left( \sum_{mn} i\bar{\psi}_m Q_{mn} \psi_n - \frac{\pi\nu}{2} \text{tr} Q^2 \right) \right]\end{aligned}$$



where the normalization factor has been absorbed into the measure. Here note that the matrices  $Q = Q_{nm}^{\alpha\beta}$  carry both replica  $\alpha$  and Matsubara  $\epsilon_n$  indices. As usual, the symmetry properties of the matrix fields reflect those of the dyadic product  $\psi \otimes \bar{\psi}$  from which we deduce the hermiticity constraint,

$$Q^\dagger = Q. \quad (42)$$

Integrating over the Grassmann fields, the average replicated partition function takes the form

$$\langle Z_0^n \rangle = \int DQ \exp \left[ - \int \text{tr} \left( \frac{\pi\nu}{4\tau_{\text{tr}}} Q^2 - \ln \hat{G}^{-1} \right) \right]$$

where, defining the matrix of Matsubara frequencies  $[\hat{\epsilon}]_{nm} = \epsilon_n \delta_{nm} \otimes \mathbb{1}$ ,

$$\hat{G} = i\hat{\epsilon} - \frac{1}{2m} \left( \hat{\mathbf{p}} - \frac{e}{c} \mathbf{A} \right)^2 + E_F + \frac{i}{2\tau_{\text{tr}}} Q.$$

From this action, the derivation of the non-linear  $\sigma$ -model is straightforward. As with the single-particle theory, a variation of the action with respect to the matrix field  $Q$  obtains the usual saddle-point equation  $Q_{\text{sp}}(\mathbf{r}) = (i/\pi\nu)\mathcal{G}(\mathbf{r}, \mathbf{r})$ . Applying the ansatz,  $Q_{nm} = Q_{nn}\delta_{nm} \otimes \mathbb{1}$ ,

the diagonal elements are identified with the solutions of the self-consistent Born approximation for the self-energy. Taking into account the analyticity properties of the average Green function one obtains the solution  $Q = \Lambda$  where  $\Lambda = \text{sgn}(\hat{\epsilon})$ . As with the supersymmetric formulation, in the limit low energy limit (i.e.  $\epsilon_n \rightarrow 0$ ), the saddle-point solution expands to the degenerate manifold of homogeneous solutions,  $Q = T\Lambda T^{-1}$ .

Finally, subjecting the effective action to a gradient expansion stabilized by the condition  $\epsilon_F \tau_{\text{tr}} \gg 1$ , one obtains the non-linear  $\sigma$ -model functional

$$\langle Z_0^n \rangle = \int DQ \exp \left[ - \frac{\pi\nu}{4} \int \text{tr} [D(\partial Q)^2 - 4\hat{\epsilon}Q] \right]$$

where  $Q(\mathbf{r}) = T(\mathbf{r})\Lambda T^{-1}(\mathbf{r})$ . As with the non-interacting theory, to identify the low-lying modes of the effective action with the diffusion modes, we employ the parameterization

$$T = e^{-W/2}, \quad W_{nm} = \begin{pmatrix} \epsilon_m > 0 & \epsilon_m < 0 \\ -B^\dagger & B \end{pmatrix} \begin{matrix} \epsilon_n > 0 \\ \epsilon_n < 0 \end{matrix}.$$

Then, expanding the action to quadratic order in the generators, we obtain the Gaussian functional

$$\langle Z_0^n \rangle = \int DB \exp \left[ - \frac{\pi\nu}{2} \int \sum_{n>0, m<0} \left[ D \nabla B_{nm}^{\alpha\beta} \nabla B_{mn}^{\beta\alpha \dagger} + (\epsilon_n - \epsilon_m) B_{nm}^{\alpha\beta} B_{mn}^{\beta\alpha \dagger} \right] \right]$$

showing the diffusive nature of the propagator.

With these preliminaries, we turn now to the consideration of the influence of the Coulomb interaction. In this case, a separate Hubbard-Stratonovich field, local in time, must be introduced to decouple the Coulomb interaction of the fields. Applying a Hubbard-Stratonovich transformation to the replicated Coulomb interaction, one finds

$$\exp \left[ - \int_0^\beta d\tau \frac{1}{2} \int \int' \bar{\psi}(\mathbf{r}) \bar{\psi}(\mathbf{r}') \frac{e^2}{|\mathbf{r} - \mathbf{r}'|} \psi(\mathbf{r}') \psi(\mathbf{r}) \right] = \int D\Phi \exp \left[ - \int d\tau \int \left( \Phi \frac{\hat{\Gamma}_0^{-1}}{2} \Phi + i\bar{\psi} e \Phi \psi \right) \right],$$

where the Fourier transform of the form factor for the Coulomb interaction takes the form  $\Gamma_0^{-1}(\mathbf{q}) = \mathbf{q}^2/4\pi$  in three dimensions, and  $\Gamma_0^{-1}(\mathbf{q}) = |\mathbf{q}|/2\pi$  in two. Here, as with  $\psi$ , the fields  $\Phi$  carry replica indices.

## B. Plasma Theory of the Free Electron Gas

We begin by studying the conventional Gell-Mann Brückner theory [127] of a clean Hamiltonian free of disorder. Covering standard material, to be found in basically any textbook on many body theory, this introductory part of the analysis has been included to keep the discussion self-contained; expert readers are invited to directly proceed to the next section. After the Hubbard-Stratonovich decoupling, the quantum partition function for the interacting electron gas formally takes the form

$$\mathcal{Z}^n = \int D[\bar{\psi}, \psi] D\Phi e^{-\int d\tau \int \left[ \Phi \frac{\hat{\Gamma}_0^{-1}}{2} \Phi - \bar{\psi} \hat{G}^{-1} \psi \right]}$$

where

$$\hat{G}^{-1} = E_F - \partial_\tau - \frac{\hat{\mathbf{p}}^2}{2m} - ie\Phi.$$

Gaussian in the Fermionic fields, the functional integral can be performed exactly and yields the formal expression

$$\mathcal{Z}^n = \int D\Phi \exp \left[ - \int d\tau \int \Phi \hat{\Gamma}_0 \Phi + \ln \det \hat{G}^{-1} \right].$$

Setting  $e = 0$ , the auxiliary photon field decouples from the determinant and we recover the formal expression

for the partition function of the non-interacting electron gas. To deal with the functional integral over  $\Phi$ , further progress is possible within an approximation. In this case, we will take the strength of the Coulomb interaction to be weak and look for a perturbative expansion in  $\Phi$ . In fact, the constraints set by the Fermi liquid theory extend the validity of the phenomenology of this

expansion beyond the regime in which it can be formally justified.

Defining the bare free particle Green function (i.e. of the unperturbed system) as  $\hat{G}_0^{-1} = E_F - \partial_\tau - \hat{\mathbf{p}}^2/2m$ , and expanding in the strength of the interaction  $e$ , we obtain

$$\ln \det \hat{G}^{-1} \equiv \text{tr} \ln (\hat{G}_0^{-1} - ie\Phi) = \text{tr} \ln \hat{G}_0^{-1} + \text{tr} \ln [1 - ie\hat{G}_0\Phi] = \text{tr} \ln \hat{G}_0^{-1} - \text{tr} \left[ ie\hat{G}_0\Phi + \frac{1}{2} (ie\hat{G}_0\Phi)^2 + \dots \right].$$

Taking each term in order, we note that, since  $\Phi(0) = 0$  (due to an implicit neutralizing background),

$$\text{tr} [\hat{G}_0\Phi] = \frac{1}{\sqrt{\beta L^d}} \sum_{\omega_n, \mathbf{k}} \frac{1}{i\omega_n + \epsilon_{\mathbf{k}} - E_F} \Phi(0) = 0.$$

Similarly, defining the *density-density response function*.

$$\chi(\omega_n, \mathbf{q}) = -\frac{1}{\beta L^d} \sum_{\omega_n, \mathbf{k}} \frac{1}{i\omega_n + \epsilon_{\mathbf{k}} - E_F} \frac{1}{i\omega_n + i\omega_m + \epsilon_{\mathbf{k}+\mathbf{q}} - E_F} \quad (43)$$

where  $\epsilon_{\mathbf{k}} = \mathbf{k}^2/2m$ , the second term in the expansion gives

$$\frac{e^2}{2} \text{tr} [\hat{G}_0\Phi]^2 = \sum_{\omega_n, \mathbf{k}; \omega_m, \mathbf{q}} G_0(\omega_n, \mathbf{k}) \frac{\Phi_{\omega_m, \mathbf{q}}}{\sqrt{\beta L^d}} G_0(\omega_n + \omega_m, \mathbf{k} + \mathbf{q}) \frac{\Phi_{-\omega_m, -\mathbf{q}}}{\sqrt{\beta L^d}} = \sum_{\omega_m, \mathbf{q}} \frac{e^2}{2} \chi(\omega_m, \mathbf{q}) \Phi_{-\omega_m, -\mathbf{q}} \Phi_{\omega_m, \mathbf{q}},$$

Collecting together the bare photon action with this expansion, to leading order in  $e$ , the quantum partition function takes the form

$$\mathcal{Z} = \mathcal{Z}_0 \int D\Phi e^{-S[\Phi]},$$

where  $\mathcal{Z}_0$  denotes the partition function of the non-interacting gas, and the effective action for the photon field is given by

$$S[\Phi] = \frac{1}{2} \sum'_{\omega_n, \mathbf{q}} \frac{e^2}{D(\omega_n, \mathbf{q})} |\Phi_{\omega_n, \mathbf{q}}|^2 + O(e^4).$$

This result has a clear physical interpretation: the interaction of the electron gas with the electromagnetic field induces a modified *screened Coulomb interaction* (see Fig. 44),

$$D(\omega_n, \mathbf{q}) = \frac{1}{\epsilon(\omega_n, \mathbf{q})} \frac{4\pi e^2}{\mathbf{q}^2}, \quad \epsilon(\omega_n, \mathbf{q}) = 1 - \frac{4\pi e^2}{\mathbf{q}^2} \chi(\omega_n, \mathbf{q}),$$

where  $\epsilon(\omega_n, \mathbf{q})$  is the energy and momentum dependent effective *dielectric function*. This result, which is known in the literature as the *Random Phase Approximation (RPA)*, amounts to treating the long-range part of the Coulomb interaction as an “external” polarization field, and  $(4\pi e^2/\mathbf{q}^2)\chi(\omega_n, \mathbf{q})$  is known as the *screened polarizability*.

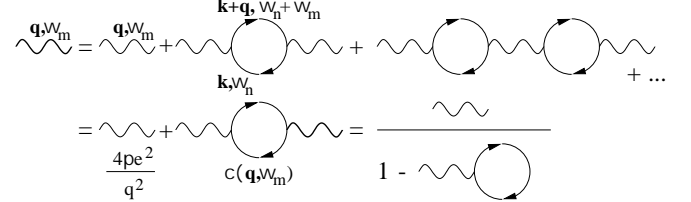


FIG. 44. The modified screened Coulomb interaction,  $D(\omega_n, \mathbf{q})$  can be viewed as the summation of an infinite ‘diagrammatic’ series expansion in the interaction: the bare Coulomb interaction vertex is ‘dressed’ by repeated particle-hole excitations of the electron gas. The corresponding summation of the geometric series (known as a *Dyson equation*) is shown schematically.

To explore the dielectric properties of the interacting electron gas it is necessary to understand the frequency and momentum dependence of the density-density response function (43). Making use of the analytical properties of the Green function, a summation over the Matsubara frequencies obtains the response function

$$\chi(\omega_m, \mathbf{q}) = -\frac{1}{L^d} \sum_{\mathbf{k}} \frac{n_{\mathbf{k}+\mathbf{q}} - n_{\mathbf{k}}}{i\omega_m + \epsilon_{\mathbf{k}} - \epsilon_{\mathbf{k}+\mathbf{q}}} \quad (44)$$

where

$$n_{\mathbf{k}} = \frac{1}{e^{\beta(E_F - \epsilon_{\mathbf{k}})} + 1}.$$

denotes the Fermi-Dirac distribution function.

To analyze the screened Coulomb interaction  $D(\omega_n, \mathbf{q})$ , we divide our consideration into two limits:

▷ **STATIC LIMIT** ( $|\omega_n| \ll k_F |\mathbf{q}|/m$ )

For frequencies small as compared to the momentum transfer (and temperatures  $T \ll E_F$ ), the response function converges to the static limit

$$\chi(0, \mathbf{q}) \simeq \frac{1}{L^d} \sum_{\mathbf{k}} \frac{\mathbf{q} \cdot \partial_{\mathbf{k}} n_{\mathbf{k}}}{\mathbf{q} \cdot \partial_{\mathbf{k}} \epsilon_{\mathbf{k}}} \simeq \int \frac{d^3 k}{(2\pi)^3} \partial_{\epsilon_{\mathbf{k}}} n_{\mathbf{k}} = \nu(E_F),$$

where  $\nu(E_F)$  represents the DoS at the Fermi level. Substituting this result into the expression for  $D(\omega_n, \mathbf{q})$ , and applying a Fourier transform, we obtain the static screened Coulomb interaction

$$V_{\text{screen}}(r) = \frac{e^2}{r} e^{-r/\lambda_{\text{TF}}},$$

where  $\lambda_{\text{TF}} = 4\pi e^2 \nu(E_F)$  defines the *Thomas-Fermi screening length*. Physically, on length scales in excess of  $\lambda_{\text{TF}}$ , the bare Coulomb interaction is screened by the collective fluctuations of the electron gas.

Taking into account higher order contributions in the interaction does not change the conclusions qualitatively. The screening behavior of the electron gas is preserved while the formula for the screen length  $\lambda_{\text{TF}}$  is modified by Fermi liquid corrections.

▷ **HIGH FREQUENCY LIMIT** ( $|\omega_n| \gg k_F |\mathbf{q}|/m$ )

By contrast, in the high frequency limit, the density-density response function takes the form

$$\begin{aligned} \chi(\omega_m, \mathbf{q}) &\simeq -\frac{1}{L^d} \sum_{\mathbf{k}} \frac{\mathbf{q} \cdot \partial_{\mathbf{k}} n_{\mathbf{k}}}{i\omega_m - \mathbf{q} \cdot \partial_{\mathbf{k}} \epsilon_{\mathbf{k}}} \\ &\simeq -\int \frac{d^d k}{(2\pi)^d} \frac{1}{i\omega_m} \left(1 - \frac{\mathbf{q} \cdot \mathbf{k}}{im\omega_m}\right) \mathbf{q} \cdot \partial_{\mathbf{k}} n_{\mathbf{k}} \\ &\simeq -\int \frac{d^d k}{(2\pi)^d} \frac{\mathbf{q}^2}{m\omega_m^2} n_{\mathbf{k}} = -\frac{\mathbf{q}^2}{m\omega_m^2} n, \end{aligned}$$

where  $n = N/L^d$  denotes the number density. Applying the analytic continuation to real frequencies,  $i\omega_n \rightarrow \omega + i0$ , we obtain

$$\lim_{m\omega/k_F|\mathbf{q}| \rightarrow \infty} D^R(\omega, \mathbf{q}) = \frac{4\pi e^2}{\mathbf{q}^2} \left[1 - \frac{\omega_p^2}{\omega^2}\right]^{-1},$$

where  $\omega_p = 4\pi e^2 n/m$  represents the *Plasma frequency*. This result has a natural physical interpretation: the response of the electron gas is not instantaneous but is retarded. At frequencies greatly in excess of the plasma frequency, the electrons are unable to screen an electromagnetic field and the bare Coulomb interaction is recovered.

How are these results modified when the particles are subject to a weak impurity potential? Qualitatively, we can expect the slow diffusive dynamics to have important manifestations on the screening and relaxation properties of the electron gas.

### C. Plasma Theory of the Disordered Electron Gas

With this background, we turn to the consideration of the influence of disorder. Applied to the impurity averaged, replicated partition function, the quantum partition of the electron gas takes the form

$$\langle Z^n \rangle = \int DQ \int D\Phi e^{-\int \left[ \frac{\pi\nu}{4\tau_{\text{tr}}} \text{tr} Q^2 - \text{tr} \ln \hat{G}^{-1} + \int d\tau \Phi \frac{\hat{G}_0^{-1}}{2} \Phi \right]}$$

where the full matrix Green function is defined by

$$\hat{G}^{-1} = i\hat{\epsilon} - \frac{1}{2m} \left( \hat{\mathbf{p}} - \frac{e}{c} \mathbf{A} \right)^2 - ie\Phi + E_F + \frac{iQ}{2\tau_{\text{tr}}}$$

Previously, with the non-interacting theory, we saw that fluctuations of the matrix fields separate into massive and massless contributions. On energy scales  $\epsilon \ll 1/\tau_{\text{tr}}$ , the latter, which are associated with the long-range diffusion mode contributions, dominate the low-energy effective action. By contrast, in the absence of the disorder potential, an expansion of the action in the fluctuations of  $\Phi$  obtains the Plasma theory of the screened Coulomb potential. A consistent theory of the interacting disordered metal must necessarily combine these two limits. To achieve a correct decoupling of the fast and slow degrees of freedom it proves convenient to take into account the gauge invariance of the action [125].

In its present form, the functional is invariant under the time and space local gauge transformation

$$Q(\tau, \tau'; \mathbf{r}) \mapsto \tilde{Q}(\tau, \tau'; \mathbf{r}) = e^{ik(\mathbf{r}, \tau)} Q(\tau, \tau'; \mathbf{r}) e^{-ik(\mathbf{r}, \tau')}.$$

Applied to the functional, taking  $k$  to be diagonal in the replica space, such a gauge transformation induces a vector potential,

$$\mathbf{A} \mapsto \tilde{\mathbf{A}} = \mathbf{A} - \frac{c}{e} \partial k, \quad e\Phi \mapsto e\tilde{\Phi} = e\Phi - \partial_\tau k.$$

In the following, we will find it convenient to leave the choice of gauge unspecified. Later, we will use (an approximation for) the saddle-point of the low-energy functional to specify a particularly convenient gauge.

Considering the high energy sector of the action,  $\epsilon \gg 1/\tau_{\text{tr}}$ , an expansion of the action obtains

$$\int \text{tr}_{\epsilon \gg 1/\tau_{\text{tr}}} \ln \left[ i\hat{\epsilon} - \frac{\hat{\mathbf{p}}^2}{2m} + E_F - ie\tilde{\Phi} \right] \simeq \frac{\nu}{2} \int \int d\tau e^2 \tilde{\Phi}^2$$

where high frequency and momentum corrections to the screened Coulomb interaction are neglected against the low energy content of the remainder of the action. In the high-frequency limit, the disorder has no influence on the dynamics of the electron degrees of freedom.

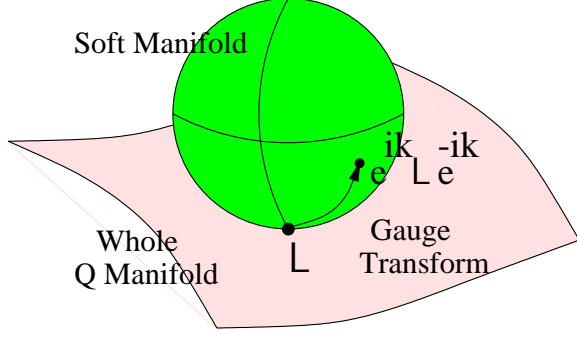


FIG. 45. Schematic diagram showing the action of the gauge transformation described in the text.

Turning to the low energy sector,  $\epsilon \lesssim 1/\tau_{tr}$ , setting  $Q = T\Lambda T^{-1}$ , and applying the gradient expansion

$$T^{-1}\hat{G}^{-1}T = E_F - \frac{\mathbf{p}^2}{2m} + \frac{i\Lambda}{2\tau_{tr}} + T^{-1} \left[ i\hat{\epsilon} - \frac{\mathbf{p}}{m} \cdot \hat{\mathbf{q}} - ie\tilde{\Phi} \right] T$$

where  $\hat{\mathbf{q}} = -i\partial - e\tilde{\mathbf{A}}/c$ , we obtain the non-linear  $\sigma$ -model action [128]

$$S[Q] = \frac{\pi\nu}{4} \int \text{tr} \left[ D(\tilde{\partial}Q)^2 - 4 \left( \hat{\epsilon} - e\tilde{\Phi} \right) Q \right]$$

where  $\tilde{\partial} = \partial - i(e/c)[\tilde{\mathbf{A}}, \cdot]$ . Combined with the high energy part of the action, and the bare Coulomb interaction, we obtain

$$\langle \mathcal{Z}^n \rangle = \int DQ \int D\Phi e^{-S[Q] - \frac{1}{2} \int d\tau \int d\mathbf{r} [\Phi \hat{\Gamma}_0^{-1} \Phi - e^2 \nu \tilde{\Phi}^2]}.$$

At this stage, it is tempting to immediately implement an expansion perturbative in the interaction, and in the diffusion modes. Indeed such an expansion recovers the results of diagrammatic perturbation theory contained in the literature [129]. However, the interaction field  $\Phi$  couples linearly to  $Q$ , which implies that the saddle-point configuration of the  $Q$  field is rotated from  $\Lambda$  (see Fig. 45). Put differently, the ground state of the interacting electron gas is modified by the impurity potential. A consistent expansion of the interaction (which avoids an infinite re-summation of diagrams) requires the identification of the true saddle-point of the theory.

#### D. Gauge Fixing: Low-Energy Saddle-Point

A variation of the low energy action with respect to  $Q$  subject to the non-linear constraint obtains the saddle-point equation,

$$D\tilde{\partial} \left( Q_{sp} \tilde{\partial} Q_{sp} \right) + \left[ \hat{\epsilon} - e\tilde{\Phi}, Q_{sp} \right] = 0.$$

Ideally, one would like to find the solution  $Q_{sp}$  which solves the equation exactly. However, for an arbitrary (in time and space) configuration of the field  $\tilde{\Phi}$ , such a program is impossible. Here, instead, we will fix the local gauge field  $k(\mathbf{r}, \tau)$  such that the saddle-point solution for  $Q$  approaches the non-interacting solution  $\Lambda$ . Thus, setting  $Q_{sp} = \Lambda$ , we obtain the non-linear equation for  $k$ ,

$$-\frac{c}{e} D\Lambda \partial^2 k \Lambda + \left( \frac{c}{e} \right)^2 Ds \partial k \Lambda \partial k \Lambda + [\partial_\tau k - e\Phi, \Lambda] = 0.$$

Neglecting the term second order in  $k$  (which is justified if the *spatial variation* of the gauge function  $k$  is small) the resulting linear equation has the (replica diagonal) solution

$$k(\omega, \mathbf{q}) = \frac{i\Phi(\omega, \mathbf{q})}{D\mathbf{q}^2 \text{sgn}(\omega) + \omega},$$

where  $\omega$  denotes a bosonic Matsubara frequency. Substituting this solution back into the action, one obtains the modified Coulomb interaction,

$$S = \frac{1}{2} \sum_\omega \int \Phi \hat{\Gamma}_{RPA}^{-1} \Phi, \quad \Gamma_{RPA}^{-1}(\omega, \mathbf{q}) = \Gamma_0^{-1}(\mathbf{q}) + \frac{\sigma \mathbf{q}^2}{D\mathbf{q}^2 + |\omega|}$$

where as usual  $\sigma = e^2 \nu D$ . This estimate, which in the present context is known as a random phase approximation, has a simple physical interpretation. The screening of Coulomb interaction in the disordered environment is modified by the diffusive dynamics of the electrons. The modification can be interpreted diagrammatically as an infinite summation of polarization loops dressed by diffuson modes (see Fig. 46).



FIG. 46. Diagrammatic representation of the RPA correction to the Coulomb interaction. The shading within the loop represents a diffusion ladder.

Now, in principle, an expansion of the action in the fluctuations of  $Q$  around the saddle-point leads to higher order quantum interference corrections. However, already at this order, we can obtain the dominant contribution to the tunneling anomaly since the latter can be interpreted physically as a consequence of diffusively slowed screening.

To illustrate the utility of the field theoretic approach, we turn to an application of the functional to examine the voltage dependence of the tunneling conductance  $G(V)$  of a particle from a point contact (or STM tip) onto a disordered metallic background. In particular, if the charge accommodation time is much longer than the transfer time from contact onto the metal, the tunneling conductance can be identified with the *single-particle* DoS,  $G(V) \sim \nu(\epsilon = eV)$ . The latter is defined as the imaginary part of the single-particle Green function

$$\nu(\epsilon) = -\frac{1}{\pi} \text{Im} \hat{G}(\mathbf{r}, \mathbf{r}; \epsilon_n) \Big|_{i\epsilon_n \rightarrow \epsilon + i0}.$$

The single-particle DoS can be expressed in terms of the functional integral above. Specifically, taking into account the gauge transformation, and performing the (trivial) replica to zero limit, the saddle-point approximation for the ensemble averaged local single-particle Green function is given by

$$\begin{aligned} \langle \hat{G}^>(\mathbf{r}, \mathbf{r}; 0, \tau) \rangle_V &= -i\pi\nu \left\langle e^{ik(0)} \Lambda_{-\tau} e^{-ik(\tau)} \right\rangle_{\Phi} = \\ &= -i\pi\nu \Lambda_{-\tau} e^{-S(\tau)} \end{aligned}$$

where  $\Lambda_{-\tau}$  represents the single-particle propagator for a clean system, and

$$S(\tau) = \frac{e^2}{2} \int \sum_{\omega_n} 4 \sin^2(\omega\tau) \frac{\Gamma_{\text{RPA}}(\mathbf{q}, \omega)}{(D\mathbf{q}^2 + |\omega|)^2}.$$

Here the self-consistency of the approach demands that the Matsubara summation and momentum integration are limited to the range  $|\omega|, v_F|\mathbf{q}| < 1/\tau_{\text{tr}}$ . Specifically, for a two-dimensional metal,

$$S(\tau) = \frac{e^2}{8\pi^2\sigma} \ln \left( \frac{\tau}{\tau_{\text{tr}}} \right) \ln (\tau\tau_{\text{tr}}\sigma^2(\nu e^2)^2).$$

Physically, the single-particle Green function  $\langle \hat{G}^>(\mathbf{r}, \mathbf{r}; 0, \tau) \rangle_V$  represents the amplitude for a particle injected into a disordered metal at a position  $\mathbf{r}$  at time  $\tau = 0$  to return to the point  $\mathbf{r}$  after a time  $\tau$ . That the action  $S(\tau)$  is imaginary expresses the fact that right after the tunneling, the particle is ‘under the energy barrier’, due to the Coulomb interaction with its own charge cloud. The structure of  $S(\tau)$  describes the diffusive relaxation of the charge density (the two diffusion poles), self-interacting through the RPA-screened Coulomb potential.

With this definition, the single-particle DoS is given by

$$\langle \nu(\epsilon) \rangle = \nu \int d\tau e^{\epsilon\tau - S(\tau)} \Lambda_{-\tau},$$

The latter is dominated by the stationary configuration of the total effective action which (to a good approximation) is obtained from the condition

$$\frac{\partial S}{\partial \tau} \Big|_{\tau_*(\epsilon)} = \epsilon.$$

Here  $\tau_*$  can be interpreted as the charge accommodation time. In two-dimensions, the latter is given by

$$\tau_* = \frac{1}{4\pi^2\epsilon g} \ln \left( \frac{\sigma\nu e^2}{\epsilon} \right),$$

a result which is self-consistent in the hydrodynamic limit  $\tau_* \gg \tau_{\text{tr}}$ , i.e. at  $\epsilon < e^2/\sigma\tau_{\text{tr}}$ . Substituting this expression back into the action, we obtain the tunneling conductance

$$\langle G(V) \rangle = G_0 e^{-\frac{e^2}{8\pi^2\sigma} \ln \left( \frac{e^2}{4\pi^2\sigma e V \tau_{\text{tr}}} \right) \ln \left( \frac{e^2 \tau_{\text{tr}} \sigma (\nu e^2)^2}{4\pi^2 e V} \right)}$$

where  $G_0$  denotes a voltage independent constant conductance. Diagrammatically, this results can be interpreted as the summation of an infinite series of diagrams for which the first is shown in Fig. 47.

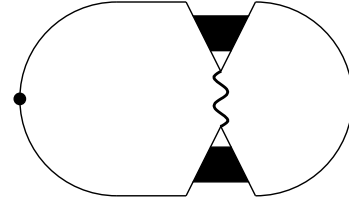


FIG. 47. Diagrammatic representation of the leading contribution to the Zero-Bias Anomaly. The exponential formula given in the text represents an infinite re-summation of a set of diagrams of which this contribution is the first.

The manifestation of Coulomb interaction in the tunneling anomaly is not unique. In particular, further analysis of the effective action, which goes beyond the leading approximation above, leads to a logarithmic enhancement of the conductivity. This quantum correction competes with the weak localization correction.

This completes our brief survey of the influence of disorder on Coulomb interaction phenomena in metallic structures. Needless to say, we have touched upon just a fragment of the literature in this field. Nevertheless, the physical concepts exhibited by screening and the zero-bias anomaly are representative of a wider class of interaction phenomena in disordered conductors. For a more comprehensive review of the field, we refer to Refs. [47,49,129–131,46].

Following on from the pioneering work of Wigner [85] on the properties of complex atomic nuclei, in a classic series of papers [22] Dyson introduced a complete classification of complex many-body systems according to their fundamental symmetries — “the three-fold way”. Using arguments based largely on mathematical grounds, Dyson proposed the existence of three universality classes which are distinguished by their invariance properties under time-reversal and spin rotation. In section IB6 we saw that the universal statistical properties of these classes are characterized by three random matrix ensembles, Unitary, Orthogonal and Symplectic. At the same time, the importance of the Wigner-Dyson scheme in the classification of the low-energy statistical properties of random and complex chaotic phase coherent quantum structures was stressed.

But is this classification exhaustive? In the course of the last few years it has become clear that the answer is negative, i.e. that various classes of stochastic quantum systems of current interest do not fall into the threefold classification scheme of Wigner and Dyson. Curiously, perhaps the most transparent ways of anticipating the existence these novel and *fundamental* symmetry classes is by purely formal mathematical reasoning:

Consider the  $N$ -dimensional Hamiltonian  $H$  of some (generally spin-full) quantum system. Besides Hermiticity, one commonly considers two additional discrete symmetries, invariance under time reversal  $\mathcal{T}$  and invariance under spin rotations  $\mathcal{S}$ :

$$\begin{aligned}\mathcal{T} : H &= \sigma_2 H^T \sigma_2, \\ \mathcal{S} : [H, \sigma_i] &= 0, \quad i = 1, 2, 3,\end{aligned}$$

where  $\sigma_i$  are Pauli matrices acting on spin. Depending on whether or not the symmetries  $\mathcal{T}$  and  $\mathcal{S}$  are realized, one has to distinguish four different cases. How can one embed these symmetry structures into the quantitative description of stochastic quantum systems?

The original method, put forward by Wigner and Dyson, did not concentrate on the Hamiltonian itself but rather on its transformation behavior. The idea was to demand that under unitary transformations  $H \mapsto U H U^\dagger$ ,  $U \in U(N)$  the fundamental symmetry of the Hamiltonian be not changed. E.g. for the case of a spin invariant ( $\mathcal{S} : +$ ) and time reversal invariant Hamiltonian, ( $\mathcal{T} : +$ ) this requirement entails  $U^* = U$ , i.e.  $U \in O(N) \subset U(N)$ , the orthogonal group in  $N$ -dimensions. A maximally entropic set of Hamiltonians, closing under all possible orthogonal transformations, forms the so-called Gaussian Orthogonal Ensemble, GOE, discussed above. Similar considerations for the other symmetry cases led to the introduction of the Gaussian Unitary and Symplectic Ensemble, respectively. (It is straightforward to show that both cases ( $\mathcal{T} : -, \mathcal{S} : +$ ) and ( $\mathcal{T} : -, \mathcal{S} : -$ ) fall into the unitary class.)

More recently an alternative scheme of classifying symmetries has been introduced. The new method, which focuses on the Hamiltonian itself rather than on its transformation behavior, has the advantage of hinting at a possible generalization of the three-fold Wigner Dyson classification. Considering the same Hamiltonian as before, we define  $X \equiv iH$ . The motivation for introducing  $X$  is that this object belongs to an *algebra*, viz. the algebra of anti-hermitian matrices,  $\mathfrak{u}(N)$  generating the unitary group  $U(N)$ . (We will denote the algebra of any group  $A$  by the corresponding small Latin character ‘ $\mathfrak{a}$ ’ throughout.  $\mathfrak{u}(N)$  generates  $U(N)$  in the sense that for  $X$  running through all of  $U(N)$ ,  $\exp(X)$  runs through all of  $U(N)$ .) As with the considerations above we next observe that the objects  $X$  corresponding to Hamiltonians of higher symmetry can not be drawn from the full algebra but rather symmetry restricted subsets thereof. Again using  $(\mathcal{T} : +, \mathcal{S} : +)$  as an example, we have  $X^T = X$ , implying that  $X \in \mathfrak{u}(N)/\mathfrak{o}(N)$ . (Here we have used the fact that the quotient vector space  $\mathfrak{u}(N)/\mathfrak{o}(N)$  forms the algebra of anti-hermitian symmetric matrices.) Exponentiating this sub-algebra we generate the *coset space*  $U(N)/O(N) \subset U(N)$ . Similar considerations for the case  $(\mathcal{T} : +, \mathcal{S} : -)$  lead to the identification of the coset space  $U(N)/Sp(N)$ . Why do we care to go through these, admittedly formal, manipulations? The motivation is that the sets  $U(N)$ ,  $U(N)/O(N)$  and  $U(N)/Sp(N)$  identified for the case of unitary, orthogonal and symplectic symmetry, respectively, possess a very high degree of mathematical structure: they are representatives of so-called compact symmetric spaces. Of such structures only ten different families, each indexed by an integer  $N$ , exist. (For simplicity, we restrict ourselves to the consideration of even  $N$ . For  $N$  odd, an eleventh symmetric space exists.) Rather than phrasing the comparatively involved definition of a symmetric space (c.f., for example, Ref. [132]) we here merely display the ten-fold classification, introduced and labeled by Cartan:

space	denotation
$U(N)$	A
$U(N)/O(N)$	AI
$U(2N)/Sp(2N)$	AII
$U(N+M)/U(N) \times U(M)$	AIII
$SO(N+M)/SO(N) \times SO(M)$	BDI
$Sp(N+M)/Sp(N) \times Sp(M)$	CII
$SO(N)$	BD
$Sp(N)$	C
$Sp(N)/U(N)$	CI
$SO(2N)/U(N)$	DIII

Above we have shown that the first three of these objects appear in the context of the established symmetry classes of Wigner and Dyson. One may now wonder whether the remaining seven spaces AIII, ..., DIII, too, might have any physical significance. Of course we would not have gone through the formal discussion above if the answer were not positive. Research done in the last few years

has shown that not only may these objects appear in principle, they even do so in rather interesting physical contexts. The principal connection between symmetric spaces on the one hand and their realization as symmetry classes of physical significance was first revealed in the seminal paper [133]. Focusing on application oriented aspects, the remainder of this section will discuss the emergence of the seven new classes in mesoscopic physics.

### A. Realizations of Novel Symmetries

Before turning to the discussion of any specific example, let us ask why the — seemingly exhaustive — Wigner-Dyson scheme might lack completeness. At the origin of the Wigner-Dyson analysis stands the assumption that the spectral properties of an ergodic quantum system are *on average translationally invariant in energy*. Even for systems where this assumption is not automatically fulfilled, e.g. due to systematic gradients in the mean DoS, the average spectrum can be made uniform by suitable ‘unfolding’ procedures. One may then proceed to analyse spectral fluctuations, as described by one of the classical symmetry ensembles. However, there are quite a few system classes where the average spectrum exhibits structure, not due to some non-universal features but due to *symmetry*. The example perhaps most familiar to condensed matter physicists is the superconductor. Here the chemical potential imposes a marked singularity on the spectrum, identified and protected through a particle-hole symmetry. It is such types of situations to which the enlarged classification scheme applies.

As a prototype system let us consider the example of a  $2N \times 2N$  matrix Hamiltonian

$$H = \begin{pmatrix} & Z \\ Z^\dagger & \end{pmatrix}, \quad (45)$$

where the matrix elements of the complex matrix  $Z$  are drawn at random from some distribution. As well as being Hermitian  $H^\dagger = H$ , the matrix Hamiltonian exhibits a *chiral symmetry* in the  $2 \times 2$  block space,

$$H = -\sigma_3 H \sigma_3. \quad (46)$$

In consequence, the eigenvalues are either zero, or come in pairs of opposite sign. In other words, the energy  $\epsilon = 0$  plays a special role implying that the average uniformity of the spectrum is broken in the vicinity of  $\epsilon = 0$ . In particular, the average spectral density of  $H$  close to zero energy is non-stationary, yet nevertheless *universal* (i.e., for sufficiently low energies, the average density is independent of the nature of the distribution of the elements  $Z$ ). Applying symmetry considerations like the ones outlined above to the chirally symmetric operator (45) one finds that  $H$  is tangent to the symmetric space  $U(2N)/U(N) \times U(N)$ , i.e. it belongs to symmetry class AIII.

In order to more explicitly assess the implications of the chiral structure of the Hamiltonian, we consider a random matrix implementation of the Hamiltonian  $H$ , i.e. a model where the blocks  $Z$  are drawn from some maximally entropic random distribution. (For the appearance of such models in physical applications, see below.) All information about the level statistics of this system is contained within the joint probability distribution function of the eigenvalues,  $P(\{\epsilon\})$ . Computing the Jacobian of the unitary transformations which bring the members of the ensemble of Gaussian distributed Hamiltonians to diagonal form,

$$H = U \begin{pmatrix} \hat{\epsilon} & \\ & -\hat{\epsilon} \end{pmatrix} U^{-1}, \quad \hat{\epsilon} = \text{diag}(\epsilon_1, \epsilon_2, \dots),$$

one obtains the distribution function [134]

$$P(\{\epsilon\})d[\{\epsilon\}] = \prod_{i < j} |\epsilon_i^2 - \epsilon_j^2|^\beta \prod_k |\epsilon_k|^\alpha e^{-\epsilon_k^2/v^2} d\epsilon_k \quad (47)$$

where  $\beta = 2$ ,  $\alpha = 2$ , and  $v$  represents the variance of the distribution. The structure of the distribution function makes both the breaking of spectral translational invariance and the special role played by  $\epsilon = 0$  manifest. (The function does not only depend on energy differences but also on the energies themselves; for levels approaching  $\epsilon = 0$ , the function vanishes.) The vanishing of spectral weight in the vicinity of  $\epsilon = 0$  has a simple physical interpretation: an energy level  $\epsilon$  attempting to approach zero encounters its partner  $-\epsilon$  approaching from the ‘other side’. The randomness implemented in the Hamiltonian implies that the two levels repel each other and that the close vicinity of 0 becomes a ‘no go zone’.

In addition to the fundamental chiral symmetry (46), the further symmetry under time-reversal (i.e.  $H^T = H$  or, equivalently,  $Z^* = Z$ ) can be imposed. According to the Cartan classification, a Hamiltonian of this type belongs to the class BDI. In this case, the corresponding distribution function takes the same general form as Eq. (47) but with  $\beta = 1$  and  $\alpha = 1$ . (An extension of (45) to a spinful structure identifies another symmetry class [133] which, for simplicity, we do not consider here.)

How does the chiral symmetry appear in the context of stochastic quantum physics? To mention one example, in the massless limit the dynamics of a relativistic fermion system is described by a Dirac operator  $\hat{D}$  anti-commutative with  $\gamma_5$  (i.e. in the basis in which  $\gamma_5$  is diagonal, the matrix elements of  $\hat{D}$  are block off-diagonal). When subjected to a random gauge field, the low-energy properties of the system are specified by one of the chiral symmetry classes. Here, the different ensembles correspond to different choices of the gauge group and the number of flavors [135]. As with generic chaotic systems, the low-energy behaviour of *finite size* systems of this type, as realized, e.g., in lattice QCD, can be

modeled by random matrix theory [136]. Later, in section VF, we will see that operators of chiral symmetry appear in other physical contexts including disordered single-electron systems.

In addition to the four chiral symmetry classes described above, there exist a further four classes associated with “particle/hole”-like structures. Again beginning with the simplest case,  $(\mathcal{T} : -, \mathcal{S} : +)$ , the Hamiltonian

$$H = \begin{pmatrix} a & b \\ b^\dagger & -a^T \end{pmatrix}, \quad (48)$$

where the block diagonal elements are Hermitian,  $a^\dagger = a$ , and the off-diagonal blocks are symmetric,  $b^T = b$ , exhibits the PH-symmetry

$$H = -\sigma_2 H^T \sigma_2. \quad (49)$$

In this case, according to the Cartan classification scheme, the Hamiltonian (48) belongs to symmetry class C. Again, the distribution function takes the general form of Eq. (47), but now with  $\beta = 2$  and  $\alpha = 2$  [137]. By imposing the further symmetry of time-reversal (i.e.  $a^* = a$  and  $b^* = b$ ), the symmetry is raised to class CI;  $\beta = 1$  and  $\alpha = 1$ . Once again, an extension to a spinful structure identifies two more symmetry classes [133].

Hamiltonians of symmetry class C and CI also find applications in various branches of physics. Of these, perhaps the one most directly motivated from the form of the Hamiltonian is superconductivity. However, as we will see below, various stochastic classical operators can be classified as members of the symmetry class CI. A summary of the classification scheme for random matrix ensembles (without a symplectic structure), together with some common applications is tabulated below.

Class	RM Ensemble	Application
A	Dyson (GUE)	Conductor in $B$ -Field
AI	Dyson (GOE)	$\mathcal{T}$ -invariant Conductor
AIID	Chiral GUE	Random Flux Model
BDI	Chiral GOE	Imaginary Vector Potential
C	NS	Superconductor in Magnetic Field
CI	NS	Dirty d-wave Superconductor

In the following, we will explore some of the unusual spectral and localization properties which accompany these different classes. Our first application is to the study of the quantum coherence properties of dirty superconductors.

## B. Dirty Superconductivity

According to the phenomenology of the **BCS theory**, in the mean-field approximation, the quasi-particle Hamiltonian of a spin-singlet superconductor is specified by

$$\hat{H}_{\text{BCS}} = \int c_\sigma^\dagger \hat{H} c_\sigma + \int [\Delta c_\uparrow^\dagger c_\downarrow^\dagger + \text{h.c.}], \quad (50)$$

where  $\hat{H} = \hat{H}_0 + V$ . Here  $\hat{H}_0 = (\hat{\mathbf{p}} - (e/c)\mathbf{A})^2/2m - E_F$  denotes the bare Hamiltonian of the particle, and  $\Delta$  denotes the (complex) order parameter. In the Nambu representation, the corresponding quasi-particle Hamiltonian takes the  $2 \times 2$  matrix form  $\hat{H}_{\text{BCS}} = \int \psi^\dagger \hat{H}_{\text{GORKOV}} \psi$  where  $\psi^\dagger = (c_\uparrow^\dagger, c_\downarrow)$ , and

$$\hat{H}_{\text{GORKOV}} = \begin{pmatrix} \hat{H} & \Delta \\ \Delta^\dagger & -\hat{H}^T \end{pmatrix} \quad (51)$$

defines the Gor'kov Hamiltonian. A comparison of  $\hat{H}_{\text{GORKOV}}$  with Eq. (49) identifies the Gor'kov Hamiltonian as a member of symmetry class C. In the absence of an external magnetic field  $\mathbf{A}$ , a gauge can be specified in which the order parameter is real. In this case the Hamiltonian is symmetric under time-reversal  $\hat{H}_{\text{GORKOV}}^T = \hat{H}_{\text{GORKOV}}$ , and belongs to the higher symmetry class CI. Introducing Pauli matrices  $\sigma^{\text{PH}}$  which operate in the matrix or PH-sector of  $\hat{H}_{\text{GORKOV}}$ , the PH-symmetry (49) translates to the condition,  $\hat{H}_{\text{GORKOV}} = -\sigma_2^{\text{PH}} \hat{H}_{\text{GORKOV}}^T \sigma_2^{\text{PH}}$ .

In the absence of an impurity potential  $V$ , the clean  $\mathcal{T}$ -invariant Hamiltonian can be brought to the diagonal form

$$\epsilon_{\text{BCS}}(\mathbf{p}) = \pm (\epsilon_{\mathbf{p}}^2 + \Delta^2)^{1/2}$$

where  $\epsilon_{\mathbf{p}}$  represents the spectrum of the normal Hamiltonian  $\hat{H}_0$ . The corresponding single-particle DoS is then given by

$$\nu_{\text{BCS}}(\epsilon) = \frac{|\epsilon|}{\epsilon^2 - \Delta^2|^{1/2}} \theta(|\epsilon| - |\Delta|). \quad (52)$$

How does disorder influence the quasi-particle spectrum? In the normal metallic conductor, disorder was shown to have no influence on single-particle properties such as the DoS. Recalling that non-trivial phenomena in mesoscopic physics typically originate in the interference of advanced and retarded Green functions, one might speculate that the average DoS of the superconductor, a quantity represented by the single Green function,  $\hat{G}^\pm(\epsilon) = (\epsilon_\pm - \hat{H}_{\text{GORKOV}})^{-1}$  does not exhibit interesting behavior. The fact is, however, that the average superconductor DoS is a highly non-trivial object, influenced by various mechanisms of quantum interference. The reason for the failure of the above naive argument is that it does not account for the high degree of symmetry of the Hamiltonian or, equivalently, for the structural information encoded in (51): applied to the Gor'kov Green function, the PH-symmetry (49) translates to the property

$$G^\pm(\epsilon) = -\sigma_2^{\text{PH}} [G^\mp(-\epsilon)]^T \sigma_2^{\text{PH}} \quad (53)$$



which brings with it two implications: firstly it shows that the PH-symmetry entails a pole ambiguity; retarded and advanced Green functions are equivalent up to a PH-transformation. This pole structure implies that a *single* Gor'kov Green function displays a degree of complexity comparable to a *pair* of normal Green functions, a phenomenon whose physical consequences we are going to discuss below. Secondly, (53) shows that finite energies  $\epsilon$  break the PH-symmetry which is just another way of expressing the special role played by the band center. In the presence of disorder, these structures manifest themselves in the existence of soft modes which become massive for finite  $\epsilon$ . To better understand the formation of these modes and the mesoscopic phenomena caused by them, we turn to an effective field theory.

### 1. Field Theory of the Dirty Superconductor

The general construction of the low energy effective action for a bulk superconductor was first discussed by Oppermann [138], and later developed by Kravtsov and Oppermann [139] within the framework of a fermion replica field theory. Their approach was subsequently generalized to the supersymmetric scheme by Altland, Simons and Taras-Semchuk [140] in a study of the coherence properties of hybrid superconductor-normal structures. As usual, the field theoretic approach begins with the representation of the generating function of the Gor'kov Green function and its products as a functional field integral. As with the  $\mathcal{T}$ -invariant normal metallic systems, to accommodate the PH-symmetry of the Hamiltonian, it is convenient to make use of the “charge conjugation” operation (53) to affect a doubling of the field space.

Following the notation of Ref. [141] (and the general scheme as outlined in section II), the generating function of the Gor'kov Green function can be represented as a functional field integral involving four component superfields  $\psi$  which carry a PH-index and BF-grading. As with  $\mathcal{T}$ -invariant normal conductors, to take into account the particle/hole symmetry,  $\int \bar{\psi}(\hat{H}_{\text{GORKOV}} - \epsilon)\psi = -\int \psi^T \sigma_2^{\text{PH}}(\hat{H}_{\text{GORKOV}} + \epsilon)\sigma_2^{\text{PH}}\bar{\psi}^T$ , it is convenient to double the field space after which the generating function takes the form

$$\mathcal{Z}[J = 0] = e^{-i \int \bar{\Psi}(\epsilon - \sigma_3^{\text{CC}} - \hat{H}_{\text{GORKOV}})\Psi},$$

where

$$\Psi = \frac{1}{\sqrt{2}} \begin{pmatrix} \psi \\ \sigma_2^{\text{PH}} \bar{\psi}^T \end{pmatrix}, \quad \bar{\Psi} = \frac{1}{\sqrt{2}} (\bar{\psi} \quad -\psi^T \sigma_2^{\text{PH}}).$$

It is in this additional sector, hereafter known as the “charge conjugation” (CC) sector, that the Pauli matrices  $\sigma^{\text{CC}}$  operate. With this definition, the superfields  $\Psi$  and  $\bar{\Psi}$  obey the symmetry relations

$$\Psi = \sigma_2^{\text{PH}} \gamma \bar{\Psi}^T, \quad \bar{\Psi} = -\Psi^T \sigma_2^{\text{PH}} \gamma^{-1}$$

where  $\gamma = \mathbb{1}^{\text{PH}} \otimes (E_{\text{BB}} \otimes \sigma_1^{\text{CC}} - E_{\text{FF}} \otimes i\sigma_2^{\text{CC}})$ . Note that, in principle, one could further extend the field space to accommodate more than a single Green function in parallel. Moreover, according to Eq. (53), an extension of the field space to accommodate advanced and retarded degrees of freedom is unnecessary as one can be presented as a transform of the other.

Proceeding as with the normal conductor, taking the impurity potential to be Gaussian  $\delta$ -correlated, the interaction of the fields generated by the ensemble averaging over the impurity configuration can be decoupled with the introduction of  $8 \times 8$  component supermatrix fields  $Q$ . As a result, the generating functional takes the form

$$\langle \mathcal{Z}[J = 0] \rangle = \int DQ e^{\int \text{str}(\frac{\pi\nu_N}{8\tau} Q^2 - \frac{1}{2} \ln \hat{G}^{-1})} \quad (54)$$

where  $\nu_N$  denotes the normal average DoS, and

$$\hat{G}^{-1} = \hat{H}_{\text{GORKOV}}(V = 0) - \epsilon_- \sigma_3^{\text{CC}} + \frac{i}{2\tau} \sigma_3^{\text{PH}} Q,$$

represents the supermatrix Green function. Here the symmetry properties of the superfields reflect those of the dyadic product  $\psi \otimes \bar{\psi}$  and induce the symmetry constraint  $Q = \sigma_1^{\text{PH}} \gamma Q^T \gamma^{-1} \sigma_1^{\text{PH}}$  [141].

Previously, with the normal conductor, progress was made by subjecting the action to a mean-field analysis and studying the influence of slow fluctuations around the saddle-point by means of a gradient expansion. Here we can attempt to formulate a similar approach. Taking the typical strength of the disorder potential  $1/\tau$  to be greatly in excess of the strength of the order parameter  $|\Delta|$ , both the superconducting component as well as  $\epsilon$  can be treated as a weak perturbation. In this case, a variation of the action with respect to  $Q$  obtains the saddle-point equation  $Q_{\text{sp}}(\mathbf{r}) = i\mathcal{G}(\mathbf{r}, \mathbf{r})\sigma_3^{\text{PH}}/\pi\nu$ . As usual, identifying the saddle-point solution with the self-consistent Born approximation for the average Green function, we obtain the solution  $Q_{\text{sp}} = \sigma_3^{\text{PH}} \otimes \sigma_3^{\text{CC}}$ .

However, as with the normal conductor, the invariance of the action as  $\mathbf{A} \rightarrow 0$ ,  $|\Delta| \rightarrow 0$  and  $\epsilon \rightarrow 0$  under the spatially homogeneous transformation  $Q(\mathbf{r}) \mapsto TQ(\mathbf{r})T^{-1}$  where  $T$  is compatible with the symmetry properties of  $Q$ , identifies an entire saddle-point manifold. A gradient expansion of the action which takes into account the soft modes of the theory associated with the saddle-point manifold obtains the non-linear  $\sigma$ -model action,

$$S[Q] = -\frac{\pi\nu_N}{8} \int \left[ D(\tilde{\partial}Q)^2 - 4i \left( \epsilon_- \sigma_3^{\text{CC}} + \hat{\Delta} \right) \sigma_3^{\text{PH}} Q \right]. \quad (55)$$

where  $\hat{\Delta} = |\Delta| \sigma_1^{\text{PH}} e^{-i\phi} \sigma_2^{\text{PH}}$ ,  $\tilde{\partial} = \partial - i(e/c)\mathbf{A}[\sigma_3^{\text{PH}}, \cdot]$  and, as usual, the supermatrix fields are subject to the non-linear constraint  $Q(\mathbf{r})^2 = \mathbb{1}$ .

As anticipated from our preliminary considerations of the Gor'kov Green function, the form of the effective action closely resembles that of the normal conductor. Indeed, removing the order parameter, and identifying the

base point  $\sigma_3^{\text{PH}} \otimes \sigma_3^{\text{CC}}$  of the manifold with  $\sigma_3^{\text{AR}} \otimes \mathbf{1}^{\text{TR}}$  the action of the normal conductor (31) and (55) coincide. By analogy with our previous discussions, the action shows that the soft modes associated with density relaxation in the PH-channel are made massive by the frequency source,  $\epsilon$ . However, in contrast to the normal metal, the order parameter  $\Delta$  further reduces the degeneracy of the saddle-point manifold even at  $\epsilon = 0$ .

## 2. Mean-Field Theory

To determine the influence of the order parameter on the low-lying structure of  $S[Q]$  it is necessary to subject the non-linear  $\sigma$ -model action to a further saddle-point analysis.

No confusion should arise as to the iterated use of saddle point analyses: our model comes with a hierarchy of energy scales,

$$E_F \gg \frac{1}{\tau}, \Delta, \epsilon \gg \delta.$$

The first saddle point analysis, stabilized through the inequality 1) has led to the general saddle point manifold  $T(\sigma_3^{\text{PH}} \otimes \sigma_3^{\text{CC}})T^{-1}$ . Symbolically, the  $T$ 's can be understood as rotations tracing out the angular degrees of freedom of the mexican hat type structure shown in Fig. 26. The radial gradients identifying the bottom of the hat are steep (1)). Looking at the model on a higher resolution scale, one notices that the bottom of the well is not energetically uniform. This is visualized in Fig. 26 for the simple case of a normal metal action coupling to an energy parameter  $\Omega$ . The latter caused some symmetry breaking and identified  $\sigma_3^{\text{AR}}$  as the energetically favourable saddle point on the low energy manifold. In the present case, the additional presence of the parameter  $\Delta$  leads to a more complex low energy structure to be discussed below. At any rate, in cases where 2) holds a second saddle point analysis will be applied to identify low-lying sub-structures on the bottom of the large scale saddle point manifold.

To keep our discussion simple, we will hereafter limit our consideration to a  $\mathcal{T}$ -invariant Hamiltonian  $\mathbf{A} = 0$ , wherein we adopt a gauge in which the phase of the order parameter  $\phi$  is set to zero. In this case, a variation of the action with respect to  $Q$  subject to the non-linear constraint  $Q^2 = \mathbf{1}$ , obtains the low-energy saddle-point equation

$$D\partial(Q_{\text{SP}}\partial Q_{\text{SP}}) + i[Q_{\text{SP}}, \mathbf{\Omega} \cdot \mathbf{\Sigma}] = 0 \quad (56)$$

where we have defined the vectors  $\mathbf{\Omega} = (0, -i|\Delta|, \epsilon)$  and  $\mathbf{\Sigma} = (0, \sigma_2^{\text{PH}}, \sigma_3^{\text{PH}} \otimes \sigma_3^{\text{CC}})$ . Homogeneity of the gap function  $\Delta$  implies homogeneity of the saddle-point solution,  $Q_{\text{SP}}(\mathbf{r}) = Q_{\text{SP}}$ . Applying the ansatz  $Q_{\text{SP}} = \hat{\mathbf{q}} \cdot \mathbf{\Sigma}$ , where  $\hat{\mathbf{q}}^2 = 1$ , the saddle-point equation translates to the condition  $\hat{\mathbf{q}} \times \mathbf{\Omega} = 0$ . From this equation we obtain the

homogeneous solution  $\hat{\mathbf{q}} \propto \mathbf{\Omega}$ . A consideration of the analytic properties of the Green function requires that the branch cut in the definition of  $\mathbf{\Omega}$  lies along the negative real axis. With this choice

$$\hat{\mathbf{q}} = \frac{\mathbf{\Omega}}{|\mathbf{\Omega}|} \times \begin{cases} 1 & |\epsilon| > |\Delta| \\ -i\text{sgn}(\epsilon) & |\epsilon| < |\Delta|. \end{cases} \quad (57)$$

Applied to the DoS, the saddle-point solution reproduces the DoS corresponding to that of a *clean* bulk superconductor,

$$\langle \nu(\epsilon) \rangle = \frac{\nu_N}{8} \text{Re} \langle \text{str}(Q\sigma_3^{\text{CC}} \otimes \sigma_3^{\text{PH}} \otimes \sigma_3^{\text{BF}}) \rangle_Q \stackrel{Q \rightarrow Q_{\text{SP}}}{\simeq} \nu_{\text{BCS}}(\epsilon).$$

On the level of the saddle-point or mean-field, disorder has no influence on the average DoS of the superconductor.

## 3. Fluctuations

In taking into account fluctuation corrections to the mean-field solution, it is first necessary to identify the different classes of soft modes that operate in the vicinity of the saddle-point. Based on our earlier considerations of the fundamental symmetries, we anticipate the existence of two separate universality classes, CI and C. With  $\epsilon = 0$ ,  $\mathbf{A} = 0$ , and  $\Delta$  (real and) arbitrary, the action is invariant under global transformations

$$Q(\mathbf{r}) \mapsto TQ(\mathbf{r})T^{-1}, \quad (58)$$

where  $T$  is constant in space and obeys the conditions  $\gamma = T\gamma T^T$  and  $\sigma_2^{\text{PH}} = T\sigma_2^{\text{PH}}T^T$ . Formally,  $T$  belongs to the manifold  $\text{OSp}(2|2) \times \text{OSp}(2|2)$ . Dividing off those transformations  $H: T \mapsto TH$  which leave  $\sigma_3^{\text{PH}} \otimes \sigma_3^{\text{CC}}$  invariant (i.e.  $H\sigma_3^{\text{PH}} \otimes \sigma_3^{\text{CC}}H^{-1} = \sigma_3^{\text{PH}} \otimes \sigma_3^{\text{CC}}$ ), the symmetry is reduced to the group manifold  $\text{OSp}(2|2) \times \text{OSp}(2|2)/\text{OSp}(2|2) = \text{OSp}(2|2)$  which defines the symmetry class CI.

Here, for completeness, we remark that under the influence of a non-vanishing external magnetic field  $\mathbf{A}$ , time-reversal symmetry is broken, the superconducting gap collapses, and the symmetry of the invariant manifold is reduced. Yet, for  $\epsilon = 0$ , the action remains invariant under global transformations  $T = \mathbf{1}^{\text{PH}} \otimes t$ , where the elements  $t \in \text{OSp}(2|2)$  obey the condition  $\gamma = t\gamma t^T$ . Dividing off those transformations  $h: t \mapsto th$  which leave  $\sigma_3^{\text{CC}}$  invariant (i.e.  $h\sigma_3^{\text{CC}}h^{-1} = \sigma_3^{\text{CC}}$ ), the symmetry is reduced to the quotient or coset space  $\text{OSp}(2|2)/\text{Gl}(1|1)$  which defines the symmetry class C.

Having specified the symmetry properties associated with the soft modes of the action, we are, at least in principle, in a position to investigate their influence on the DoS. Here, instead of carrying out that program in detail, to keep our discussion concise we merely state the outcome of such an analysis. Referring to Ref. [140] for technical details, an investigation of the influence of fluctuations on the average DoS reveals the existence of only

small corrections to the mean-field solution, perturbative in the parameter  $E_c/\Delta$ , above the gap edge. At least in the non-interacting model considered here, the integrity of the superconducting energy gap itself is *maintained* in the presence of an impurity potential!

In fact, this result is consistent with the celebrated **Anderson theorem** [142], and could have been anticipated from the outset: going back to the quasi-particle Hamiltonian (50), even in the presence of disorder, a canonical transformation which diagonalizes the bare Hamiltonian  $\hat{H}_{\text{GORKOV}}$  can be used to bring the matrix Hamiltonian to a block diagonal form. Diagonalized, the quasi-particle Hamiltonian has the spectrum  $E_i = \pm(\epsilon_i^2 + \Delta^2)^{1/2}$  where  $\epsilon_i$  denotes the eigenvalues of the disordered Hamiltonian  $\hat{H}$ . Evidently, the gap  $\Delta$  is preserved by the impurity potential. Put differently, Cooper pairs can be formed out of the exact time-reversed eigenstates of the random single-particle Hamiltonian, the DoS of which is largely unaffected by static disorder.

This conclusion also has a natural interpretation at the level of the diffusion modes. The soft modes associated with the PH-symmetry rely on the constructive phase interference of a particle with energy  $\epsilon$  and a hole with energy  $-\epsilon$ . Since the clean Hamiltonian exhibits no quasi-particle states below the gap, the “soft modes” are guaranteed to have a mass of at least  $\Delta$ .

At first sight, the conclusion of this investigation might seem disappointing: low-energy fluctuations associated with novel modes of density relaxation (in this case in the PH-sector) seem to have little role to play in the environment of a superconductor with a large uniform energy gap. However, as we will see shortly, such modes can have a dramatic effect on the phase coherence properties of gapless superconductors (e.g. those of  $d$ -wave symmetry), as well on the properties of a normal metal brought into contact with a superconductor.

### C. Hybrid Superconductor-Normal Systems

With this preparation, let us now consider the influence of disorder on the spectral properties of a hybrid superconductor-normal system. A superconductor brought into contact with a normal metal tends to impart aspects of its superconducting character onto the normal region. Underlying this effect is the mechanism of **Andreev scattering** by which an electron from the normal region is reflected at the SN-interface as a hole, and a Cooper pair is added to the superconducting condensate. This phenomenon has a striking effect on spectral and transport properties, known collectively as the **proximity effect**.

The essential features that distinguish Andreev scattering from normal scattering are summarized below:

- ▷ As opposed to ordinary specular reflection, Andreev reflection represents a process of **retro-reflection**. Apart from a slight angular mismatch proportional to the excitation energy  $\epsilon$  of a quasi-particle above the Fermi energy  $E_F$ , the hole is reflected back along the trajectory of the incoming electron (see Fig. 48).
- ▷ An electron with excitation energy  $\epsilon$  is scattered into a hole with energy  $-\epsilon$ .
- ▷ The hole acquires a scattering phase shift  $\pi/2 - \phi$  where  $\phi$  is the phase of the superconducting order parameter at the interface.

FIG. 48. Schematic diagram showing a typical pair of Feynman paths which, by the mechanism of Andreev scattering off the superconductor (the dark region), induce a non-zero expectation value of the anomalous average  $\langle c_{\uparrow}^{\dagger}(\mathbf{r})c_{\downarrow}^{\dagger}(\mathbf{r}) \rangle$ . Notice the propagation of the particle-hole pair-amplitude can be interpreted as classical diffusion along a trajectory  $\gamma$ .

An important consequence of Andreev processes is the formation of a Cooper pair amplitude  $\langle c_{\uparrow}^{\dagger}(\mathbf{r})c_{\downarrow}^{\dagger}(\mathbf{r}) \rangle$  in the normal metal region which, survives even in the disordered environment. The creation of a local pairing field expectation value can be heuristically understood from simple semi-classical considerations: consider the creation of an electron somewhere at a point  $\mathbf{r}$  inside a disordered metal adjacent to a superconductor (see Fig. 48). Due to the presence of disorder, the electron propagates diffusively. In doing so it may eventually strike the SN-interface and be Andreev reflected. In general the newly created hole may now diffuse along its own path. However, a particularly interesting situation arises if the hole happens to propagate along the path of the

incoming electron back to the point of creation. As a result we not only obtain a non-vanishing pairing field expectation value but also a quantity that is insensitive to disorder averaging: during their propagation through the disordered background, both the incoming electron and the outgoing hole accumulate a quantum mechanical scattering phase which depends sensitively on microscopic details of the disorder. However, owing to the fact that the two particles propagate along the same path these phases cancel each other to a large extent. (For an excitation energy  $\epsilon = 0$  the cancellation is, in fact, perfect. For non-vanishing  $\epsilon$  one obtains a phase mismatch  $\sim \epsilon L^2/D$ , where  $L$  denotes the separation of  $\mathbf{r}$  from the interface.) Of course, more generic paths, where the electron and hole follow different trajectories, also contribute to the pairing field amplitude. However such contributions vanish upon disorder averaging due to their strong phase dependence.

The non-vanishing of the anomalous average  $\langle c_{\uparrow}^{\dagger}(\mathbf{r})c_{\downarrow}^{\dagger}(\mathbf{r}) \rangle$  even within the normal region is the basic content of the proximity effect. Besides being robust against disorder, the pairing field amplitude possesses a number of important features (all of which are related to the phase argument above):

- ▷  $\langle c_{\uparrow}^{\dagger}(\mathbf{r})c_{\downarrow}^{\dagger}(\mathbf{r}) \rangle$  varies weakly as a function of  $\mathbf{r}$ . Specifically, it does not fluctuate on the scale of the wavelength, but rather on length scales set by the diffusion length  $L_{\epsilon} \equiv (D/\epsilon)^{1/2}$ .
- ▷ While phase coherent (i.e.  $\epsilon \gg T, \tau_{\varphi}^{-1}$ ), the anomalous average  $\langle c_{\uparrow}^{\dagger}(\mathbf{r})c_{\downarrow}^{\dagger}(\mathbf{r}) \rangle$  decays exponentially as a function of  $\epsilon L^2/D$  as one moves further into the normal region away from the SN interface.
- ▷ Quantitative expressions for the diffusive pairs of quantum paths entering the physics of the proximity effect are provided by diffuson modes in the PH-channel.
- ▷ Finally, the pairing field amplitude depends on the phases of the order parameters of the adjacent superconductors. If only a single superconducting terminal with constant phase  $\phi$  is present, the phase is inessential and can be eliminated by means of a global gauge transformation. More interesting situations arise when more than one superconductor is present. In such cases, the phase sensitivity of the pairing amplitude provides the mechanism for the stationary Josephson effect.

The non-vanishing of the pairing field amplitude heavily influences the properties of the normal metal compounds of SN-systems. Widely known examples of proximity effect induced phenomena are the DC and AC Josephson effect, which allow for the accommodation of supercurrent across an SNS-junction. Another important phenomenon is the dependence of the normal conductance on the phases of adjacent superconductors —

again triggered by the phase sensitivity of the proximity amplitude. However, for brevity, we again limit our consideration to the influence of the proximity effect on the quasi-particle spectrum inside the normal region.

FIG. 49. Schematic diagram showing phase coherent path configurations contributing to the renormalization of the DoS at the position  $\mathbf{r}$ . Top: first order diffusive contribution suppressing the metallic DoS. Middle: quantum correction to the leading order process. (Notice the structural similarity to the previously discussed Hikami box forming the origin of the weak localization correction in normal metals.) Bottom: higher order process. Contrary to the weak localization, the quantum corrections to the metallic DoS and must be summed to infinite order. This is effectively achieved by the solution of the Usadel equation (56).

Why should the local DoS be influenced by the Proximity Effect? An answer to this question, at least qualitatively, is provided by the identification of relevant phase coherent corrections. Referring to Fig. 49, a particle injected at a position  $\mathbf{r}$  can propagate diffusively through the normal region. In the simplest case, a phase coherent contribution to the local DoS at  $\mathbf{r}$  is provided by a closed path in which a particle is Andreev scattered into a hole and then, later, back to a particle. Taking into account the total  $\pi$  phase shift due to the Andreev scattering processes, the local DoS is diminished from the normal value by such a process.

At higher order in the number of Andreev scatterings, one can identify “weak localization” type processes (now in the PH-channel) which induce further corrections to the local DoS (see Fig. 49). Now, although such contributions are higher order in the number of Andreev scatterings, they nevertheless contribute at the same order. As a result, to account quantitatively for the influence of the proximity effect on the local DoS, it is necessary to take into account the accumulation of the infinite hierarchy of such contributions. Fortunately, this is achieved more efficiently within the framework of an effective low-energy action.

To investigate the influence of Andreev processes on the spectral properties of phase coherent SN devices we can again construct an effective low-energy field theory. For this purpose, we can immediately import the formalism developed for the bulk superconductor above. In particular, if the contact between the normal metal and superconductor is metallic, it suffices to consider the quasi-particle Hamiltonian (50) with an order parameter which takes a non-zero value only within the superconducting regions. (Strictly speaking, a rigorous approach would demand a self-consistent treatment of the order parameter particularly in the vicinity of the interface. However, at least for s-wave symmetry, the self-consistent solution is only slightly modified and the phenomenology of our discussion below applies.) By taking, for simplicity, the normal average DoS  $\nu_N$ , and scattering time  $\tau$  to be uniform throughout the S and N regions, the effective low-energy theory is represented by the same non-linear  $\sigma$ -model action as (55), with the inhomogeneity of  $\Delta$  understood.

Similarly, varying the action with respect to  $Q$ , the low-energy mean-field equation is given by Eq. (56). Historically, within this context, the saddle-point equation was first derived within the framework of a quasi-classical theory of the average Green function [71], and is known in the literature as the **Usadel equation** [143]. (For a review, see Ref. [144].)

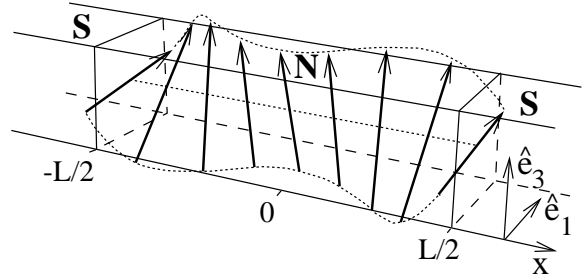


FIG. 50. Arrows showing the real part of the solution  $\hat{Q}$  applied to an SNS junction for a typical range of parameters (courtesy of Ref. [140]).

The qualitative form of the solution can be easily deduced from the asymptotic dependences: deep within the superconducting region, the solution to the saddle-point equation converges to the bulk value (57). While, deep within the normal region,  $Q_{\text{sp}} = \hat{\mathbf{q}} \cdot \boldsymbol{\Sigma}$  is dominated by the quasi-particle energy scale  $\epsilon$ , and converges on the bulk solution for the normal region,  $Q_{\text{sp}} = \sigma_3^{\text{PH}} \otimes \sigma_3^{\text{CC}}$ . To accommodate the spatial inhomogeneity of the gap function across the SN-interface, the matrix  $Q_{\text{sp}}$  “rotates” on a length scale set by the diffusion length  $L_\epsilon$ . Finally, current conservation at the SN-interface implies the boundary condition [145],  $\sigma_S Q \partial_\perp Q|_{\text{SN}} = \sigma_N Q \partial_\perp Q|_{\text{SN}}$ , where  $\sigma_S$  and  $\sigma_N$  denote the normal conductivity of the S and N

regions.

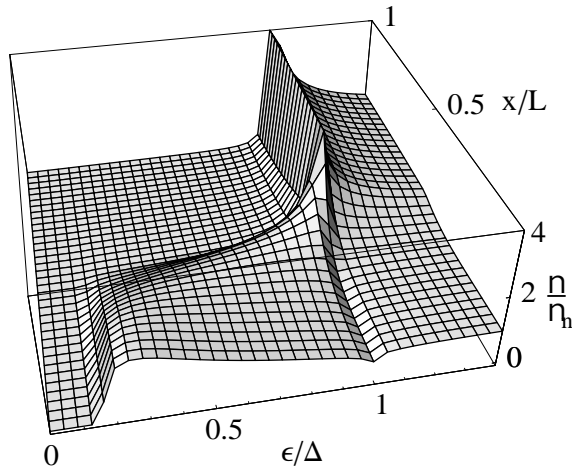


FIG. 51. Local DoS  $\nu$  of the SNS structure of Fig. 50 shown as a function of energy and position for a typical range of parameters (courtesy of Ref. [140]).

As with the bulk superconductor, an explicit solution of the saddle-point equation can be obtained by applying the ansatz,  $Q_{\text{sp}} = \hat{\mathbf{q}} \cdot \Sigma$ , after which Eq. (56) takes the form

$$\hat{\mathbf{q}} \times (D\partial^2 \hat{\mathbf{q}} - 2i\Omega) = 0.$$

An angular parameterization of  $\mathbf{q}$  brings the non-linear Usadel equation to the form of a sine-Gordon equation. A solution for the latter can be found in closed form. Again, leaving the details to Ref. [140], we focus on the qualitative form of the solution. Applied to an SNS-junction (with the geometry shown in Fig. 50) with a zero phase difference between the superconducting terminals, the solution to the Usadel equation is shown in Fig. 50 for a typical range of parameters. The corresponding local DoS, obtained as the projection of  $\hat{\mathbf{q}}$  onto  $\sigma_3^{\text{ph}}$ ,  $\nu(\mathbf{r}) = \nu_N \text{Re}[\hat{q}(\mathbf{r})]_3$  is shown in Fig. 51.

The most striking feature of the solution is the appearance of a spatially constant minigap of width  $\sim D/L^2$  in the local quasi-particle DoS of the normal metal region. While, within the superconductor, in the vicinity of the SN-interface, a non-zero local DoS develops below the gap. Away the interface, the latter decays exponentially on a scale set by the bulk coherence length  $\xi = (D/2\Delta)^{1/2}$ . Going beyond the quasi-classical mean field level, one may ask what happens to the gap once higher order quantum fluctuations around the mean field level are included. Interestingly, the gap turns out to be quite ‘hard’; it is robust to all orders in perturbation theory. (More precisely, a one-loop renormalization group analysis [140] ‘shifts’ the gap edge to  $D_{\text{ren}}/L^2$ , where  $D_{\text{ren}}$  denotes the renormalized diffusion constant discussed in section I, but leaves the hard gap edge intact.)

For completeness we should mention that a closer and essentially non-perturbative analysis [146–148] reveals the existence of DoS tails, *exponentially* small in the conductance, extending into the sub-gap region. Such tail-states form in the (exponentially improbable) case of a potential configuration that leads to almost perfect decoupling of superconductor and parts of the normal region, respectively. Within the field theoretical formalism, tail state formation is described by instantons connecting the quasi-classical mean field with perturbatively inaccessible configurations. The action associated with such configurations scales with  $g$  [140,147,148] (i.e. the overall statistical weight associated to tail state formation is  $\sim \exp(-g)$ ).

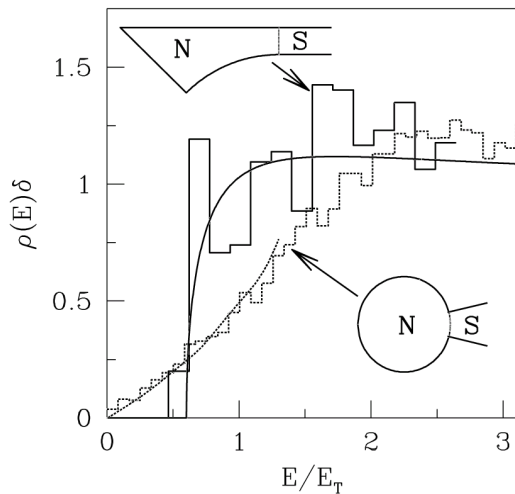


FIG. 52. Numerically computed DoS profile of an integrable and a chaotic Andreev quantum dot. Courtesy of Ref. [149].

It is interesting to compare the DoS structure of diffusive Andreev systems with that of more general system classes, i.e. integrable and generically chaotic. In a seminal paper [150] de Gennes and Saint-James theoretically considered a clean quasi two-dimensional (i.e. integrable) metallic film superimposed on a superconductor substrate, and found a DoS that vanished linearly upon approaching zero energy. This result exemplifies a general rule: the Andreev DoS of integrable systems vanishes upon approaching zero energy, but is non-gapped. In contrast, the DoS of finite chaotic SN systems is gapped, no matter whether chaoticity is caused by diffusive disorder or otherwise (c.f. Fig. 52). This was first formulated as a conjecture [149] and has since then been (theoretically) confirmed for numerous test-systems. Thus, the proximity effect acts like some kind of ‘litmus test’ sharply discriminating between cases of integrable and chaotic dynamics, respectively. To appreciate the relevance of the statement, one should keep in mind that traces of quantum chaos are usually sought for in rela-

tively subtle observables measuring spectral *correlations* or related. Here, one encounters a massive indication of chaos in a *mean* observable.

So far, there is no satisfactory theory of the gap in generic chaotic systems. (The test systems mentioned above have been studied numerically.) Semi-classical approaches to the problem have met with some limited success [151,152], i.e. it has been possible to understand the smallness of the DoS in the chaotic case, but not the formation of a gap. This is, again, due to the fact that semi-classics is not able to capture weak localization corrections, let alone the non-perturbative accumulation of weak localization type processes that is responsible for the formation of the gap. On this background, it is interesting to note that a theory of the proximity effect in non-stochastic structures can be cast in the form of the ballistic  $\sigma$ -model. The corresponding “kinetic equation” associated with the saddle-point also finds a counterpart in the early literature and is known as the Eilenberger equation [71]. Integration over fluctuations around the Eilenberger mean field [153], produces a DoS profile suppressed below the semi-classical prediction. However, largely due to the regularization problems mentioned above, this approach, too, does not have the status of a complete theory. Summarizing, the proximity DoS of chaotic systems represents a very basic observable, difficult to get under control theoretically, on which future theories of chaotic systems can be put to test.

This concludes our preliminary survey of the influence of quantum interference on the phase coherence properties of disordered hybrid SN-structures. Our discussion has focussed specifically on the influence of the proximity effect on the single-particle properties of the system. A discussion of the two-particle properties and the interplay of fluctuations in different channels can be found in Ref. [140].

Finally, we should note that Coulomb interaction effects can play an important role in the shaping the properties of dirty superconductors. Again, a generalization of the statistical field to account for interaction effects is achieved straightforwardly, while its analysis remains the subject of on-going research (for a review see, e.g., Ref [154].

The investigation of quantum coherence phenomena in hybrid SN-structures emphasizes the importance of discrete symmetries on the properties of weakly disordered systems. While the low-lying diffusion modes in the PH-channel were rendered massive by the gap function in the bulk superconductor, in the SN-environment the influence of these modes in the normal region can dramatically influence the quasi-particle spectrum. These results also beg the question as to whether the disorder can influence the properties of bulk superconductors with a non-trivial symmetry.

## D. Dirty d-Wave Superconductivity

To close our survey of coherence properties of disordered superconductors, we turn to the investigation of the influence of static disorder on the long-range properties of superconductors of unconventional *d*-wave symmetry. In recent years, the latter have come under intense scrutiny [155–166] in relation to the hole-doped high temperature cuprate superconductors. Indeed, these attempts to resolve the impact of impurity scattering on the low temperature spectral and transport properties of a disordered *d*-wave superconductor have ignited great controversy in the literature.

The key feature which distinguishes *d*-wave from conventional *s*-wave superconductors, and makes the influence of disorder harder to resolve, is the existence of low-lying gapless Dirac-like quasi-particle excitations at the Fermi energy. Beginning with the work of Gor’kov and Kalugin [155], and later by Lee [157], early considerations based on approximate self-consistent treatments suggested that an arbitrarily weak impurity potential induces a finite DoS at the Fermi surface, and leads to weak localization of all quasi-particle states in the two-dimensional system. This conclusion found support in an analysis of a Lorentzian distributed impurity potential by Ziegler *et al.* [161].

However, these conclusions were found to be in contradiction with those of Nersesyan *et al.* [158]. Mapping the *d*-wave system onto a conformally invariant Fermion replica field theory, the latter obtained a power law dependence of the quasi-particle DoS,  $\nu(\epsilon) \sim |\epsilon|^{1/7}$ , and proposed “critical” or power law localization properties of the quasi-particle states at the Fermi level. To further add to this controversy, a mechanism was proposed by Balatsky and Salkola [160] whereby the weak coupling of “marginally-bound” impurity states at the Fermi level lead to the absence of quasi-particle localization.

Very recently, in a study by Senthil *et al.* [163], a novel transition between a “spin insulating” phase and “spin metallic” phase was proposed again within the framework of replica field theory. There, great emphasis was placed on the existence of both particle/hole and time-reversal symmetry of the random Hamiltonian. This property, which places the model in symmetry class *CI*, affords the existence of low energy (spin) diffusion modes which influence strongly the long-range localization behavior of the states near zero energy.

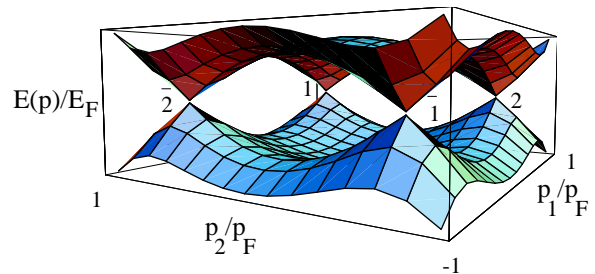


FIG. 53. The clean quasi-particle spectrum of a d-wave superconductor showing the existence of four Dirac nodes at the Fermi level

With this background, we begin our analysis with a simple model of the d-wave superconductor. In the vicinity of the Fermi energy, the phenomenology of a two-dimensional d-wave superconductor can be described by a Gor'kov Hamiltonian (51) with the real inhomogeneous order parameter,

$$\hat{\Delta} = \frac{|\Delta|}{p_F^2} [\hat{p}_1^2 - \hat{p}_2^2].$$

In the absence of disorder, the clean quasi-particle spectrum  $\epsilon_{\mathbf{p}} = \pm(\epsilon_{\mathbf{p}}^2 + \Delta^2)^{1/2}$  is characterized by the existence of four Dirac nodes at the Fermi level located at the momentum coordinates  $\mathbf{p}_a = (\pm 1, \pm 1)p_F/\sqrt{2}$  where  $a = 1, \bar{1}, 2$  and  $\bar{2}$ . (The assignment of the coordinates is shown in Fig. 53.) After subjecting the Hamiltonian to a  $\pi/2$  rotation in the PH-sector of the theory,  $\psi \rightarrow \exp[-i\pi\sigma_1^{\text{PH}}]\psi$ , an expansion of the Gor'kov Hamiltonian obtains

$$H_{\text{GORKOV}} = \sum_{\mathbf{p}a} \psi_{\mathbf{p}a}^\dagger \hat{\mathcal{H}}_{\text{DIRAC}}^{(a)} \psi_{\mathbf{p}a} \quad (59)$$

where, setting  $v_+ = p_F/m$ ,  $v_- = 2\Delta/p_F$ , and  $\hat{p}_\pm = \hat{p}_1 \pm \hat{p}_2$ ,

$$\begin{aligned} \hat{\mathcal{H}}_{\text{DIRAC}}^{(1)} &= -\hat{\mathcal{H}}_{\text{DIRAC}}^{(\bar{1})} = v_+ \hat{p}_+ \sigma_2^{\text{PH}} + v_- \hat{p}_- \sigma_1^{\text{PH}} \\ \hat{\mathcal{H}}_{\text{DIRAC}}^{(2)} &= -\hat{\mathcal{H}}_{\text{DIRAC}}^{(\bar{2})} = v_+ \hat{p}_- \sigma_2^{\text{PH}} + v_- \hat{p}_+ \sigma_1^{\text{PH}}. \end{aligned}$$

Adding disorder to the linearized Hamiltonian, the impurity potential can be separated into forward (intra-node)  $\hat{H}_{\text{FS}} = \hat{V}_0 \delta_{aa'} \sigma_2^{\text{PH}}$ , and backward (inter-node) scattering channels  $\hat{H}_{\text{BS}}$ . To formulate the effective field theory of the d-wave Hamiltonian, our strategy will be first to consider the forward scattering component, focusing on the properties of a single node, and then treat the backward scattering perturbatively.

### 1. Field Theory of a Single Dirac Node

To construct an effective field theory for a single node (say 1) we can make use of the preliminary analysis of the bulk s-wave superconductor. In particular, since the formulation of the functional (54) made no assumption about the symmetry of the order parameter, we can immediately cast the ensemble averaged generating functional for the d-wave case in the same general form but with the supermatrix Green function,

$$\hat{\mathcal{G}}^{-1} = \hat{\mathcal{H}}_{\text{DIRAC}}^{(1)} - \epsilon_- \sigma_3^{\text{CC}} + \frac{i\sigma_2^{\text{PH}}}{2\tau} Q.$$

Note that, according to the  $\pi/2$  rotation implemented earlier, the  $Q$  matrices obey a modified symmetry constraint.

As usual, further progress is possible only within a saddle-point approximation. However, in contrast to the bulk s-wave superconductor, the influence of the order parameter, and its effect on the structure of the clean quasi-particle spectrum demands a careful consideration of the saddle-point equation,  $Q_{\text{SP}}(\mathbf{r}) = i\mathcal{G}(\mathbf{r}, \mathbf{r})\sigma_2^{\text{PH}}/\pi\nu$ . Applying the ansatz  $Q_{\text{SP}} = q\sigma_2^{\text{PH}} \otimes \sigma_3^{\text{CC}}$ , the saddle-point solution is found from the (properly UV regularized) self-consistency condition,

$$q = \int \frac{d\mathbf{p}}{(2\pi)^2} \frac{1}{v_+^2 p_+^2 + v_-^2 p_-^2 + q^2/4\tau^2}.$$

However, as with the normal metallic conductor, at  $\epsilon = 0$ , the solution  $Q_{\text{SP}}$  is not unique, but rather the saddle-point is spanned by a whole manifold of solutions parameterized by

$$\sigma_2^{\text{PH}} Q = q \begin{pmatrix} \sigma_3^{\text{CC}} T & \\ & T^{-1} \sigma_3^{\text{CC}} \end{pmatrix}_{\text{PH}}.$$

where the spatially homogeneous  $4 \times 4$  supermatrices  $T$  belong to the *group* manifold  $\text{GL}(2|2)$ . Taking into account the slow variation of the fields  $T(\mathbf{r})$ , at  $\epsilon = 0$ , the low-energy effective action takes the form

$$S[T] = -\frac{1}{2} \text{str} \ln \left[ 1 + \frac{4\tau^2}{q^2} T^{-1} \hat{O} T \hat{O}^\dagger \right]$$

where  $\hat{O} = v_- \hat{p}_- - i v_+ \hat{p}_+$ .

### 2. Gradient Expansion

In this form, the effective action can be subjected to a gradient expansion. However, the Dirac structure of the clean quasi-particle action leads to UV divergences whose regularization must be treated with care. Fortunately, there exists a regularization procedure based on a “heat kernel expansion” [167] which provides a manifestly UV and IR regular scheme for expanding determinants of Dirac operators. In the present case, the analysis of Ref. [167] can be applied directly. Referring to Ref. [168] for a detailed discussion, we note that at  $\epsilon = 0$ , the effective action separates into two contributions,  $S = S_0 + S_{\text{WZNW}}$ : the first term in the action,

$$S_0 = -\frac{1}{16\pi v_+ v_-} \int \text{str} \left[ v_+^2 \partial_+ T \partial_+ T^{-1} + v_-^2 \partial_- T \partial_- T^{-1} \right]$$

denotes the standard gradient term of a non-linear  $\sigma$ -model action while, defining  $\tilde{T}(t=0) = \mathbb{1}$ , and  $\tilde{T}(t=1) = T$ , the second term

$$S_{\text{WZNW}} = \frac{i}{6\pi} \int_0^1 dt \int \epsilon^{\sigma\mu\nu} \text{str} \left[ \tilde{T}^{-1} \partial_\sigma \tilde{T} \tilde{T}^{-1} \partial_\mu \tilde{T} \tilde{T}^{-1} \partial_\nu \tilde{T} \right]$$

represents a Wess-Zumino-Novikov-Witten (WZNW) model (of level  $k = -1$ ). (Evidently, at least in the case



of a single node, a trivial rescaling of the coordinates allows the velocity scales  $v_+$ , and  $v_-$  to be removed from the action.) The forward scattering disorder couples to the action through

$$S_{\text{dis}} = \frac{g}{\pi^2} \int d^2r \text{str}(T^{-1} \partial_\mu T) \text{str}(T \bar{\partial}_\mu T^{-1}),$$

where  $g$  is a dimensionless constant measuring the strength of the disorder. Finally, at non-zero values of the energy  $\epsilon$ , the action acquires the relevant symmetry breaking perturbation

$$S_\epsilon = -\frac{\pi\epsilon}{2} \int \text{str}[T^{-1} + T].$$

Notice an intriguing feature of the field theory defined through  $S = S_0 + S_{\text{WZNW}} + S_{\text{dis}} + S_\epsilon$ : even if we switch off the disorder,  $S_{\text{dis}} = 0$ , it looks quite non-trivial. On the other hand, the non-disordered problem is just free relativistic fermions and, therefore, be exactly solvable. This means that the field theory must, in some way that is certainly not manifest from the appearance of its action, exactly solvable, too. The key to the solution of the problem lies in some fundamental connections between theories of free relativistic fermions on the one hand and group valued nonlinear  $\sigma$ -models on the other hand. Roughly speaking, the equivalence between the two theories represents a non-Abelian generalization of the celebrated bosonization approach to one-dimensional fermions: (1+1)-dimensional relativistic fermions can be represented in terms of a free bosonic field theory, a connection that forms the basis of the long success-story of theories of 1d-fermion materials (see [169] for a review). Indeed, it is straightforward to verify that a restriction of the matrix fields  $T$  to the Abelian sector, i.e. to their diagonal components, lets the action  $S$  collapse to a Gaussian form. The full matrix character of the  $T$ 's encodes the non-trivial  $\text{GL}(1|1)$  rotation invariance of the fermionic parent theory.

Further discussion of this point would directly lead us into the realm of **non-Abelian bosonization** and **conformal field theory** which lie well beyond the scope of the present text. Instead, we just summarize a few principal features of the WZNW theory. Two-dimensional models of this type have been studied extensively in the literature [170–172] and many of their properties are known independently of the specific realization of the field manifold. In particular it is known that the WZNW theory (i.e. at  $\epsilon = 0$ ) is *critical* and possesses an infrared attractive fixed point. The conformal invariance of the action indeed admits an exact computation of the scaling behavior of various physical observables. Without going into great detail, let us remark on some results of this analysis [172].

Now according to standard RG arguments (see, for example Ludwig *et al.* [173]) the local DoS can be shown to obey the homogeneity relation

$$\nu(E) = b^{-q} \nu(b^{2-q} E),$$

where  $q$  (which in the present case is equal to 1/3) denotes the scaling dimension of the primary field  $T$  and its inverse  $T^{-1}$  (i.e. the fields coupling to the DoS). Applying scaling concepts of conformal field theory [173,158,168] one identifies the dimension of the relevant combination  $T + T^{-1}$  as  $q = 1 - 2g/\pi$ . Solving the homogeneity equation for this value of  $q$  leads to

$$\nu(E) \sim |E|^\alpha, \quad \alpha = \frac{q}{2-q} = \frac{1-2g/\pi}{1+2g/\pi}. \quad (60)$$

Therefore, under the influence of disorder, a Dirac node spectrum is transformed to one in which the DoS vanishes as a power law with a disorder dependent exponent. Similarly, under renormalization, the bare coupling constant of the contribution  $S_0$  to the action, which in turn determines the spin conductance [163], flows to a universal value.

This completes our study of the spectral and transport properties associated with a *single* Dirac node. However, in the context of the *d*-wave superconductor, we must recall that four nodes contribute to the low-energy properties of the quasi-particle spectrum.

### 3. Mode Locking

Dealing first with the *intra-node* or forward scattering potential, an extension of the field manifold to accommodate all four Dirac nodes, reveals that no soft modes operate within the node-space: the soft manifold is described by four copies of a field theory with target manifold  $\text{GL}(2|2)$ . In fact, these field theories are not quite independent as can be seen from the following heuristic argument. (For a rigorous discussion of these aspects, see Ref. [168].) Consider quasi-particle excitations belonging to node 1. Low energy soft modes operating in this sector are characterized by a center of mass momentum  $\simeq (\pi/2, \pi/2)$ . What happens when the dynamics of the system is subjected to a time reversal operation? Clearly, the average component of the momentum will be flipped to its opposite, i.e.  $\simeq (-\pi/2, -\pi/2)$ , which is simply to say that time reversal maps node 1 onto  $\bar{1}$  and vice versa. From this picture it is plausible that the low energy field configurations of node 1 and  $\bar{1}$  are not entirely independent but rather related through some symmetry operations.

Yet this type of correlation is irrelevant as long as the nodes are not coupled through some concrete physical scattering mechanism. This is illustrated in Fig. 54 where the disorder dependent scaling exponents of a numerically simulated soft scattering *d*-wave superconductor are compared with the analytical prediction (60).

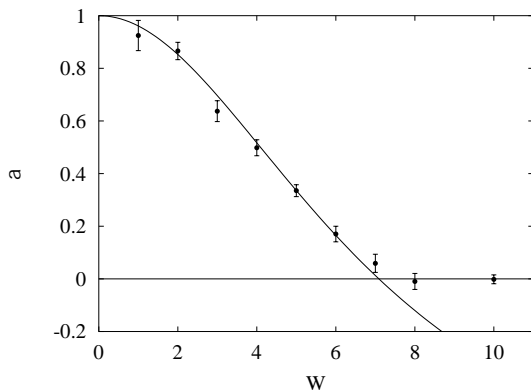


FIG. 54. Numerically computed scaling exponents of the DoS of a  $35 \times 35$  lattice  $d$ -wave superconductor in comparison with the analytical prediction (solid line). The parameter  $W$  parameterizes the strength of the disorder. Notice that the DoS exponents level off at a value of  $W$  that corresponds to a sign change of the scaling exponent. This conforms with a recent analytical prediction of a ‘phase transition’ in the  $d$ -wave quasi-particle system at large disorder,  $g = \pi/2$  [164]. Courtesy of Ref. [165].

But what happens when the influence of the *inter-node* scattering channels is taken into account? In the presence of an isotropic inter-node scattering potential, the low energy action of the theory contains an extra contribution

$$S_{\text{INT}} = -c_{\text{INT}} \int \sum_{aa'} \text{str} [T_a T_{a'}^{-1} + \text{h.c.}],$$

where  $c_{\text{INT}}$  represents the coupling constant associated with the scattering potential and the index  $a = (1, \bar{1}, 2, \bar{2})$  labels the nodes. For low enough energies  $\epsilon$ , the massive coupling locks the fields associated with each node. Roughly speaking, this has two consequences: first, the locking of the (symmetry related!) fields at nodes 1 and  $\bar{1}$  (similarly for 2 and  $\bar{2}$ ) leads to a symmetry reduction: the target manifold of the locked theory is  $\text{OSp}(2|2) \subset \text{GL}(2|2)$ . Second, the superposition of the separate theories leads to a *cancellation* of the WZNW term. As a result, the total effective action takes the form

$$S = - \int \text{str} \left[ \frac{1}{4\pi g} \partial T \partial T^{-1} + 4c_1 \epsilon (T + T^{-1}) \right],$$

where  $g = 2v_+ v_- / (v_+^2 + v_-^2)$  and  $T = T_1 = \doteq T_2$  is the ‘equilibrated’ field configuration. This is the generic form of the field theory of a time reversal invariant spin singlet superconductor, i.e. a superconductor belonging to symmetry class  $CI$  [138,139,163,168].

What conclusions can be drawn on the spectral properties of the  $d$ -wave superconductor? The one loop renormalization group equations of the field theory predict localization on some scale  $\xi$ . Following the logics of section IB 8 one expects that the low energy quasi-particle

spectrum will resemble that of a random matrix ensemble with a level spacing  $\Delta_\xi$ , i.e. the level spacing of a system with linear extent  $\xi$ . The matrix ensemble relevant for our present discussion is of type  $CI$  [137]. One of its hallmarks is a *linear* vanishing of the DoS at zero energy, on a scale set by the level spacing. (c.f. the disorder dependent power law vanishing obtained in the soft case.) Indeed, regimes with linearly vanishing DoS have been numerically identified [166]. However, given that localization lengths in two-dimensional systems are large, it is not obvious that the numerical analyses really probe a massively localized phase.

So far we have discussed the influence of *continuously* distributed disorder potentials on spectral properties of the  $d$ -wave superconductor. For completeness, let us mention that there is another way to model the disorder which has not been discussed so far. Rather than starting from some kind of smooth distribution, one may contemplate a set of *isolated* scattering centers, each described by some potential envelope function. Within this latter approach, which is commonly referred to as **Poisson distributed disorder**, averaging amounts to integrating over the impurity centers. In most mesoscopic applications, the specifics of the modeling are of no real concern, and one may employ the model that one finds technically most convenient. In the  $d$ -wave superconductor, however, the situation is different. The point is that infinitely strong repulsive impurities, so-called impurities at the unitary limit, may lead to the creation of zero energy impurity bound states [157]. I.e. for unitary scatterers, the DoS does not vanish at zero energy, it rather diverges. The qualitatively different spectral properties obtained from different modelings of the  $d$ -wave system ignited a lively debate as to which model is the ‘correct’ one. Interestingly, it took almost a decade to realize that there is no real contradiction, i.e. that the  $d$ -wave superconductor supports a number of different spectral profiles, depending on the realization of the disorder.

But which type of disorder is ‘real’, i.e. which comes closest to the situation encountered in experiment. This question is difficult to answer, especially for a theorist. On the face of it, disorder in  $d$ -wave superconductors is mostly realized in terms of Zn-donor atoms, which come fairly close to what one would term a unitary scatterer. However, too strong an amount of isotropic ( $s$ -wave) impurity scattering would not sit comfortably with the very formation of a  $d$ -wave order parameter phase. Indeed, it has been argued that the *effective* disorder potential seen by quasi-particles might be predominantly soft [174]. At any rate, the present body of experimental works on spectral and transport properties of the  $d$ -wave system does not allow for an unambiguous identification of both, the ‘relevant’ type of disorder and its localization properties. Our discussion above also entails that, for any given realization of the impurity potential, complex crossover scenarios between different universal regimes may be realized. E.g. for large energies, the inter-node coupling of a moderately soft potential may not suffice to effectively

lock the nodal soft modes (class AIII.) However, for lower energies, the relevancy of the inter-node coupling might stabilize a node-equilibrated phase (class CI.)

This concludes our survey of the influence of disorder on the quasi-particle properties of a  $d$ -wave superconductor. For completeness, we remark that, under the influence of an external magnetic field, the fundamental symmetry is reduced from class CI to class C. In the present context, this symmetry breaking transforms the WZNW term into a topological Pruisken term and admits, at least in principle, to the existence of a spin quantum Hall effect [175]. Whether such a state is realized in practice is the subject of continuing investigation.

The analysis above emphasizes the importance of discrete PH-symmetries in providing novel mechanisms of quantum coherence. Yet, as we have discussed earlier, PH-like symmetries represent just one class of models in which discrete symmetries play a crucial role. In the following we will examine how sublattice or chiral symmetries lead to unusual spectral and localization properties in so-called stochastic sublattice models.

### E. Systems with Chiral Symmetries

In section V A we had argued that there are basically two different categories of matrix systems with non-standard symmetry: systems with superconductor particle/hole symmetry and systems with chiral symmetry, i.e. systems whose Hamiltonian that can be cast into an off-diagonal structure (45). That superconductors play a prominent role in condensed matter physics does not need further explanation but what can be said about systems of the latter class? Indeed, there are quite a few condensed matter problems that possess inherent chiral symmetries:

- ▷ In the section on  $d$ -wave superconductivity, we have encountered a Fermion system that behaves essentially relativistic, i.e. a system whose dynamics is described by a massless Dirac operator. **Relativistic fermion systems** find numerous applications in condensed matter physics. They are realized in effectively one-dimensional conductors [176], narrow-gap semiconductors [177], anomalous superconductors [178], and others.
- ▷ In the next section we will discuss **bond-disordered lattice fermion systems**, i.e. lattice systems with stochastic inter-site hopping matrix elements. In cases where the host lattice is bipartite (e.g. cubic), such systems possess a chiral symmetry which leads to highly non-trivial localization behaviour in the vicinity of the tight binding band center.
- ▷ A number of problems of condensed matter and general statistical physics can be described in terms

of effectively **non-hermitian dynamical systems**. The behaviour of such systems, too, is affected by chiral symmetries, albeit in a less obvious sense than with the previously mentioned classes.

In the next section we will discuss bond-disordered fermion systems as an example of a problem with inherent chiral symmetry.

### F. Bond-Disordered Fermion Systems

The classes of disordered systems we discussed so far were described in terms of some continuum microscopic Hamiltonian  $\hat{H} = \hat{H}_0 + \hat{V}$ , where  $\hat{H}_0$  modeled the underlying ‘clean’ system (e.g.  $\hat{H}_0 = \hat{\mathbf{p}}^2/2m$ ), and disorder was introduced via some randomly distributed operator  $\hat{V}$  (e.g.  $\hat{V} = V(\mathbf{r})$  random). However, in lattice models, disorder is often implemented in terms of stochastic operators which operate in purely off-diagonal elements,

$$\hat{H} = - \sum_{\langle ij \rangle} \left[ c_{i\alpha}^\dagger U_{ij}^{\alpha\beta} c_{j\beta} + \text{h.c.} \right], \quad (61)$$

where  $\langle ij \rangle$  denote neighboring sites of a  $d$ -dimensional hypercubic lattice, the  $N$ -component operators  $c_{i\alpha}^\dagger$ ,  $\alpha = 1, \dots, N$ , create lattice Fermions, and  $U_{ij}^{\alpha\beta}$  represent  $N$ -dimensional matrices residing on the links of the lattice. Stochasticity is introduced by drawing the (generally complex) matrix elements  $U$  from some random distribution (subject to the Hermiticity requirement  $U_{ij} = U_{ji}^\dagger$ ). For  $N = 1$ , Hamiltonians of the type (61) are commonly referred to as **random flux** (RF) models, a denotation we will hereafter adopt for the cases  $N \neq 1$ . (Also notice that our Hamiltonian has dimensionality unity, i.e. all energies are measured in units of the tight binding band width.)

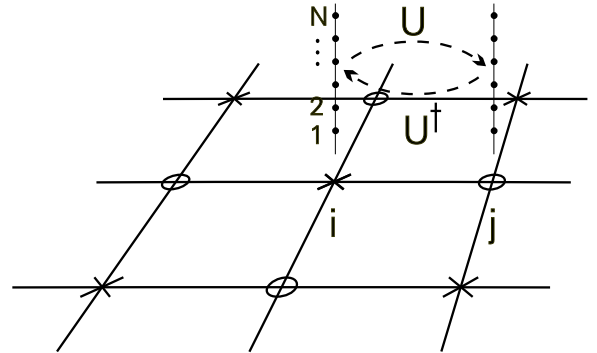


FIG. 55. The generalized random flux model.

In fact RF-models appear in a variety of different physical contexts: the two-dimensional  $N = 1$  version describes the dynamics of lattice Fermions subject to a random magnetic field or, more accurately, a random vector potential [179–183]. This model has also been discussed in connection with the physics of the half-filled fractional quantum Hall phase [184], the physics of the spin-split Landau level [181,197], and the gauge theory of high  $T_c$  superconductivity [186]. Identifying the two fermion components of the  $N = 2$  RF-model with a spin degree of freedom, (61) describes the propagation of lattice electrons on a spin-disordered background, a situation that occurs, for example, in connection with the physics of manganese oxides [187].

At first sight it would seem that the random flux Hamiltonian falls into the general category of Anderson Hamiltonians for disordered systems. Being Hermitian but not real, the Hamiltonian (61) is therefore expected to belong to the general class of models with unitary symmetry. As such, according to the one-parameter scaling theory, all states are expected to be Anderson localized in two-dimensions. However, as will be discussed below, this picture is correct only as long as one stays away from zero energy.

Being of pure nearest neighbor type (i.e. having no matrix elements connecting orbitals on the same site), the RF-Hamiltonian (61) possesses an implicit discrete symmetry which, as will be explored below, heavily influences the physical properties of the model. The nature of the symmetry can easily be understood by inspection of Fig. 55. As mentioned above, our model is defined on a bi-partite lattice, i.e. a lattice that can be subdivided into two nested sublattices (the  $\circ$ 's and the  $\times$ 's in Fig. 55). When represented in a  $(\circ, \times)$ -basis the lattice Hamiltonian becomes purely off-diagonal,

$$\hat{H} = \begin{pmatrix} & \hat{H}_{\circ, \times} \\ \hat{H}_{\times, \circ} & \end{pmatrix}.$$

This sublattice off-diagonal form of the Hamiltonian has led to the alternative denotation **sublattice** model for the bond-disordered system. More importantly for us, the form of  $H$  exposes an implicit chiral symmetry (46) and shows the spectrum to be symmetric,  $\epsilon \rightarrow -\epsilon$ . Therefore, according to the Cartan classification introduced in section V A, a generic member of the random flux Hamiltonian belongs to the chiral symmetry class AIII.

As with the  $d$ -wave superconductor, the existence of a chiral symmetry has far reaching consequences for the physics of the model at the band-center. Although the Hamiltonian is *always* chiral, i.e. not just in the band center, for finite energies the chiral symmetry is ineffective. The reason is that the information about both thermodynamic and transport properties of the system is encoded in the single-particle Green function  $G^\pm(\epsilon) \equiv (\epsilon^\pm - \hat{H})^{-1}$  rather than in the Hamiltonian itself. Now, as with the superconductor, since  $G^\pm(\epsilon) = -\sigma_3 G^\mp(-\epsilon) \sigma_3$ , where the

Pauli matrices operate in the space of the sublattice, the inversion property under adjunction with  $\sigma_3$  is broken by finite  $\epsilon$ .

In the vicinity of the band center, the chiral symmetry of the Hamiltonian gives rise to the existence of soft modes. To explore the influence of these modes on the spectral and delocalization properties of the states near the band center we will again look for an effective low-energy field theory. To keep our discussion specific, we begin by identifying different types of disorder and geometry that may be considered.

▷ One obvious choice would be to model the tight binding hopping matrix elements according to  $U_{ij}^{\alpha\beta} = 1 + R_{ij}^{\alpha\beta}$  where  $R_{ij} = R_{ji}^\dagger$  are Gaussian distributed matrices with variance  $\langle R_{ij}^{\alpha\beta} R_{ij}^{\beta'\alpha'} \rangle = \lambda^2 \delta_{\alpha\beta} \delta_{\alpha'\beta'} / N$ , and  $\lambda \ll 1$ . This is the weakly disordered limit, i.e. the bond-disordered analog of the weakly disordered Anderson model discussed before. Beginning with the early paper of Gade [188] various replica and supersymmetric field theory approaches to this model have been formulated [189–192]. While most of these theories focused on the two-dimensional lattice, the quasi one-dimensional bond-disordered *chain* has been analysed too, notably by transfer-matrix methods [193], but also by field theory [192]. The  $1d$ -variant is of particular interest because (a) it stands intermediate in complexity between the zero-dimensional ergodic limit and the two-dimensional case, (b) it is to a large extent exactly solvable and (c) it exhibits strikingly different behaviour from conventional disordered wires.

▷ Alternatively, one may consider a maximally disordered version of the sublattice system. By which we mean a model where the  $U_{ij}$  are unitary matrices uniformly distributed over  $U(N)$ . Interestingly, this maximally disordered version of the sublattice system is amenable to analytical analysis, too [194].

Taking the strongly disordered variant as an example, the next two sections will review the construction of a low energy field theory for RF-model. It's — interesting — low energy spectral and transport properties will then be discussed in section V F 3.

### 1. Field Theory of the RF-Model

Previously, the construction of an effective field theory has relied on a separation of energy scales in which the influence of disorder is assumed to be weak (i.e.  $1/E_F \tau \ll 1$ ). However, in the present case, there is no separation of energy scales — the disorder potential is manifestly strong. In principle, to implement the usual scheme, we could deliberately limit our considerations to sublattice models of the general form of Eq. (61) but

where the disordered components of the matrix elements  $U_{ij}$  are small as compared to some uniform part. Indeed, beginning with the seminal work of Gade [188], sublattice models of this kind have been studied in the literature within the framework of conventional (replica) field theory approaches [189].

However, instead, we will introduce a second kind of approach tailored to the study of *unitary* stochastic operators. This approach, known in the literature as the ‘color-flavor transformation’, provides a formal method for mapping model systems of this kind onto functional integrals containing a low-energy sector describing the large distance physics [195]. One could legitimately argue that such a generalization is gratuitous — if we believe that the form of the low-energy action is universal, dictated solely by fundamental symmetries, we could work with a weak coupling theory, and ultimately, in the spirit of Ginzburg-Landau theory, extend the effective action into the strong coupling regime. However, apart from an obvious aesthetic appeal, our motivation for developing this novel approach is to emphasize the bridge that exists between mesoscopic physics, and other branches of theoretical physics. At the same time, one can view the coincidence of the strong and weak coupling theories as a microscopic or “*ab initio*” confirmation of universality.

As a first step towards establishing the transformed theory, we consider the ensemble average of the usual generating functional  $\langle \mathcal{Z}[J] \rangle$  where

$$\mathcal{Z}[J=0] = \int D\psi e^{i \sum_i \bar{\psi}_i \epsilon^+ \psi_i + i \sum_{(i \in A, j \in B)} (\bar{\psi}_i U_{ij} \psi_j + \bar{\psi}_j U_{ij}^\dagger \psi_i)}.$$

Here  $\langle \cdots \rangle \equiv \prod_{(i,j)} \int dU_{ij}(\cdots)$  represents the non-Abelian generalization of a phase average, and  $dU_{ij}$  denotes the Haar measure on  $U(N)$ . As usual, the fields  $\psi = \{\psi_{i,a}^\alpha\}$  carry three types of indices: a lattice index  $i$ , a ‘color’ index  $\alpha$  (coupling to the internal group indices of the  $U$ ’s), and a ‘flavor’ index  $a = B, F$  referring to the boson/fermion grading. (An extension of the field space to accommodate  $n$ -point functions is easily achieved by increasing the number of flavor components. Here, for simplicity, we focus on the one-point function.)

## 2. Color-Flavor Transformation

The ensemble average over the bond matrices  $U_{ij}$  induces a complicated interaction of the fields. The color-flavor transformation provides a method of decoupling of the interaction effectively trading the group integrals over the  $U_{ij}$  for integrations over a set of auxiliary field variables  $Z_{ij}$ . Remarkably, despite the complicated nature of the interaction, the transformation is exact! (And straightforwardly generalized to other groups.) Following

Ref. [195], an application of the transformation to link  $ij$  of the lattice, one obtains

$$\langle e^{i(\bar{\psi}_i U_{ij} \psi_j + \bar{\psi}_j U_{ij}^\dagger \psi_i)} \rangle = \int D(Z, \tilde{Z}) M_{ij} e^{i(\bar{\psi}_i Z_{ij} \psi_i + \bar{\psi}_j \tilde{Z}_{ij} \psi_j)},$$

where  $M_{ij} = \text{sdet}(1 - Z_{ij} \tilde{Z}_{ij})^N$  represents the invariant measure, and the fields

$$Z_{ij} \in \text{GL}(1|1), \quad \tilde{Z}_{ij} \in \text{GL}(1|1) \quad (62)$$

are  $2 \times 2$ -dimensional supermatrices living on the directed link from the  $A$  site  $i$  to the nearest neighbor  $B$ -site  $j$ . (By ‘directed’ we mean that there is no  $Z_{ji}$ .) The integration  $\int D(Z, \tilde{Z})$  over all pairs  $(Z_{ij}, \tilde{Z}_{ij})$  is subject to the further set of constraints:

$$Z_{ij,FF} = -\tilde{Z}_{ij,FF}^*, \quad \tilde{Z}_{ij,BB} = Z_{ij,BB}, \quad (63)$$

while the Grassmann valued components,  $Z_{ij,BF}$ ,  $Z_{ij,FB}$ ,  $\tilde{Z}_{ij,BF}$ , and  $\tilde{Z}_{ij,FB}$  are independent.

Conceptually, the color-flavor transformation has a status similar to that of the Hubbard-Stratonovich transformation employed in the study of continuum Hamiltonians. The motivation for introducing the  $Z$ -fields is that they rearrange the coupling between the fields (see Fig. 56). Qualitatively, the  $Z$ ’s connect pairs of fields that, by construction, represent segments of ‘paired paths’. Segments of this structure are stabilized by mechanisms of quantum interference, implying that the  $Z$ ’s connect to a sector of the theory which contains information about the long-range behavior. In addition, the  $Z$ ’s couple non-trivially to the ‘flavor’ space. The remainder of the analysis will essentially amount to extracting the low-energy sector of the  $Z$ -functional stabilized by the interference.

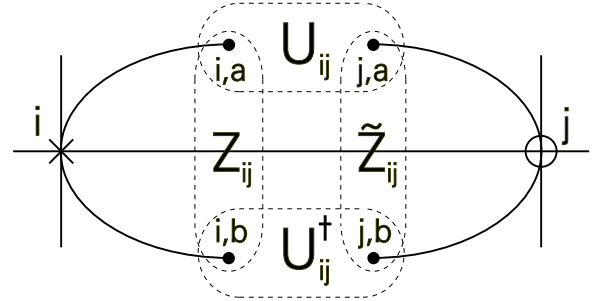


FIG. 56. Visualization of the different coupling of the  $U$ ’s and the  $Z$ ’s, respectively, to the field variables  $\psi$  (represented by the solid dots).

Applying the color-flavor transformation to each link of the lattice, and integrating over the  $\psi$ -fields, we obtain the functional

$$\langle \mathcal{Z}[J=0] \rangle = \int D(Z, \tilde{Z}) \prod_{\langle i \in A, j \in B \rangle} M_{ij} e^{-N \sum_{i \in A} \text{str} \ln \left( \epsilon^+ + \sum_{j \in N_i} Z_{ij} \right) - N \sum_{j \in B} \text{str} \ln \left( \epsilon^+ + \sum_{i \in N_j} \tilde{Z}_{ij} \right)}, \quad (64)$$

where the symbol  $\sum_{j \in N_i}$  denotes a summation over all sites  $j$  which neighbor  $i$ .

So far all manipulations have been exact. Further progress is made possible by subjecting the functional (64) to a saddle-point analysis. At  $\epsilon = 0$ , the variation of the action with respect to  $Z_{ij}$  and  $\tilde{Z}_{ij}$  obtains a saddle-point equation with the homogeneous solution  $\tilde{Z}_{\text{sp}} = Z_{\text{sp}} \simeq ix \mathbb{1}^{\text{BF}}$  where  $x \equiv (2d-1)^{-1/2}$ . However, as usual, this solution is not unique. The isotropy of the  $\epsilon = 0$  action in the BF-sector, which follows directly from the chiral structure of the Hamiltonian, implies a manifold of degeneracy spanned by the transformations

$$Z_{\text{sp}} = ix \bar{T} T, \quad \tilde{Z}_{\text{sp}} = ix (\bar{T} T)^{-1}, \quad (65)$$

where  $T, \hat{T} \in \text{GL}(1|1)$ . Taking into account the fact that  $\text{GL}(1|1) \times \text{GL}(1|1) = \text{GL}(1|1)$ , we conclude that the full extent of the saddle-point manifold is given by  $\text{GL}(1|1)$  [196]

Eq. (65) defines the maximum manifold of solutions of the saddle-point equations. In order to complete the determination of the global structure of the theory, we next need to explore how the manifold (65) intersects with the domain of the field integration (as specified by (62), and (63)). To this end, we represent a general pair of matrices as

$$(Z, \tilde{Z}) \equiv ix(PT, T^{-1}P), \quad (66)$$

where  $P, T \in \text{GL}(1|1)$  and we have omitted the site index ( $ij$ ) for notational transparency. The restriction of Eq. (63) leads to the relations,

$$\begin{aligned} P_{\text{FF}} &\in \text{GL}(1)/\text{U}(1), & T_{\text{FF}} &\in \text{U}(1) \\ P_{\text{BB}} &\in \text{U}(1), & T_{\text{BB}} &\in \text{GL}(1)/\text{U}(1), \end{aligned} \quad (67)$$

while the off-diagonal elements  $P_{\text{BF}}, P_{\text{FB}}, T_{\text{BF}}$  and  $T_{\text{FB}}$  are independent. Since Eqs. (65) and (66) imply that the saddle-point configurations of the theory are specified by  $P = \mathbb{1}$ , the measure of the  $P$ -integration is flat Euclidean,

whilst the  $T$ -integration is over the invariant measures on the manifolds (67).

The saddle-point decomposition (67) can now be used to reduce the exact functional (64) to a simpler effective functional describing the long-range behavior of the model. Technically, the procedure is based on a continuum approximation in combination with a gradient expansion around the spatially constant saddle-point manifold. It is important to realize that this evaluation scheme is, in fact, problematic: as compared to analogous treatments of *weakly* disordered models, the gradient expansion is not stabilized by the presence of a small parameter (e.g.  $1/E_F \tau$ ). Apart from the external parameter  $\epsilon$ , all energy scales are rather of the same order. With the non-Abelian versions of the RF-model,  $N > 1$ , the situation is less problematic, the reason being that the mean field analysis is stabilized by the parameter  $1/N$ .

Keeping these words of caution in mind, we now turn to the discussion of the continuum expansion of the theory. On general grounds, it may be anticipated that after integration over massive modes  $P$ , the effective action takes the form  $S[P, T] \rightarrow S_{\text{eff}}[T] = S_{\epsilon}[T] + S_{\text{fl}}[T] + S_{\text{m}}[T]$ , where  $S_{\epsilon}[T]$  is the contribution due to finite energies  $\epsilon$ ,  $S_{\text{fl}}[T]$  is the action associated with fluctuations of the Goldstone modes (the  $T$ 's), and  $S_{\text{m}}[T]$  represents a residual action induced by the interaction between massive and Goldstone modes, respectively. (Note that, in conventional disordered models, to leading order in  $1/k_F \ell$ , no coupling between the massless and massive modes survives.) Assuming that the field configurations relevant to the long-range physics are smooth, the different contributions to the action can then be computed by a gradient expansion followed by a continuum limit. Albeit conceptually straightforward, the explicit formulation of this program is somewhat involved and we therefore choose to omit it here. Referring instead to the original literature [194] for technical details, we simply note that the outcome of the gradient expansion is the effective *group* action

$$S[T] = - \int \left[ c_1 \text{str}(\partial T^{-1} \partial T) + i c_2 \text{str}(\epsilon(T + T^{-1})) + c_3 (\text{str}(T^{-1} \partial T))^2 \right] + S_{\text{b}}[T], \quad (68)$$

where  $T \in \text{GL}(1|1)$  (i.e.  $T$  belongs to the group of invertible supermatrices of dimension 2). Defining  $N_i$ ,  $i = 1, \dots, d$  as the number of sites in the  $\hat{\mathbf{e}}_i$ -direction,

$$S_{\text{b}}[T] = \frac{N}{2^d} \sum_{s_i=0,1} (-)^{\sum_i (N_i+1)s_i} \text{str} \ln(T(s_1 L_1, \dots, s_d L_d)),$$

represents a boundary action that depends on the values of the fields  $T$  at the corner points of the lattice. The coupling constants are defined by  $c_1 = N a^{2-d}/8d$ ,  $c_2 = N(2d-1)^{1/2} a^{-d}/4d$ ,  $c_3 = a^{2-d} C/16d$  where  $a$  represents the lattice spacing, and  $C$  denotes a geometry-dependent numerical constant  $O(1)$ .

Thus, for the ensemble of random flux lattice mod-

els whose matrix elements belong to the unitary group  $U(N)$ , we have succeeded in formulating a low energy effective field theory. Based on the fundamental symmetries of the action, we can expect (68) to describe the long-range properties of any stochastic Hamiltonian which belongs to the symmetry class AIII, a conjecture which finds support in the analysis of the weak coupling version of the random flux model [188]. As a caveat, we remark that, as with the class CI action for the disordered  $d$ -wave superconductor, the group structure of the field manifold, in principle, admits the existence of a WZWN-term. However, at least for the random flux model considered here, such a term does not appear.

### 3. Properties of the Field Theory

What information can be drawn from the field theory? To answer this question, it is convenient to distinguish the very low energy, or “ergodic regime” from the diffusive. As usual, on energy scales  $\epsilon \ll E_c \equiv c_1/(c_2 L^2)$ , the functional is dominated by the spatially constant zero mode configuration  $T_0 = \text{const.}$ ,

$$S_0[T_0] = -\frac{\pi\nu}{2} \text{str}(\hat{\epsilon}(T_0 + T_0^{-1})) + S_b[T_0], \quad (69)$$

where  $\nu$  is the bulk mean DoS of the system. As expected, up to the boundary term, correlation functions computed with respect to the zero mode action coincide with those otherwise obtained from an analysis of the chiral unitary random matrix ensemble ChGUE [134,197,198,135], (the matrix ensemble of symmetry class AIII in the classification scheme of Ref. [133]). In particular, an explicit calculation of the mean DoS shows that [135]

$$\nu(\epsilon) = \frac{\pi^2 \epsilon \nu^2}{2} (J_0^2(\pi \epsilon \nu) + J_1^2(\pi \epsilon \nu)),$$

if the total number of lattice sites is even (and therefore  $S_b = 0$ ), while, for  $N$  orbitals,

$$\nu(\epsilon) = \frac{\pi^2 \epsilon \nu^2}{2} (J_N^2(\pi \epsilon \nu) - J_{N-1}(\pi \epsilon \nu) J_{N+1}(\pi \epsilon \nu)),$$

if the number of sites is odd. These results show that, as  $\epsilon \rightarrow 0$ , the DoS vanishes on a scale set by the mean level spacing. (Moreover, in contrast to conventional disordered systems, the limit  $\epsilon \rightarrow 0$  does not behave *absolutely* universally: the fine structure of the DoS close to  $\epsilon = 0$  depends sensitively on the ‘parity’ of the lattice, i.e. on whether the number of sites is even or odd [135,199,193]. Without going into detail, we remark that the information about this effect is encoded in the boundary term  $S_b$ .)

Leaving the random matrix regime, we turn to the more interesting case of a quasi one-dimensional sublattice *chain*. Let us briefly recapitulate the central characteristics of conventional  $N$ -channel disordered wires: the

average DoS is structureless and all states are localized on the scale of a localization length  $\xi \sim N\ell$ . In contrast, the phenomenology of the sublattice wire [193,192]

- ▷ depends sensitively on the number of channels,  $N$ , being even or odd.
- ▷ For  $N$  even, the system exhibits conventional localization behaviour while the DoS exhibits a gap on the scale of  $\Delta_\xi$ . This gap is direct manifestation of a mechanism discussed in section IB 8: a localized system can be imagined as an assembly of isolated “localization volumes”. For small energies  $\epsilon < \Delta_\xi$  each of these behaves ergodic. As a consequence, the system exhibits RMT type phenomenology where the role of the level spacing is assumed by  $\Delta_\xi$ . In contrast,
- ▷ for  $N$  odd, the sublattice chain supports a delocalized mode. Its conductance decays algebraically with the system size,  $g \sim (\xi/L)^{1/2}$ , while the DoS diverges for small energies,  $\nu(\epsilon) \sim 1/(|\epsilon| \ln^3(|\epsilon|))$ .

As with the zero dimensional case, it is the term  $S_b$  that is responsible for the unusual  $N$  even/odd staggering behaviour. In the  $1d$ -case, this term can be cast into the form [192]

$$S_b = -\frac{N}{2} \int \text{str}(T \partial T^{-1}).$$

At first sight it looks like this operator is at odds with the left  $\leftrightarrow$  right parity invariance of the microscopic parent model. (The derivative changes sign under a mapping  $x \rightarrow -x$  which, on the other hand, leaves the averaged microscopic system invariant.) To resolve the paradox let us (a) focus attention on the phase valued compact sector of our theory,  $T_{\text{FF}}(x) = e^{i\phi(x)}$  (for the role of the non-compact sector, see Ref. [192]) and (b) appeal to the standard analogy:  $1d$  statistical field theory  $\leftrightarrow$  single particle quantum mechanics. Within this latter picture, our field integral acquires the meaning of a *path integral* of a particle on a ring (the latter being parameterized by the phase variable  $\phi$ ); and the length  $L$  of our system has become time. Looking at the Lagrangian, we identify  $2(c_1 + c_3)$  as the mass of our particle,  $c_2\epsilon$  as the coefficient of a  $\cos\phi$ -potential, and, most importantly,  $N/2$ -as the vector potential of a magnetic flux  $N/2$  threading the ring. (Remember that a vector potential couples through a Lagrangian as  $\sim \int \mathbf{A} \cdot \dot{\mathbf{x}}$ , where  $\mathbf{x}$  is coordinate.) This resolves our puzzle. The magnetic flux is quantized to half-integer multiples of the flux quantum. Since an integer flux quantum has no effect, the fluxes  $N/2$  and  $-N/2$  are equivalent, which explains why the sign of the derivative operator is inessential. More importantly, we can intuitively understand the origin of the staggering phenomena. A non-integer flux alters the spectrum of a particle on a ring. This in turn leads to modified long-time behaviour of the Green function. Within the statistical field theory context, “long-time” becomes “large length”.

Working out this analogy in quantitative terms one finds that for  $N$  odd, i.e. for a half integer flux quantum, the Green function becomes long-ranged: delocalization.

To which extent do these anomalies carry over to the two-dimensional case? Although no longer exactly solvable, conclusions regarding the physical behavior of the RF-model, most notably about its localization behavior, can be directly inferred from the RG analysis of Ref. [188]. There it was shown that the conductance of the weakly disordered  $2d$  model at the band center (which is essentially determined by the coupling constant  $c_1$ ) did not change under one-loop perturbative renormalization. This observation suggests that a non-localized state might exist in the middle of the band. Since the stability of the perturbative RG merely relies on the smallness of the parameters  $a^{2-d}c_1^{-1}$ , and  $a^{4-d}c_2/c_1^2 \ll 1$ , its results can be straightforwardly carried over to the  $N \gg 1$  non-Abelian RF model: the one-loop renormalization indicates that for  $N \gg 1$  the strongly disordered RF model exhibits metallic behavior at the band center.

As for the validity the RG results in the Abelian case ( $N = 1$ ), from the results presented here, there appears to be only one useful test of consistency: the existence of a metallic state for  $N = 1$  with strong disorder would at least be compatible with the behavior in the limiting cases:  $N = 1$  and weak disorder, and  $N \gg 1$  with arbitrary disorder. Moreover, this conclusion does also seem to be consistent with the most recent numerical investigations [179]. More concrete analytical evidence in favor of band center delocalization is not currently available.

Besides the conductance, the DoS of the extended model also behaves in an unusual manner: in particular, the analysis of Ref. [188] predicts divergent behavior upon approaching the band center, where the detailed functional form of the divergence depends on the dimensionality of the system. In particular, at energy scales  $E_c \ll |\epsilon| \ll 1$ , in two-dimensions the RG analysis predicts

$$\nu(\epsilon) \sim \frac{e^{-\kappa\sqrt{\ln(-|\epsilon|)}}}{|\epsilon|}.$$

The scale below which the  $|\epsilon|^{-1}$  divergence begins to dominate over the exponential factor is determined by the constant  $\kappa$ . Unfortunately the dependence of that constant on the relevant parameters of the model can not be reliably extracted from the perturbative RG analysis. The only statement that can safely be made is that a divergence forms at some point upon approaching the band center. Ultimately, the divergent behavior is cut-off by the onset of the non-perturbative ergodic regime discussed above. A quantitative understanding of both the formation of the divergence and its truncation in the close vicinity of the band center would necessitate a combination of an RG analysis with a non-perturbative treatment of the zero mode contribution. Nevertheless, these conclusions bare at least qualitative comparison with numerics (see Fig. 57).

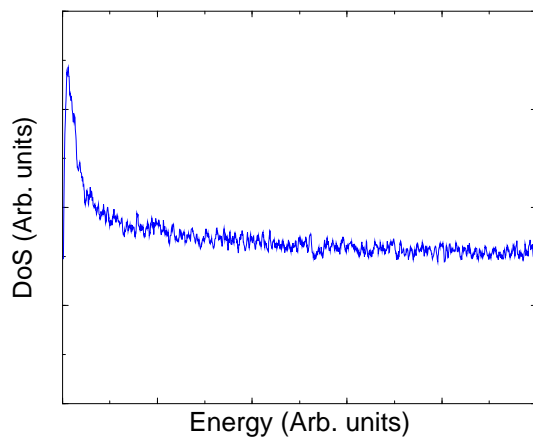


FIG. 57. Measurement of the DoS of an  $N = 1$  random flux Hamiltonian for a  $20 \times 20$  tight-binding lattice Hamiltonian. The data clearly shows a divergence in the vicinity of zero energy together with a “microgap” corresponding to the ergodic regime of the model.

A third piece of information that can be extracted from Ref. [188] is how finite energy arguments  $\epsilon$  affect the localization properties of the model: in the spirit of the RG, finite energies have the significance of relevant perturbations. Thus, the band center represents a critical manifold whilst for finite  $\epsilon$ , the model flows into a different universality class. More precisely, the band center field theory — belonging to the universality class AIII — develops into an ordinary GUE type model. (Note that this conclusion is in accord with the analysis in Ref. [182] where a continuum random field model far away from the band center was shown to be described by a supersymmetric unitary model.)

In that context, one may ask how the degrees of freedom of the model of reduced, unitary symmetry, denoted by  $Q$  [58], emerge from the fields  $T$  of the present model upon crossing over to the unitary regime. In fact the full RF model could have been formulated in terms of  $Q$ -matrices (albeit  $Q$ 's of a symmetry different from the standard unitary symmetry) from the outset: defining  $Q = \tilde{T}\sigma_3\tilde{T}^{-1}$ , where  $\tilde{T} = \exp[W\sigma_2]$  and the  $\sigma_i$  operate in sublattice space, the matrices  $\tilde{T}$  are then related to our  $T$ 's by the identity  $T = \exp[W]$ . The price to pay for this more common  $Q$ -formulation of the theory would be a certain amount of redundancy: a description in terms of structures  $Q \sim \tilde{T}\sigma_3\tilde{T}^{-1}$  is the natural one for problems with *coset space* symmetry. However, the present problem has the *group* symmetry  $GL(1|1)$  implying that a modeling directly in terms of group degrees of freedom is more natural.

Besides the weakly disordered sublattice model explored by Gade, the field theory (68) has at least two other close relatives: in QCD, (68) has been suggested on phenomenological grounds as relevant for the determination of the low energy spectrum of the Dirac opera-



tor (see Ref. [136] for review). (In QCD, ‘randomness’ is represented by gauge field fluctuations in the Yang-Mills Hamiltonian.) The simplest lattice action of a matter field with  $N$  ‘color’ indices subject to a non-Abelian local gauge symmetry is given by

$$S = - \sum_{\langle i,j \rangle} c_i^\dagger U_{ij} c_j^a - \frac{1}{2g} \sum_{\square} \left[ \left( 1 - \frac{1}{N} \text{tr}_{\square} U^4 \right) + \text{h.c.} \right].$$

where  $a = 1, \dots, n$  has the physical significance of a fermionic flavor index,  $\sum_{\square}$  is a sum over all plaquettes of the lattice, and  $\text{tr}_{\square}(U^4) \equiv \text{tr}(U_{ij}U_{jk}U_{kl}U_{li})$  represents the trace over all  $U$ ’s residing on the links of the plaquette. Physically, the plaquette action represents the discrete version of a continuum field strength tensor. In the strong coupling limit,  $g \rightarrow \infty$  (i.e. the long distance, confinement phase of the theory) the gauge fields become free and the Hamiltonian is governed by a structure like (61). In this context, the base manifold is  $4 + 1$ -dimensional whilst the fields  $T \in U(n_f + 1|1)$ , where  $n_f$  is the number of quark flavors. For a comprehensive discussion of the QCD-analogue of (68), its connection with ChRMT and its relevance for lattice QCD-analyses, we refer the reader to Refs. [24,136]. The similarity between the theories is again a manifestation of the universality of chiral  $\sigma$ -models or, more physically, the universal consequences chiral symmetries have for the long-range properties of random systems.

This concludes our investigation of the unusual low-energy properties of the ensembles that make up the novel symmetry classes. Our survey has been incomplete missing the ensembles exhibiting a symplectic structure. However, the generic features of these models and the unusual localization properties have been explored.

---

[1] N. Ashcroft and D. Mermin, *Solid State Physics* (Holt, Rinehart, Winston, 1976).  
[2] P. W. Anderson, *Basic Notions of Condensed Matter Physics* (Benjamin, Menlo Park, CA, 1984).  
[3] L. D. Landau and I. M. Lifshitz, *Physical Kinetics* (Pergamon Press, 1982).  
[4] B. L. Altshuler, P. A. Lee, and R. A. Webb, editors, *Mesoscopic Phenomena in Solids* (North-Holland, Amsterdam): p. 1, 1991.  
[5] Y. Imry, in *Introduction to Mesoscopic Physics* (Oxford University Press, Oxford) 1996.  
[6] Y. Alhassid, *Rev. Mod. Phys.* **72**, 895 (2000).  
[7] For a review see L. P. Kouwenhoven *et al.*, *Electron Transport in Quantum Dots*, proceedings of the Summer School on Mesoscopic Electron Transport (Kluwer 1997); C. M. Marcus *et al.*, *Quantum Chaos in Open versus Closed Quantum Dots: Signatures of Interacting Particles*, to appear in *Chaos, Solitons and Fractals* (July 1997), preprint cond-mat/9703038.

[8] M. J. Kelly, *Low-dimensional Semiconductors*, (Clarendon Press, Oxford 1995).  
[9] C. W. J. Beenakker and H. Van Houten, *Quantum Transport in Semiconducting Nanostructures*, Solid State Physics (Academic Press, New York) **44** (1991) p. 1  
[10] D. Mailly and M. Sanquer, *J. Phys. France* **2**, 357 (1992).  
[11] P. A. Lee and A. D. Stone, *Phys. Rev. Lett.* **55**, 1622 (1985).  
[12] B. L. Altshuler, *JETP Lett.* **41**, 649 (1985).  
[13] C. M. Marcus, Private communication  
[14] S. Washburn, in *Mesoscopic Phenomena in Solids*, eds. B. L. Altshuler, P. A. Lee, and R. A. Webb, Elsevier (1991); See also, S. Washburn and R. A. Webb, *Adv. Phys.* **35** (1986) 375; R. A. Webb, S. Washburn, C. P. Umbach, and R. B. Laibowitz, *Phys. Rev. Lett.* **54**, 2696 (1985); R. A. Webb *et al.*, in: *Physics and Technology of Submicron Structures*, eds., H. Heinrich, G. Bauer, and F. Kuchar (Springer, Berlin, 1988), Vol. **83**, p. 98.  
[15] B. L. Altshuler, A. G. Aronov, D. E. Khmel’nitskii, and A. I. Larkin, in *Quantum Theory of Solids*, Mir Publishers, Moscow, p 130 (1982).  
[16] D. E. Khmel’nitskii, *Physica B+C* **126**, 235 (1984).  
[17] L. P. Gor’kov, A. I. Larkin, and D. E. Khmel’nitskii, *JETP Lett.* **30**, 228 (1979).  
[18] B. L. Altshuler, A. G. Aronov, and B. Z. Spivak, *JETP Lett.* **33**, 94 (1981).  
[19] D. Y. Sharvin and Y. V. Sharvin, *JETP Lett.* **34**, 272 (1981).  
[20] B. L. Altshuler and B. I. Shklovskii, *JETP* **64**, 127 (1986).  
[21] Y. Imry, *Europhys. Lett.* **1**, 249 (1986).  
[22] F. J. Dyson, *J. Math. Phys.* **3**, 140, 157, 166 (1962); F. J. Dyson and M. L. Mehta, *J. Math. Phys.* **4**, 701 (1963).  
[23] M. L. Mehta, *Random Matrices* (Academic Press, New York, 1991).  
[24] T. Guhr, A. Müller-Groeling, and H. A. Weidenmüller, *Phys. Rep.* **299**, 189 (1998).  
[25] P. W. Anderson, *Phys. Rev.* **109** (1958) 1492.  
[26] J. Zittartz and J. S. Langer, *Phys. Rev.* **148**, 741 (1966).  
[27] B. I. Halperin and M. Lax, **148**, 722 *Phys. Rev.* (1966).  
[28] J. T. Edwards and D. J. Thouless, *J. Phys. C* **5**, 807 (1972).  
[29] D. J. Thouless, in: *III Condensed Matter*, eds., R. Balian, R. Maynard, and G. Toulouse, Les Houches, Session XXXI (North-Holland, Amsterdam, 1978), p. 1.  
[30] E. Abrahams, P. W. Anderson, D. C. Licciardello, and T. V. Ramakrishnan, *Phys. Rev. Lett.* **42**, 673 (1979).  
[31] V. N. Prigodin, B. L. Altshuler, K. B. Efetov, and S. Iida, *Phys. Rev. Lett.* **72**, 546 (1994).  
[32] A. Altland and D. Fuchs, *Phys. Rev. Lett.* **74**, 4269 (1995).  
[33] R. I. Shekhter, *Zh. Eksp. Teor. Fiz.* **63**, 1410 (1972) [*Sov. Phys. JETP* **36**, 747 (1973)].  
[34] I. O. Kulik and R. I. Shekhter, *Zh. Eksp. Teor. Fiz.* **68**, 623 (1975) [*Sov. Phys. JETP* **41**, 308 (1975)].  
[35] D. V. Averin, and K. K. Likharev, in *Mesoscopic Phenomena in Solids*, edited by B. L. Altshuler, P. A. Lee,

- and R. A. Webb (North-Holland, Amsterdam): p. 173, (1991).
- [36] H. Van Houten, C. W. J. Beenakker, and A. A. M. Staring, in: *Single Charge Tunneling*, edited by H. Grabert and M. H. Devoret (Plenum, New York): p. 167, (1992).
  - [37] U. Meirav, and E. B. Foxman, *Semicond. Sci. Technol.* **10**, 255 (1995).
  - [38] I. L. Aleiner, P. W. Brouwer, and L. I. Glazman, preprint cond-mat/0103008
  - [39] C. M. Marcus, private communication
  - [40] L. P. Kouwenhoven *et al.*, preprint cond-mat/9708229
  - [41] L. P. Kouwenhoven and P. L. McEuen, *Single Electron Tunneling Through a Quantum Dot*, in Nano-Science and Technology, ed. G. Timp (AIP Press, New York, 1996).
  - [42] M. A. Kastner, *Rev. Mod. Phys.* **64**, 849 (1992).
  - [43] L. S. Levitov and A. V. Shytov, preprint cond-mat/9607136.
  - [44] B. L. Altshuler and A. G. Aronov, *Sol. State. Commun.* **39**, 115 (1979)
  - [45] A. A. Abrikosov, L. P. Gorkov, and I. E. Dzyaloshinski, *Methods of Quantum Field Theory in Statistical Physics*, Dover 1963.
  - [46] B. L. Altshuler, M. E. Gershenson, and A. I. Aleiner, *Physica E* **3**, 58 (1998); I. L. Aleiner, B. L. Altshuler, and M. E. Gershenson, *Waves in Random Media* **9**, 201 (1999).
  - [47] B. L. Altshuler, A. G. Aronov, and D. E. Khmel'nitskii, *J. Phys. C* **15**, 7367 (1982).
  - [48] G. Bergmann, *Phys. Rep.* **107**, 1 (1984).
  - [49] P. A. Lee and T. V. Ramakrishnan, *Rev. Mod. Phys.* **57**, 287 (1985).
  - [50] S. Chakravarty and A. Schmid, *Phys. Rep.* **140**, 193 (1986).
  - [51] B. L. Altshuler and B. D. Simons, *Universalities: from Anderson Localization to Quantum Chaos*, a course of 10 lectures in the proceedings of the 1994 Summer Session LXI on "Mesoscopic Quantum Physics" at Les Houches, Nato ASI, eds. E Akkermans, G Montambaux, J.-L. Pichard and J. Zinn-Justin.
  - [52] T. V. Ramakrishnan, in: *Chance and Matter*, eds., J. Souletie, J. Vannimenus, and R. Stora, Les Houches, Session XLVI 1986 (North-Holland, Amsterdam, 1987), p. 213.
  - [53] B. L. Altshuler, A. G. Aronov, D. E. Khmel'nitskii, and A. I. Larkin, in: *Quantum Theory of Solids*, ed., I. M. Lifshits (Mir Publishers, Moscow, 1982), p. 130.
  - [54] S. F. Edwards, *Philos. Mag.* **3**, 1020 (1958).
  - [55] J. S. Langer and T. Neal, *Phys. Rev. Lett.* **16** (1966) 1984.
  - [56] F. J. Wegner, *Z. Phys. B* **35**, 207 (1979).
  - [57] K. B. Efetov, *Sov. Phys. JETP* **82**, 872 (1982); *ibid* **83**, 833 (1982).
  - [58] K. B. Efetov, *Adv. Phys.* **32**, 53 (1983); K. B. Efetov, *Supersymmetry in Disorder and Chaos*, Cambridge University Press, New York (1997).
  - [59] J. J. M. Verbaarschot, H. A. Weidenmüller and M. R. Zirnbauer, *Phys. Rep.* **129**, 367 (1985).
  - [60] Y. V. Fyodorov, in *Mesoscopic Quantum Physics* (Les Houches 1994), ed. E. Akkermans, G. Montambaux, J.-L. Pichard, and J. Zinn-Justin (North-Holland, Amsterdam) p. 493, 1995.
  - [61] A. D. Mirlin, in the Proceedings of the International School of Physics "Enrico Fermi", Course CXLIII, Eds. G. Casati, I. Guarneri and U. Smilansky (IOS Press, Amsterdam, 2000), pp. 223-298.
  - [62] A. D. Mirlin, *Phys. Rep.* **326**, 259 (2000).
  - [63] S. F. Edwards and P. W. Anderson, *J. Phys. F* **5**, 965 (1975).
  - [64] V. J. Emery, *Phys. Rev. B* **11**, 239 (1975).
  - [65] J. J. M. Verbaarschot and M. R. Zirnbauer, *J. Phys. A* **17**, 1093 (1985).
  - [66] M. R. Zirnbauer, preprint cond-mat/9903338.
  - [67] A. Kamenev and M. Mezard, *J. Phys. A* **32**, 4373 (1999); *Phys. Rev. B* **60**, 3944 (1999).
  - [68] I. V. Yurkevitch and I. V. Lerner, *Phys. Rev. B* **60**, 3955 (1999).
  - [69] F. A. Berezin, *Introduction to Superanalysis* (Reidel, Dordrecht, 1987).
  - [70] B. D. Simons, O. Agam and A. V. Andreev, *J. Math. Phys.* **38**, 1982 (1997).
  - [71] G. Eilenberger, *Z. Phys.* **182**, 427 (1965); *ibid.* **214**, 195 (1968).
  - [72] These rules can be proven (a) by direct calculation, i.e. explicit parameterization of the generators in terms of two commuting and two anticommuting variables and doing the Gaussian integrals or (b) more elegantly, by symmetry arguments: global rotation invariance of the theory implies that a functional expectation value  $\sim \langle \text{str} [B(\mathbf{r}) P \bar{B}(\mathbf{r}') R] \rangle_B$  must be invariant under the transformation  $P \rightarrow k P k^{-1}$ ,  $R \rightarrow k' R k'^{-1}$ , where  $k, k' \in SU(1|1)$  are constant supermatrices. This condition determines the rhs of the contraction to be proportional to  $\text{str}(P) \text{str}(R)$ . That the prefactor equals the propagator  $\Pi(\mathbf{r}, \mathbf{r}')$  follows from general properties of Gaussian functional integrals.
  - [73] V. E. Kravtsov and I. V. Lerner, *Phys. Rev. Lett.* **74**, 2563 (1995).
  - [74] A. Altland, S. Iida, and K. B. Efetov, *J. Phys. A* **14**, 3545 (1993).
  - [75] B. D. Simons and B. L. Altshuler, *Phys. Rev. Lett.* **70**, 4063 (1993); *ibid.*, *Phys. Rev. B* **48**, 5422 (1993); B. D. Simons, P. A. Lee, and B. L. Altshuler, *Phys. Rev. Lett.* **70**, 4122 (1993).
  - [76] As a footnote, we remark on the existence of a surprising connection between the parametric eigenvalue correlations of random matrix ensembles, and the quantum dynamical properties of an interacting one-dimensional electron gas. The correspondence is drawn by interpreting the energy levels with the position of the particles, and their parametric dependence on some arbitrary external perturbation with time — i.e. the spaghetti of energy levels of a disordered quantum Hamiltonian can be viewed as the "world lines" of a gas of interacting quantum particles. In the simplest case, Eq. (34) can then be interpreted as the equal-time density-density correlation function of a one-dimensional free electron gas — the eigenvalue integrations correspond to momentum integrations for the particle/hole excitations. A review of these connections and a discussion of the implications

on interacting theories can be found in Ref. [51].

- [77] O. N. Dorokhov, Pis'ma Zh. Eksp. Teor. Fiz. **36**, 259 (1982). [JETP Lett. **36**, 318 (1982)].
- [78] P. A. Mello, P. Pereyra, and N. Kumar, Ann. Phys. (N.Y.) **181**, 290 (1988).
- [79] C. W. J. Beenakker, Rev. Mod. Phys. **69**, 731 (1997).
- [80] *Supersymmetry and Trace Formulae: Chaos and Disorder* (I. V. Lerner, J. P. Keating, and D. E. Khmel'nitskii, eds.) Plenum Press (1999).
- [81] For a review, see M. C. Gutzwiller, *Chaos in Classical and Quantum Mechanics*, Springer, New York, 1990; F. Haake, *Signatures of Quantum Chaos* (Springer, Berlin, 1991).
- [82] D. Delande, in Proceedings of Les-Houches Summer School, Session LII, 1989, eds. M. -J. Giannoni, A. Voros and J. Zinn-Justin, North-Holland, Amsterdam 1991.
- [83] V. N. Prigodin, N. Taniguchi, A. Kudrolli, V. Kidambi, and S. Shridar, Phys. Rev. Lett. **75**, 2392 (1995).
- [84] C. Gmachl, F. Capasso, E. E. Narimanov, J. U. Nöckel, A. D. Stone, J. Faist, D. L. Sivco, A. Y. Cho, Science **280**, 1556 (1980).
- [85] E. P. Wigner, Ann. Math. **53**, 36 (1953).
- [86] C. E. Porter, ed. *Statistical Theories of Spectral Fluctuations*, Academic Press, New York, 1965.
- [87] L. P. Gor'kov and G. M. Eliashberg, Sov. Phys. JETP **21**, 940 (1965).
- [88] L. Schäfer and F. J. Wegner, Z. Phys. B **38**, 113 (1980).
- [89] K. B. Efetov, A. I. Larkin, and D. E. Khmel'nitskii, Sov. Phys. JETP **52**, 568 (1980).
- [90] A. Houghton, A. Jevicky, R. D. Kenway, and A. M. M. Pruisken, Phys. Rev. Lett. **45**, 394 (1980).
- [91] K. Junglich and R. Oppermann, Z. Phys. B **38**, 93 (1980).
- [92] S. Hikami, Phys. Rev. B **24**, 2671 (1981).
- [93] A. J. MaKane and M. Stone, Ann. Phys. (NY) **131**, 36 (1981).
- [94] O. Bohigas, M. J. Giannoni and C. Schmidt, Phys. Rev. Lett. **52**, 1 (1984); J. Physique Lett. **45**, L1615 (1984).
- [95] M. C. Gutzwiller, J. Math. Phys. **8**, 1979 (1967); **10**, 1004 (1969); **11**, 1791 (1970); **12**, 343 (1971).
- [96] M. V. Berry, Proc. Roy. Soc. London A **400**, 229 (1985).
- [97] M. V. Berry, in *Chaos and Quantum Physics*, eds., M. -J. Giannoni, A. Voros, and J. Zinn-Justin, Les Houches, Session LII 1989 (North-Holland, Amsterdam, 1991), p. 251.
- [98] P. Cvitanović and B. Eckhardt, J. Phys. A **24**, L237 (1991).
- [99] O. Agam, B. L. Altshuler and A. V. Andreev, Phys. Rev. Lett. **75**, 4389 (1995).
- [100] E. Bogomolny and J. P. Keating, Phys. Rev. Lett. **77**, 1472 (1996).
- [101] R. S. Whitney, I. V. Lerner and R. A. Smith, preprint cond-mat/9902328
- [102] B. A. Muzykantskii and D. E. Khmel'nitskii, JETP Lett. **62**, 76 (1995)
- [103] A. V. Andreev, O. Agam, B. D. Simons and B. L. Altshuler, Phys. Rev. Lett. **76** 3947 (1996).
- [104] A. Altland, C. R. Offer, and B. D. Simons, in *Supersymmetry and Trace Formulae: Chaos and Disorder* (I. V. Lerner, J. P. Keating, and D. E. Khmel'nitskii, eds.) Plenum Press (1999), p17.
- [105] M. R. Zirnbauer, in *Supersymmetry and Trace Formulae: Chaos and Disorder* (I. V. Lerner, J. P. Keating, and D. E. Khmel'nitskii, eds.) Plenum Press (1999), p153, chao-dyn/9812023
- [106] S. Nonnenmacher and M. Zirnbauer, in preparation.
- [107] P. Gaspard, G. Nicolis, A. Provata, and S. Tasaki, Phys. Rev. E **51**, 74 (1995).
- [108] D. Ruelle, Phys. Rev. Lett **56**, 405 (1986).
- [109] M. Pollicot, Ann. Math. **131**, 331 (1990).
- [110] G. Nicolis and C. Nicolis, Phys. Rev. A **38**, 427 (1988).
- [111] H. H. Hasegawa and D. J. Driebe, Phys. Rev. E **50**, 1781 (1994).
- [112] I. L. Aleiner and A. I. Larkin, Chaos, Solitons and Fractals **8**, 1179 (1997).
- [113] K. von Klitzing, G. Dorda and M. Pepper, Phys. Rev. Lett. **45**, 494 (1980); K. von Klitzing, Rev. Mod. Phys. **50**, 655 (1987).
- [114] J. Nicholls, private communication
- [115] A. M. M. Pruisken, Nucl. Phys. B **235**, 277 (1984); H. Levine, S. Libby, and A. A. M. Pruisken, Nucl. Phys. B **240**, 30, 49, 71 (1985)
- [116] D. E. Khmel'nitskii, JETP Lett. **38**, 552 (1983).
- [117] H. P. Wei, D. C. Tsui, M. A. Paalanen and A. M. M. Pruisken, Phys. Rev. Lett. **61**, 1294 (1988).
- [118] M. R. Zirnbauer, preprint hep-th/9905054
- [119] *The Quantum Hall Effect*, eds. R. E. Prange and S. M. Girvin (Springer-Verlag, New York, 1987).
- [120] M. Janssen, O. Viehweger, U. Fastenrath and J. Hajdu, *Introduction to the Theory of the Integer Quantum Hall Effect*, (VCH Verlagsgesellschaft mbH, D-69451 Weinheim, Germany, 1994).
- [121] J.W. Negele and H. Orland, *Quantum Many-Particle Systems*, Addison-Wesley Publishing Company, 1988.
- [122] J.J.M Verbaarschot and M.R. Zirnbauer, Ann. Phys. **158**, 78 (1984).
- [123] L. V. Keldysh, Zh. Eksp. Teor. Fiz. **47**, 1515 (1964) [Sov. Phys. JETP **20**, 1018 (1965)].
- [124] M. L. Horbach, and G. Schön, Ann. Phys. **2**, 51 (1993).
- [125] A. Kamenev and A. V. Andreev, Phys. Rev. B **60**, 2218 (1999).
- [126] A. Altland and A. Kamenev, Phys. Rev. Lett. **85**, 5615 (2000).
- [127] M. Gell-Mann and K. A. Brückner, Phys. Rev. **106**, 364 (1957); M. Gell-Mann, Phys. Rev. **106**, 369 (1957).
- [128] A. M. Finkelshtein, Sov. Sci. Rev. A Phys. **14** (1990) 1.
- [129] B. L. Altshuler and A. G. Aronov, in: *Electron-Electron Interactions in Disordered Systems*, eds., A. L. Efros and M. Pollak (North-Holland, Amsterdam, 1985), p. 1.
- [130] A. G. Aronov and Y. V. Sharvin, Rev. Mod. Phys. **59**, 755 (1987).
- [131] B. L. Altshuler, A. G. Aronov, M. E. Gershenson, and Y. V. Sharvin, in: *Physics Reviews*, ed., I. M. Khalatnikov (Harwood Academic Publishers, Switzerland, 1987), p. 225.
- [132] S. Helgason, *Differential geometry, Lie groups and symmetric spaces*, (Academic Press, New York, 1978).
- [133] M. R. Zirnbauer, J. Math. Phys. **37**, 4986 (1996).
- [134] T. Nagao, S. Slevin, J. Math. Phys. **34**, 2075 (1993);

- ibid.* **34**, 2317 (1993).
- [135] J. J. M. Verbaaschot and I. Zahed, Phys. Rev. Lett. **70**, 3852 (1993); J. J. M. Verbaaschot, Phys. Rev. Lett. **72**, 2531 (1994).
  - [136] See J. J. M. Verbaaschot and T. Wettig, hep-ph/0003017 for a review.
  - [137] A. Altland and M. R. Zirnbauer, Phys. Rev. Lett. **76**, 3420 (1996); Phys. Rev. B **55**, 1142 (1997).
  - [138] R. Oppermann, Nuclear Phys. B **280**, 753 (1987).
  - [139] V. E. Kravtsov and R. Oppermann, Phys. Rev. B **43**, 10865 (1991).
  - [140] A. Altland, B. D. Simons, and D. Taras-Semchuk, Adv. in Phys. **49**, 321 (2000).
  - [141] R. Bundschuh, C. Cassanello, D. Serban, and M. R. Zirnbauer, Nucl. Phys. B **532**, 689 (1998).
  - [142] P. W. Anderson, J. Phys. Chem. Solids **11**, 26 (1959).
  - [143] K. D. Usadel, Phys. Rev. Lett. **25**, 507 (1970).
  - [144] For a review, see *Nonequilibrium Superconductivity*, ed. V. L. Ginzburg, Nova Science Publications, 1988.
  - [145] M. Yu. Kupriyanov and V. F. Lukichev, Zh. Eksp. Teor. Fiz. **94**, 139 (1988) [Sov. Phys. JETP **67**, 1163 (1988)].
  - [146] M. G. Vavilov, P.W. Brouwer, V. Ambegaokar, and C. W. J. Beenakker, preprint cond-mat/0006375.
  - [147] A. Lamacraft and B. D. Simons, preprint cond-mat/0101080.
  - [148] P. M. Ostrovsky, M. A. Skvortsov and M. V. Feigelman, preprint cond-mat/0012478.
  - [149] J. Melsen, P. Brouwer, K. Frahm, and C. Beenakker, Europhys. Lett. **35**, 7 (1996); Physica Scripta T **69**, 223 (1997).
  - [150] P. de Gennes and D. Saint-James, Phys. Lett. **4**, 151 (1963).
  - [151] A. Lodder and Y. V. Nazarov, Phys. Rev. B **9**, 5783 (1998).
  - [152] W. Ihra, M. Leadbeater, J. L. Vega, and K. Richter, cond-mat/9909100.
  - [153] D. Taras-Semchuk and A. Altland, cond-mat/0010413.
  - [154] M. V. Feigel'man, A. I. Larkin, and M. A. Skvortsov, Phys. Rev. B **61**, 12361 (2000).
  - [155] L. P. Gor'kov and P. A. Kalugin, Pis'ma Zh. Eksp. Teor. Fiz. **41**, 208 (1985) [JETP Lett. **41**, 253 (1985)].
  - [156] E. Fradkin, Phys. Rev. B **33**, 3257 (1986); **33**, 3263 (1986).
  - [157] P. A. Lee, Phys. Rev. Lett. **71**, 1887 (1993).
  - [158] A. A. Nersesyan, A. M. Tsvelik, and F. Wenger, Phys. Rev. Lett. **72**, 2628 (1994); Nucl. Phys. B **438**, 561 (1994).
  - [159] A. V. Balatsky, A. Rosengren, and B. L. Altshuler, Phys. Rev. Lett. **73**, 720 (1994).
  - [160] A. V. Balatsky and M. I. Salkola, Phys. Rev. Lett. **76**, 2386 (1996).
  - [161] K. Ziegler, M. H. Hettler, and P. J. Hirschfeld, Phys. Rev. Lett. **77**, 3013 (1996).
  - [162] L. Balents, M. P. A. Fisher, and C. Nayak, Int. J. Mod. Phys. B **12**, 1033 (1998).
  - [163] T. Senthil *et al.*, Phys. Rev. Lett. **81**, 4704 (1998); T. Senthil and M. P. A. Fisher, preprint cond-mat/9810238.
  - [164] V. Gurarie, preprint cond-mat/9907502.
  - [165] B. Huckestein and A. Altland, preprint cond-mat/0007413.
  - [166] W. A. Atkinson, P. J. Hirschfeld, A. H. MacDonald, and K. Ziegler, preprint cond-mat/0005487.
  - [167] O. Alvarez, Nucl. Phys. B **238**, 61 (1984).
  - [168] A. Altland, B. D. Simons, and M. R. Zirnbauer, unpublished
  - [169] For review see A. O. Gogolin, A. A. Nersesyan, and A. M. Tsvelik, *Bosonization and strongly correlated systems*, Cambridge University Press, 1998 and references therein.
  - [170] E. Witten, Comm. Math. Phys. **92**, 455 (1984).
  - [171] A. M. Polyakov and P. B. Wiegmann, Phys. Lett. **B131**, 121 (1983).
  - [172] V. G. Khniznik and A. B. Zhamolodchikov, Nucl. Phys. **B247**, 83 (1984).
  - [173] A. W. W. Ludwig *et al.*, Phys. Rev. B **50**, 7526 (1994).
  - [174] O. V. Dolgov, O. V. Danylenko, M. L. Kulić, and V. Oudovenko, Int. J. Mod. Phys. B **12**, 3083 (1998); Eur. Phys. J. B **9**, 201 (1999).
  - [175] T. Senthil, J. B. Marston and M. P. A. Fisher, cond-mat/9902062
  - [176] For review see, e.g., H. J. Schulz, G. Cuniberti, and P. Pierie, in *Field Theories for Low-Dimensional Condensed Matter Systems*. G. Morandi *et al.* eds. Springer (2000); J. Voit, in the Proceedings of the International Winterschool on Electronic Properties of Novel Materials 2000, Kirchberg, March 4-11, 2000.
  - [177] A. A. Ovchinnikov and N. Erikhman, Sov. Phys. JETP **46**, 340 (1977).
  - [178] This example shows that there is no rigid assignment of symmetry classes to physical applications. E.g. the *d*-wave superconductor supports regimes with chiral symmetry (viz. the node-decoupled regime of symmetry class AIII). Later on we will see that some 'chiral' systems effectively behave like superconductors.
  - [179] P. A. Lee and D. S. Fisher, Phys. Rev. Lett. **47**, 882 (1981); T. Sugiyama and N. Nagaosa, Phys. Rev. Lett. **70**, 1980 (1993); Y. Avishai *et al.*, Phys. Rev. B **47**, 9561 (1993); D. Z. Liu *et al.*, Phys. Rev. B **52**, 5858 (1995); D. N. Sheng and Z. Y. Weng, Phys. Rev. Lett. **75**, 2388 (1995); K. Yakubo and Y. Goto, Phys. Rev. B **54**, 13432 (1996); K. Yang and R. N. Bhatt, Phys. Rev. B **55**, R1922 (1997); M. Batsch *et al.*, Physica B **249-251**, 792 (1998); X. C. Xie *et al.*, Phys. Rev. Lett. **80**, 3563 (1998); A. Furusaki, preprint, cond-mat/9808059.
  - [180] G. Gavazzi *et al.*, Phys. Rev. B **47**, 15170 (1993); V. Kalmeyer *et al.*, Phys. Rev. B **48**, 11095 (1993); S. - C. Zhang and D. P. Arovas, Phys. Rev. Lett. **72**, 1886 (1994); Y. B. Kim *et al.*, Phys. Rev. B **52**, 16646 (1995).
  - [181] D. K. K. Lee and J. T. Chalker, Phys. Rev. Lett. **72**, 1510 (1994)
  - [182] A. G. Aronov *et al.*, Phys. Rev. B **49**, 16609 (1994).
  - [183] J. Miller and J. Wang, Phys. Rev. Lett. **76**, 1461 (1996).
  - [184] B. I. Halperin, P. A. Lee, and N. Read, Phys. Rev. B **47**, 7912 (1993).
  - [185] S. Hikami *et al.*, Nucl. Phys. B **408**, 2454 (1993); D. K. Lee, Phys. Rev. B **50**, 7743 (1994); K. Minakuchi and S. Hikami, Phys. Rev. B **53**, 10898 (1996); S. Hikami and K. Minakuchi, Phys. Rev. B **55**, 7155 (1997)
  - [186] N. Nagaosa and P. A. Lee, Phys. Rev. Lett. **64**, 2450

- (1990); X. -G. Wen and P. A. Lee, Phys. Rev. Lett. **76** 503 (1996).
- [187] E. Müller-Hartmann and E. Dagotto, Phys. Rev. B **54**, R6819 (1996).
- [188] R. Gade, Nucl. Phys. B **398**, 499 (1993); R. Gade and F. Wegner, Nucl. Phys. B **398**, 499 (1991).
- [189] T. Fukui, Nucl. Phys. B **562**, 477 (1999).
- [190] S. Guruswamy, A. LeClair, and A. W. W. Ludwig, Nucl. Phys. B **583**, 475 (2000).
- [191] M. Favrizio and C. Castellani, cond-mat/0002328.
- [192] A. Altland and R. Merkt, preprint cond-mat/0102124.
- [193] P. W. Brouwer, C. Mudry, B. D. Simons, and A. Altland, Phys. Rev. Lett. **81**, 862 (1998); P. W. Brouwer, C. Mudry, and A. Furusaki, Nucl. Phys. B **565**, 653 (2000); Phys. Rev. Lett. **84**, 2913 (2000); P. W. Brouwer, C. Mudry, and A. Furusaki, Physica E **9**, 333 (2000).
- [194] A. Altland and B. D. Simons, J. Phys. A **32**, L353 (1999); Nucl. Phys. B **562**, 445 (1999).
- [195] M. R. Zirnbauer, J. Phys. A **29**, 7113 (1996).
- [196] This is an example of what in QCD is known as the phenomenon of ‘chiral symmetry breaking’: Neglecting quark masses, the microscopic Yang-Mills action (corresponding to our  $\psi$ -action in the small  $\epsilon$ -limit), is invariant under  $G \times G$  where  $G$  is a symmetry group whose detailed structure depends on the flavour content of the theory, etc. (In our formalism, its rôle is played by  $GL(1|1)$ .) Now, in the *effective* low energy QCD Lagrangian the microscopic chiral symmetry is spontaneously broken down to  $G \times G \mapsto G$  in very much the same way as the symmetry group of our low energy  $Z$ -functional is broken down to  $GL(1|1)$  from  $GL(1|1) \times GL(1|1)$ .
- [197] S. Hikami and A. Zee, Nucl. Phys. B **408**, 415 (1993); E. Brezin, S. Hikami, and A. Zee, Nucl. Phys. B **464**, 411 (1996).
- [198] A. V. Andreev, B. D. Simons, and N. Taniguchi, Nucl. Phys. B **432** [FS], 487 (1994).
- [199] For an odd number of sites, the block matrix elements of the Hamiltonian assume a *rectangular* form, the determinant vanishes and states at zero energy appear.